September 1997 ● NREL/SR-540-22967 ● UC Category: 1504

Fabrication and Testing of an Enhanced Ignition System to Reduce Cold-Start Emissions in an Ethanol (E85) Light-Duty Truck Engine

D. Gardiner, R. Mallory, and M. Todesco
Nexum Research Corporation
Thermotech Engineering Division

NREL Technical Monitor: Margaret Whalen

National Renewable Energy Laboratory
1617 Cole Boulevard
Golden, Colorado 80401-3393
A national laboratory of the
U.S. Department of Energy
Managed by the Midwest Research Institute
For the U.S. Department of Energy
Under Contract No. DE-AC36-83CH10093

Prepared under Subcontract Number ACI-6-16602-01
September 1997

NOTICE

Available to DOE and DOE contractors from:
Office of Scientific and Technical Information (OSTI)
P.O. Box 62
Oak Ridge, TN 37831
Prices available by calling (423) 576-8401

Available to the public from:
National Technical Information Service (NTIS)
U.S. Department of Commerce
5285 Port Royal Road
Springfield, VA 22161
(703) 487-4650

EXECUTIVE SUMMARY

This report describes an experimental investigation of the potential for an enhanced ignition system to lower the cold-start emissions of a light-duty vehicle engine using fuel ethanol (commonly referred to as E85). Plasma jet ignition and conventional inductive ignition were compared for a General Motors 4-cylinder, alcohol-compatible engine. Emission and combustion stability measurements were made over a range of air/fuel ratios and spark timing settings using a steady-state, cold-idle experimental technique in which the engine coolant was maintained at 25°C to simulate cold-running conditions. These tests were aimed at identifying the degree to which calibration strategies such as mixture enleanment[1] and retarded spark timing could lower engine-out hydrocarbon emissions and raise exhaust temperatures, as well as determining how such calibration changes would affect the combustion stability of the engine (as quantified by the coefficient of variation, or COV, of indicated mean effective pressure calculated from successive cylinder pressure measurements).

Retarding the spark timing to well after piston top dead centre was highly effective for reducing hydrocarbon emissions when used in combination with stoichiometric or slightly lean mixtures. This approach could increase exhaust temperatures by about 200°C over the usual values, which would be expected to cause the catalytic converter to "light-off" (attain high oxidation efficiency) earlier than normal. The ability to use such a calibration strategy was limited with conventional ignition as engine stability would degrade excessively.

At equal air/fuel ratio and spark-timing settings, plasma jet ignition provided lower COV levels and lower specific fuel consumption than conventional inductive

[1] Throughout this report, the term "enleanment" has been used to refer to calibration changes that are intended to increase the air/fuel ratio of the mixture. Enleanment is the opposite of enrichment (a term which is much more commonly used), where the air/fuel ratio is reduced to provide excess fuel for situations such as cold starting.

ignition, but caused higher hydrocarbon emissions and lower exhaust temperatures. However, plasma jet ignition provided a better trade-off between decreasing hydrocarbon emissions and increasing COV levels than inductive ignition when air/fuel ratio and spark timing were optimized. For an upper COV threshold of 10% (considered to be the upper limit that might be acceptable in practice), minimum hydrocarbon mass emission flow rates with plasma jet ignition were about 13% of those using inductive ignition.

TABLE OF CONTENTS

ACRONYMS

ATDC	:	after top dead centre
BTDC	:	bottom top dead centre
COV	:	coefficient of variation
ECM	:	electronic control module
EGO	:	exhaust gas oxygen
EGR	:	exhaust gas recirculation
EMI	:	electromagnetic interference
EPROM	:	Erasable Programmable Memory
FID	:	flame ionization detector
FTP	:	Federal Test Procedure
GM	:	General Motors
IAC	:	idle air control
IMEP	:	indicated mean effective pressure
ISFC	:	indicated specific fuel consumption
MAF	:	mass air flow
NMOG	:	non-methane organic gas
NRCan	:	Natural Resources Canada
PCM	:	powertrain control module
PJI	:	plasma jet ignition
RFI	:	radio frequency interference
UBHC	:	unburned hydrocarbon concentrations
UEGO	:	universal exhaust gas oxygen sensor
ULEV	:	ultra-low-emission vehicle

LIST OF FIGURES

1. INTRODUCTION

This report describes an experimental investigation of the potential for an enhanced ignition system to lower the cold-start emissions of a light-duty vehicle engine using fuel ethanol. The 4-cylinder test engine was a pre-production prototype representative of future alcohol-compatible engines considered for future mass production by General Motors (GM) for light-truck (S10, Sonoma) applications. The main test fuel was representative of the maximum ethanol content fuel intended for the engine and contained a total of 20% gasoline and 80% ethanol. Because fuel-grade ethanol normally contains 5% gasoline as a denaturant prior to blending for automotive use, 15% gasoline is added in the final blending process and the fuel is most commonly referred to as E85 (more correctly, E_d85) despite the fact that it is actually E80.

The ignition system that was evaluated is a type of plasma jet system using high-current/short-duration spark discharges and special recessed surface-gap spark plugs. The electrical energy of a single spark used during normal warm running is about equal to that of a conventional inductive ignition system. In order to increase ignition energy during cold starting, a series of additional sparks can be produced at short intervals (<100 μs) or the energy of a single spark can be increased. Improving the ignition process offers the potential to use leaner fuel/air mixtures and later spark timing with a cold engine than would be possible with conventional ignition systems, which normally require fuel enrichment to avoid excessive cyclic variation (combustion instability) or misfiring. Because such excess fuel requirements are a major cause of high hydrocarbon emissions for the Federal Test Procedure (FTP) cycle, it was anticipated that reducing or eliminating enrichment would represent a significant advance towards the attainment of ultra-low-emission vehicle (ULEV) standards.

The new ignition system was conceived, designed, and reduced to practice in earlier work funded by Natural Resources Canada (NRCan) that included bench tests and single-cylinder testing on the engine. In this project, the first complete multicylinder version of the ignition system was fabricated and the first tests in which this ignition system was implemented on a multicylinder engine were carried out. The emission and combustion stability tests for the

project were carried out using simulated cold-running conditions. The engine was force-cooled using a coolant heat exchanger system such that continuous steady-state testing was possible while maintaining the engine coolant temperature at 25°C. This degraded hydrocarbon emissions and combustion stability relative to a normal warmed-up condition, and permitted the effects of ignition system variables, air/fuel ratio, and spark timing to be evaluated in greater detail than transient cold-start testing would have allowed.

The remainder of this report provides background information regarding strategies for reducing cold-start hydrocarbon emissions and details regarding the apparatus and test procedures used. Measurements of the spark discharge characteristics of the enhanced ignition systems are presented, and the results of engine tests to compare hydrocarbon emissions and combustion stability between the standard and enhanced ignition systems are documented and analyzed for E85 fuel as well as (to a limited extent) E99 and gasoline.

2. BACKGROUND

2.1 The Importance of Cold-Transient Hydrocarbon Emission Characteristics in attaining ULEV Emission Levels with Alcohol Fuels

California ULEV standards (that may also be adopted by other U.S. and Canadian jurisdictions) specify maximum levels of non-methane organic gas (NMOG) of 0.04 g/mile as determined using the FTP. This presents a major challenge for automotive manufacturers, as the oxidation of unburned hydrocarbons by the exhaust catalyst is normally delayed for a significant period during the FTP drive cycle. As shown in Figure 2.1 [1], a conventional gasoline vehicle may exceed the ULEV limit after less than a minute of operation. Overall, approximately 60% of the hydrocarbon emissions for the entire FTP drive cycle are produced during the first 125 seconds of the cold-transient test phase (commonly called "Bag 1"), as the hydrocarbon oxidation efficiency of the exhaust catalyst tends to be at least 93%-95% thereafter [2].

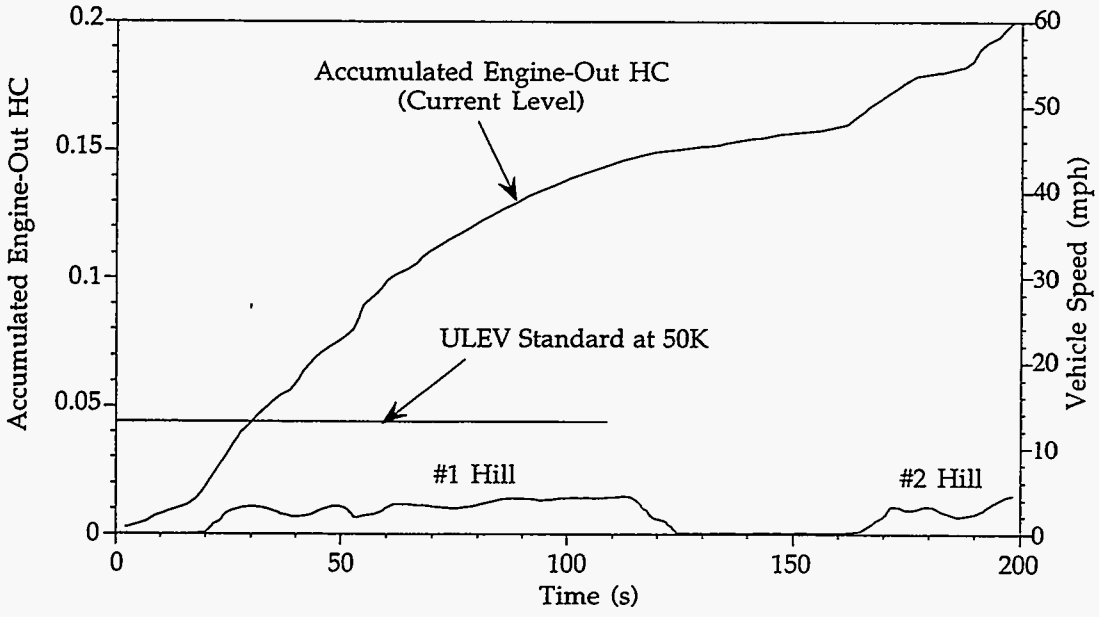

Figure 2.1: Engine-Out Hydrocarbon Emission in FTP Cold Phase (Adapted from Nakamura et al. [1])

During the period prior to catalyst activation or "light-off", engine-out hydrocarbon emissions are abnormally high. This is due largely to the rich (i.e., excess fuel) air/fuel mixtures that are usually employed, although flame quenching by cold surface walls and crevices and oil layer absorption/desorption may also play significant roles. Mixture enrichment is used to compensate for poor fuel vaporization in a cold engine, where the final vapour/air equivalence ratio existing at the time of ignition will be leaner than the liquid/air equivalence ratio originally delivered to the cylinder. Because gasoline is a multicomponent fuel spanning a wide volatility range, adding excess fuel supplies additional low-boiling-point "light end" components that vaporize easily even in a cold engine and increase the overall vapour/air equivalence ratio. Enrichment requirements for engine calibrations are normally determined empirically, but the available fundamental studies suggest that minimum delivered fuel enrichment requirements are set by the need to achieve an approximately stoichiometric (chemically correct) vapour/air equivalence ratio in the cylinder to permit cold starting and avoid poor combustion stability and driveability [3,4,5].

The problems related to mixture enrichment are compounded when high alcohol/gasoline blends such as E_d85 and M85 (85% methanol) are used. The alcohol portion of the fuel is a single boiling point component of relatively low volatility, so it is mainly the light ends contained in the gasoline fraction that are effective in increasing the vapour/air equivalence ratio as the delivered liquid/air equivalence ratio is increased. Consequently, cold-enrichment requirements tend to be somewhat higher with high alcohol blends than with gasoline. The emission situation is further worsened by the fact that the combustion of rich alcohol/air mixtures inevitably produces high levels of toxic exhaust aldehydes (predominantly acetaldehyde for ethanol and formaldehyde for methanol), which are highly reactive and have an effect on ULEV NMOG emissions that is disproportionately large compared with that of normal gasoline unburned hydrocarbons.

In summary, the need to employ fuel enrichment while the engine is cold represents a major barrier to the attainment of ULEV emission levels, particularly where alcohol fuels are

concerned. Eliminating this requirement (which otherwise makes engine-out emissions unavoidably high) forms the first step towards an effective ULEV strategy. Further steps to provide excess air in the exhaust stream (through still leaner mixtures) and optimize ignition timing offer the potential to further lower engine-out emissions, enhance the effectiveness of both conventional and enhanced (i.e., heated or insulated catalyst) after-treatment systems, and avoid the need for auxiliary hardware such as exhaust air injection pumps. In this study, an enhanced ignition system was evaluated as a means of enabling a cold engine to tolerate lean mixtures and late ignition timing so that these calibration approaches may be used as part of a ULEV emission control strategy.

2.2 Existing Knowledge Concerning the Effects of Engine Calibration Variables on Cold-Transient Hydrocarbon Emissions

Were it not for emission concerns, engine calibration for running immediately following start-up would consist of selecting values of mixture enrichment and ignition advance that provided the best idle stability characteristics. However, idle stability and low engine-out hydrocarbon emissions are, to a great extent, conflicting calibration goals for a cold engine. The influence of calibration changes on exhaust temperature is also important as higher exhaust temperatures are beneficial for achieving rapid light-off (i.e., transition to high oxidation efficiency) of the exhaust catalyst. Thus, a final calibration strategy will require some degree of compromise and the success of this compromise will depend both on the basic engine design and the characteristics of components such as the ignition and fuel delivery systems. Moreover, it may be argued that the potential cold-emission benefits of advanced hardware such as high-energy ignition and fine atomizing fuel injection may be realized mainly through the expanded range of calibration options provided by their implementation.

As an example of the influence that an emission-oriented recalibration can have on cold-start hydrocarbon emissions, data from Kaiser et al. [6] of Ford Motor Company was replotted in Figure 2.2. In this case the revised calibration strategy included a leaner air/fuel mixture, later spark timing, and an increase in idle speed. The air/fuel ratio was expressed as an excess air ratio relative to a stoichiometric or chemically correct mixture (commonly referred to as lambda); this

means of defining the air/fuel mixture will be used throughout this report. Also, engine-out total hydrocarbon emissions were reduced substantially by the revised calibration. It should be noted, however, that Kaiser et al. warned that recalibration could also alter the species distribution of the exhaust hydrocarbons and, in some cases, increase the photochemical reactivity of the emissions.

Detailed evaluations of the effects of air/fuel ratio and ignition timing on hydrocarbon emissions, combustion stability, and exhaust temperature are reported by Nakayama et al. of Honda Research and Development Co. Ltd. [2]. Rather than using actual cold starts as with Kaiser et al., Nakayama et al. performed tests under idle operation at a constant speed of 1500 rpm and a constant coolant temperature of 30°C. Apparently, some form of force-cooled, steady-state experimental technique was used, as will be discussed in the following section. Data from Nakayama et al. was replotted in Figures 2.3 and 2.4. For these figures and the remainder of the report, the coefficient of variation of indicated mean effective pressure (COV of IMEP) has been used, as this is a widely accepted means of quantifying engine stability. IMEP for individual combustion cycles is calculated from cylinder pressure measurements, and the COV is the standard deviation in IMEP expressed as a percentage of the mean IMEP.

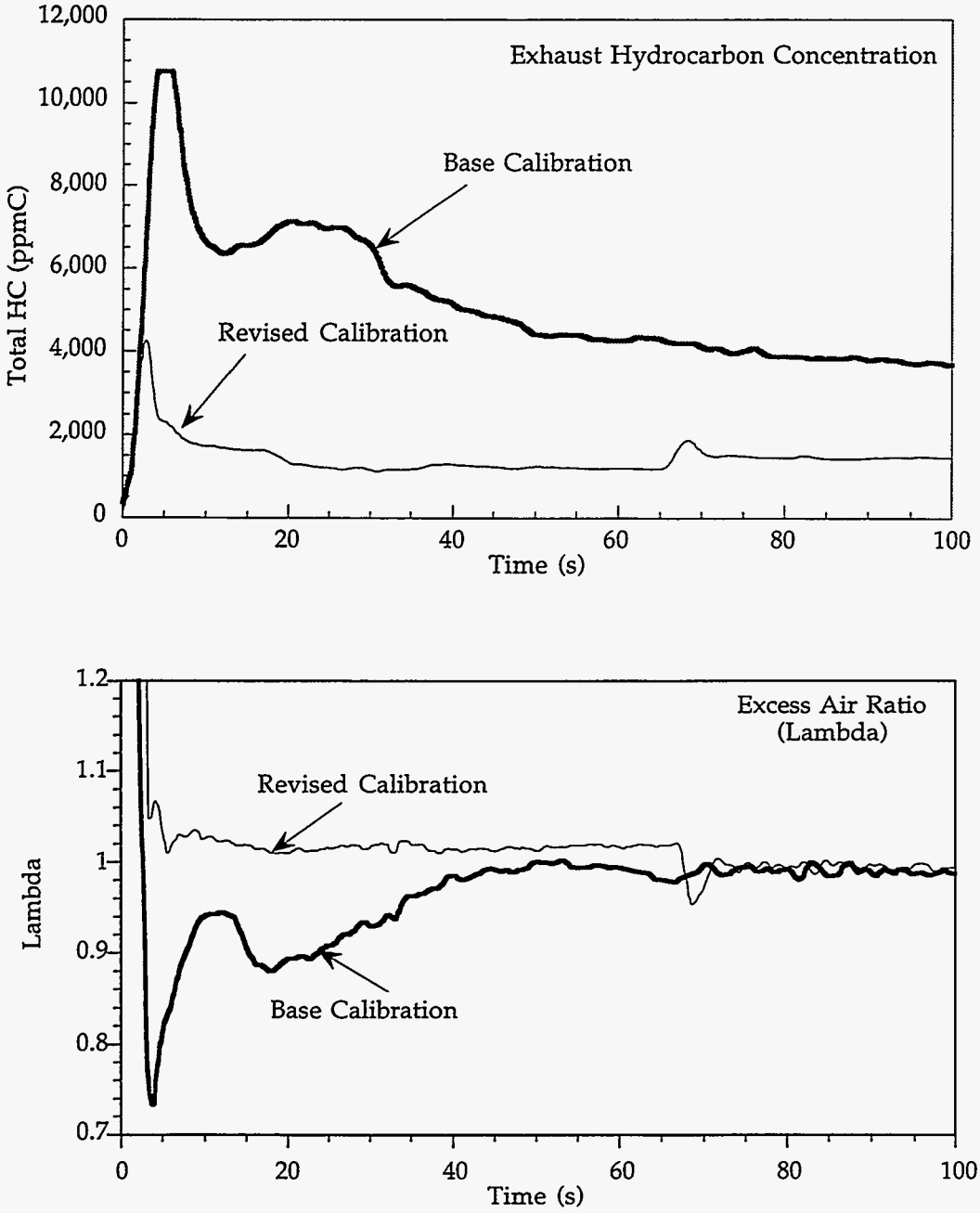

Figure 2.2: Effect of Revised Calibration Strategy on Cold-Start Hydrocarbon Emissions. Revised strategy includes leaner mixture, 200-400 rpm higher idle speed, and 15° less spark advance (Adapted from Kaiser et al. [6])

As shown in Figure 2.3, leaning the air/fuel ratio from the typical enrichment values to lambda=1 provides both a large reduction in hydrocarbon emissions and a beneficial increase in exhaust temperature. This is accompanied by increasing COV values such that the use of the leaner lambda values would not be feasible in practice. In general, good combustion stability is limited to COV values of 5% or less [2], whereas COV values in excess of 10% normally indicate extreme engine roughness or risk of stalling. Thus, in the example shown, some enrichment (i.e., lambda < 1) would be required for a vehicle.

The effects of varying ignition timing at a constant lambda value are shown in Figure 2.4. In this example, substantial reductions in hydrocarbon emissions are possible through retarded ignition timing. This can be attributed to improved oxidation of unburned fuel due to higher gas temperatures during expansion and exhaust (because burning is delayed until later in the cycle), as indicated by increased exhaust temperatures. However, COV values are shown to degrade to unacceptably high levels before the majority of the potential emission and exhaust temperature benefits can be obtained.

The relationships shown in Figures 2.3 and 2.4 are highly dependent on engine characteristics, so identical characteristics would not be expected (and were not found) for the engine used in this test program. Nevertheless, this information illustrates the potential value of technology that can improve the combustion stability under cold-running conditions so as to allow desirable combinations of lambda enleanment and ignition timing retard to be used. Nakamura et al. [2] also introduced the authors to the use of steady-state engine tests under "simulated" (i.e., force-cooled) cold-running conditions as an expedient experimental approach for evaluating new technology intended to reduce cold-start emissions.

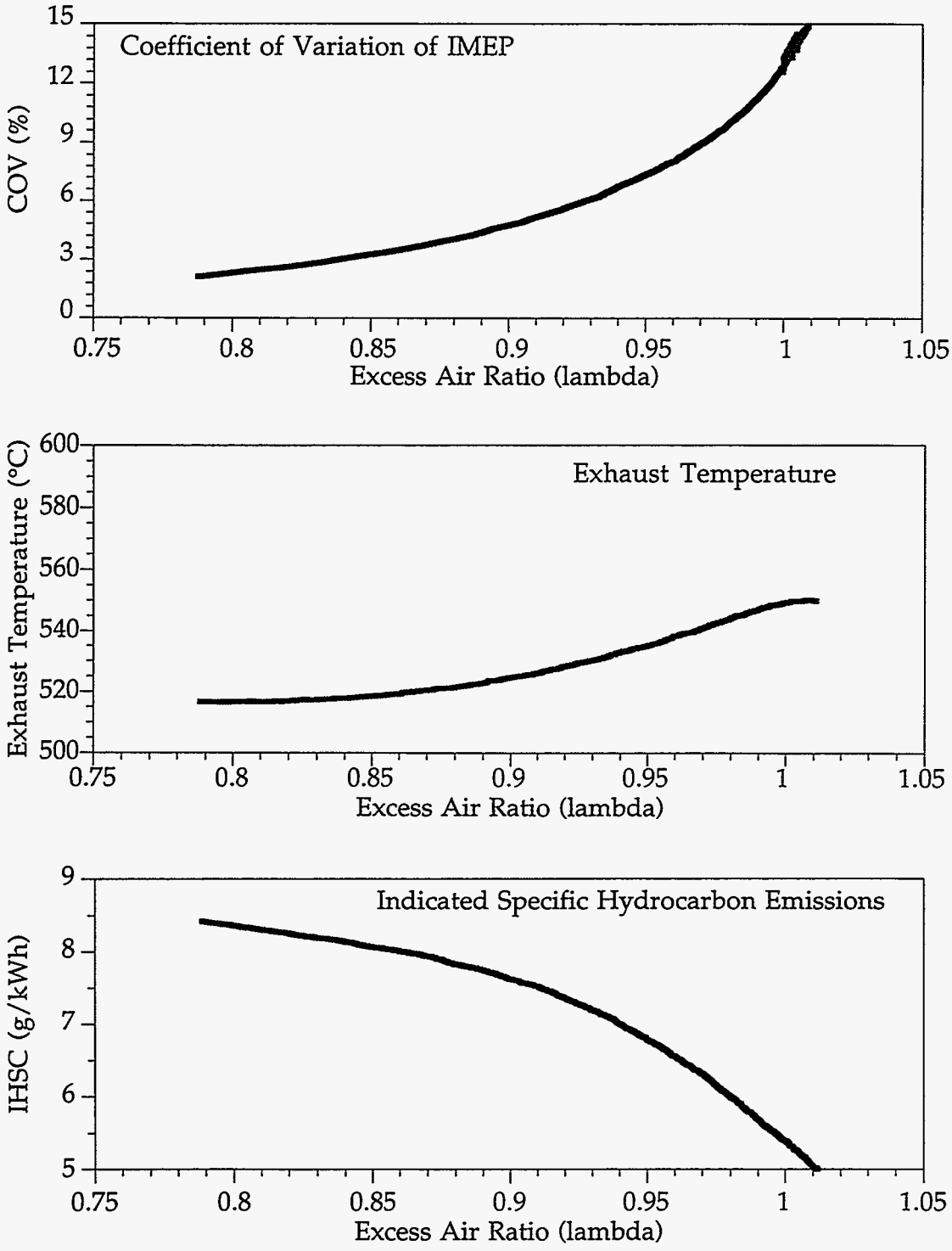

Figure 2.3: Effect of Excess Air/Fuel Ratio on Cyclic Variation, Hydrocarbon Emissions, and Exhaust Temperature (Adapted from Nakayama et al. [2])

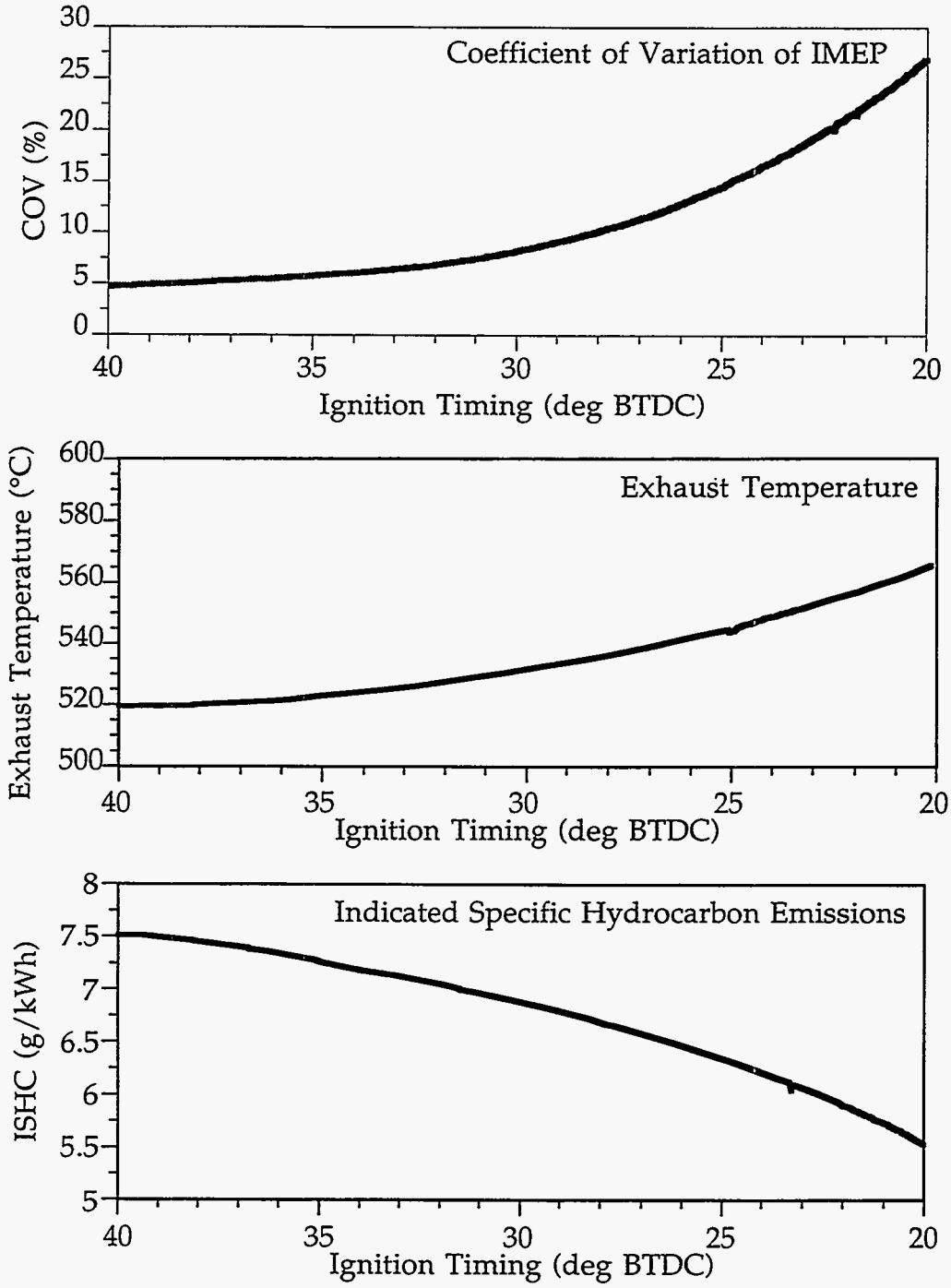

2.4

Figure 2.4: Effect of Ignition Timing on Cyclic Variation, Hydrocarbon Emissions, and Exhaust Temperature (Adapted from Nakayama et al. [2])

2.3 Rationale for Using Steady-State, Cold-Running Engine Tests

Actual cold-starting tests are very time consuming and costly to carry out if many variables (such as air/fuel ratio, ignition timing, and ignition energy) are to be investigated. The engine must be cooled prior to each test, and the transient nature of the engine's operating conditions and in-cylinder temperatures makes it difficult to discern the influence of small changes in calibration variables from the inherent test-to-test variations. In recognition of these difficulties, a number of researchers have chosen to use test procedures that create steady-state, cold operating conditions in studies aimed at identifying promising means of reducing cold-start emissions. In such cases, the engine is operated at constant speed and load while an auxiliary cooling system is used to prevent the engine coolant from warming up. This is not as severe a condition as an actual cold start, as in-cylinder surface temperatures during force-cooled, steady-state running will be higher than those that would exist immediately following starting. However, hydrocarbon emissions and combustion stability are degraded significantly relative to normal warm running conditions, such that the qualitative or directional influence of calibration variables or hardware changes may be assessed.

The work at Honda Research and Development referred to earlier [2] was obviously performed using some kind of steady-state cold testing, although no experimental details were provided in the paper. In the same year (1994) another paper describing steady-state cold testing was published by Institute Francais du Pétrole and Renault S.A. [7]. Since then, this experimental approach has been used in experiments described in two papers from Ford [8,9], three papers from GM/Saturn [10,11,12], and a paper from Volkswagen AG [13]. Thus, it appears that steady-state cold testing is now well established as a credible experimental technique for studying the problems that exist during cold-transient operation.

In the case of the study described in this report, the desire to evaluate the effects of different combinations of air/fuel ratio, spark timing, and ignition energy dictated a test matrix that would have been impractical for transient cold-start testing. Therefore, it was decided that steady-state cold testing would be used at this stage. Of course, obtaining conclusive evidence of

the ability of the hardware and calibration changes described in this report to provide reductions in FTP cycle emissions will require future research under actual operating conditions.

3. APPARATUS

3.1 Engine Test Bed

The basic engine test bed was provided by GM of Canada Ltd., Product Engineering, Oshawa, and is shown in Figure 3.1. It consisted of an engine and transmission mounted to a test stand, as well as auxiliary components such as the cooling system, exhaust system, fuel tank, instrument panel, and manual throttle and transmission controls. This setup was intended to simulate an installation of the engine in a GM S-Series/Sonoma pickup truck. It was previously used by GM staff for cold-start calibration work as part of their ethanol-compatible truck program.

3.1.1 Engine

The engine is a 2.2-litre, 4-cylinder design with a pushrod-actuated valvetrain, two valves per cylinder and sequential-port fuel injection. The engine specifications are shown in Table 3.1. The particular engine supplied by GM as part of the test bed was a preproduction prototype for the 1996 model year that had been modified by GM to incorporate features being considered for future model year vehicles. These modifications included the addition of alcohol-tolerant fuel injectors, fuel rail and fuel pump, and an alcohol concentration sensor. The engine was calibrated for gasoline and gasoline/alcohol blends containing up to 80% ethanol.

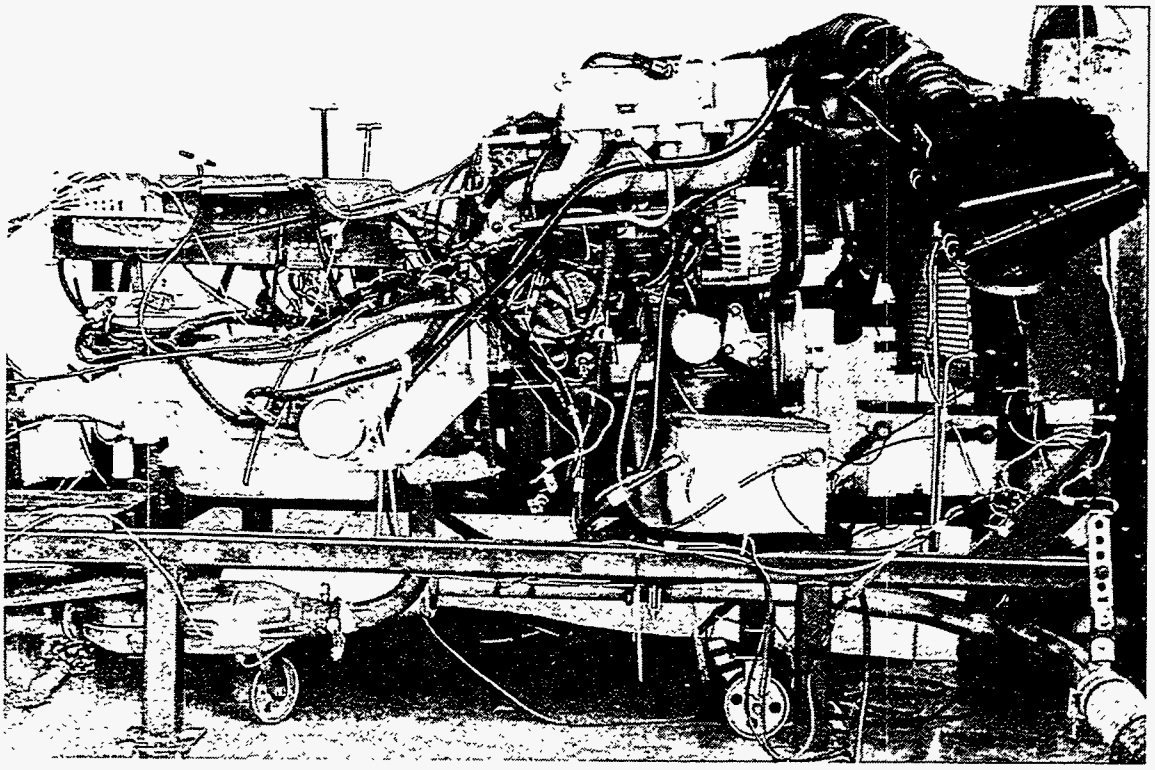

Figure 3.1: Engine Test Stand

Table 3.1: Test Engine Specifications

Engine Type:	Inline 4-cylinder
Bore:	84 mm
Stroke:	88 mm
Swept Volume:	2.2 litre
Compression Ratio	8.85:1
Valve Arrangement:	Overhead valve pushrod with 1.5:1 rockers and roller hydraulic lifters
Fuel Metering System:	Speed-density control

3.1.2 Engine Electronic Control Systems

The test bed included a special version of the GM powertrain control module (PCM), which made it possible to modify the engine control calibration. Standard PCMs of this vintage have a permanently mounted memory chip to prevent tampering. The test bed setup had a bus leading from the PCM to an external module housing a removable erasable programmable memory (EPROM) chip. The EPROM could be removed and mounted in an EPROM programmer to facilitate calibration changes. General Motors Experimental Engineering initially supplied Thermotech Engineering with a confidential manual that listed the addresses, hexadecimal values, and conversion factors to obtain engineering-unit values for relevant calibration parameters. Additional addresses and calibration technical support were supplied during the project in response to requests from Thermotech Engineering as the need for further calibration modifications became apparent.

Variations in air/fuel ratio were obtained using a wide-range air/fuel ratio sensor in the exhaust (NTK universal exhaust gas oxygen sensor [UEGO]) in combination with a UEGO signal processor equipped with an adjustable simulated exhaust gas oxygen (EGO) sensor output. The simulated output was supplied to the engine control system in place of the

standard EGO sensor. With this arrangement, the engine could be operated under closed-loop air/fuel ratio control at setpoints rich or lean of the usual stoichiometric setpoint. The UEGO-based control loop was used for both the GM PCM and the aftermarket electronic control system used during the latter part of the project.

Changes in ignition timing were initially accomplished by recalibrating the GM PCM, which either operated the standard GM inductive ignition system or was used as a timing trigger for the enhanced ignition system. The most retarded ignition timing possible with the GM PCM was 0° (top dead centre). It was eventually apparent that more retarded ignition timing could lower hydrocarbon emissions further, so an aftermarket electronic control system was installed along with trigger delay circuitry so that extreme spark retard could be tested with the enhanced ignition system. During the final phase of the project, a revised aftermarket electronic control setup was added to the apparatus, which allowed extreme spark retard to be tested with conventional inductive ignition and provided a more stable and repeatable timing signal for the enhanced ignition system. The aftermarket controller was eventually also used for fuel-injection control, as it was possible to achieve a better control loop match with the UEGO-based simulated EGO signal, thereby providing improved air/fuel ratio stability.

3.1.3 Engine Instrumentation and Data Acquisition

Diagrams depicting the instrumentation and data acquisition for the engine test bed are shown in Figures 3.2 and 3.3. Data was recorded both on a crankshaft position basis and a real-time basis. The engine cylinder head had previously been modified by GM to permit pressure transducers to be installed in each cylinder. Kistler 6121 transducers and Kistler 5010 charge amplifiers were used for cylinder pressure measurement in this study. These measurements were used for calculating the IMEP of consecutive cycles so that the COV of IMEP could be determined to quantify combustion stability.

Engine speed was measured using the crank angle encoder signal and a frequency-to-voltage converter. The exhaust air/fuel ratio was measured using the NTK wide-range UEGO sensor and electronic control module (ECM) air/fuel ratio recorder, which supplied the control loop signal. The built-in pressure sensor in the ECM unit was used to measure intake pressure and intake air flow was measured using a hot-wire mass air flow (MAF) meter.

Exhaust hydrocarbon concentration was measured using a California Analytical model 300-HFID flame ionization detector (FID), which was calibrated using 2500 ppm propane in nitrogen calibration gas. Exhaust mass flow rates were calculated based on measured intake air flow and air/fuel ratio values. Exhaust mass flow values were used along with measured hydrocarbon concentrations to calculate hydrocarbon mass flow rates in equivalent grams per second of propane.

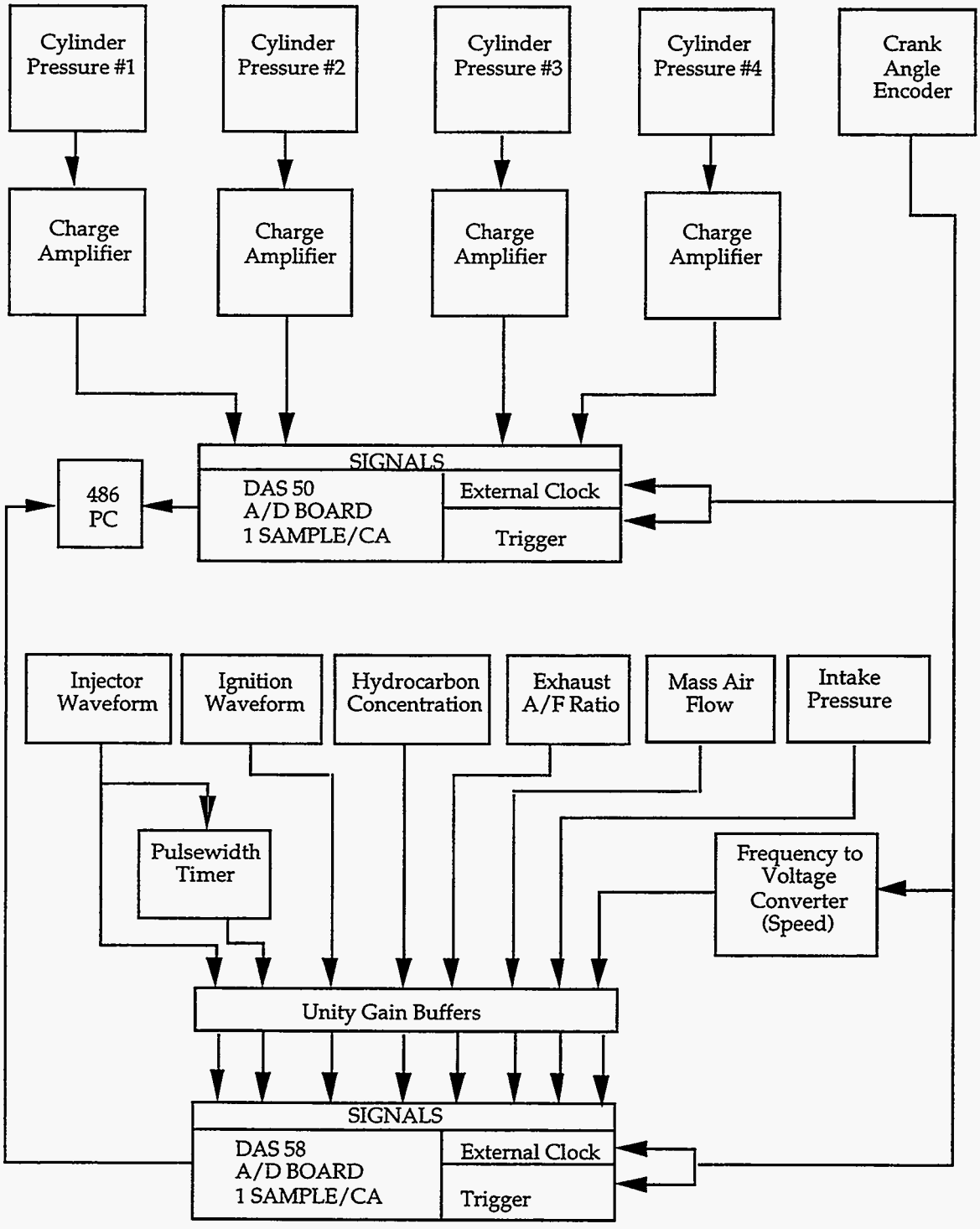

Figure 3.2: Crank-Angle-Based Instrumentation and Data Acquisition for Engine Test Bed

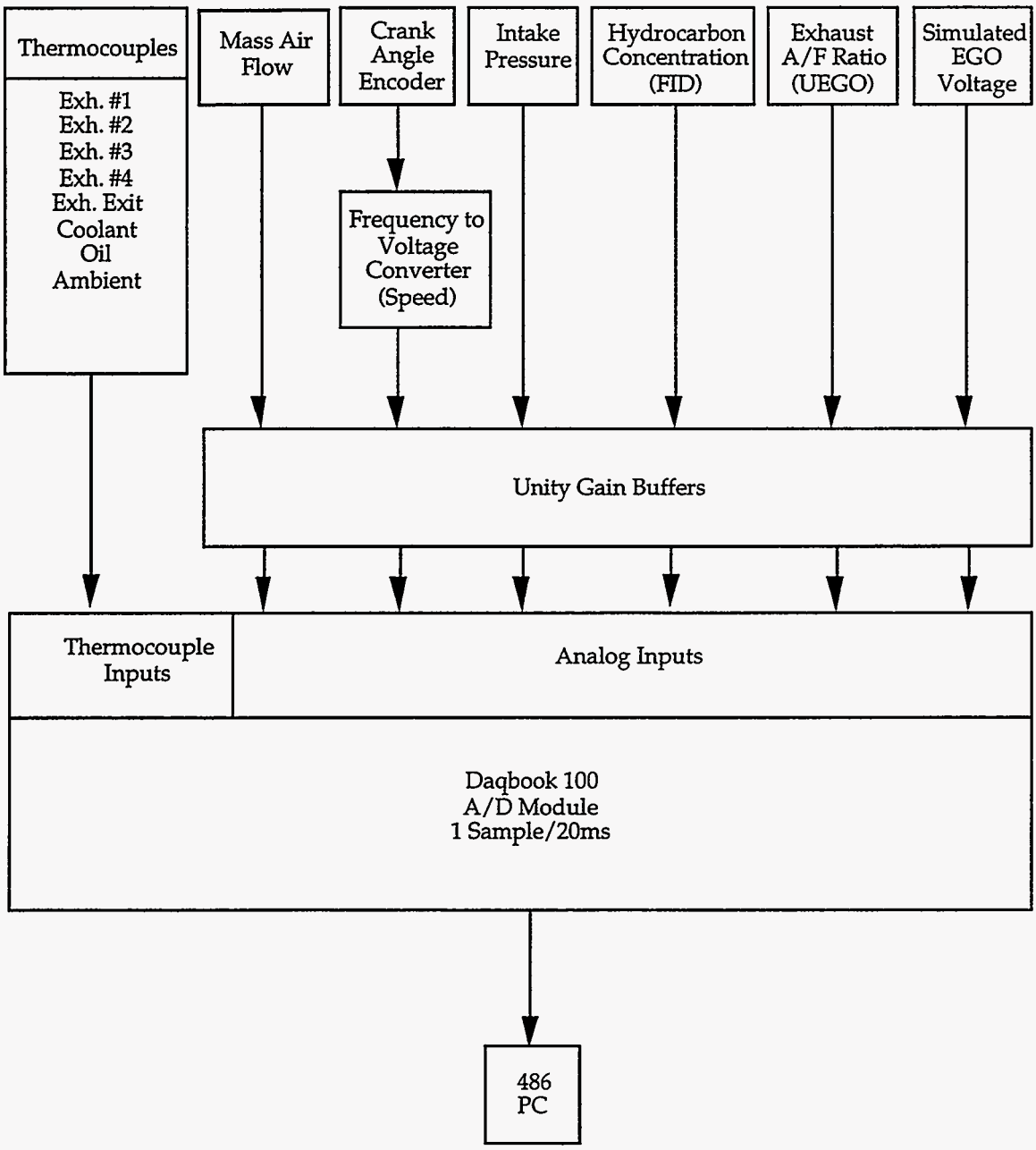

Figure 3.3: Time-Based Instrumentation and Data Acquisition for Engine Test Bed

3.2 Engine Enhanced Ignition System

The enhanced ignition system used on the GM 4-cylinder engine is depicted in Figure 3.4. This ignition system was the first multicylinder engine implementation of a novel ignition circuit originally developed in earlier work funded by NRCan and was fabricated specifically for this National Renewable Energy Laboratory (NREL) project. The system was configured for distributorless operation using one coil per engine cylinder and four independent energy storage and discharge sub-circuits. Ignition timing triggering was provided by the existing inductive ignition coil drivers of the standard GM coil module (under control of the electronic spark timing signal from the GM PCM or the programmable aftermarket engine control system used later in the project).

The coil drivers would normally each have provided primary current for an inductive ignition coil serving two cylinders. The ignition would be fired during both the compression and expansion strokes of a given cylinder (termed a "waste spark" system). With the enhanced ignition system, firing only during the compression stroke would be desirable to minimize ignitor wear; the provision of four coils and sub-circuits made this feasible. However, rather than increase the complexity of the apparatus by adding an additional timing circuit (to gate the coil driver signals relative to the camshaft sensor for each cylinder), pairs of individual cylinder circuits were paralleled to a single driver and the system was operated in waste spark mode for the tests described in this report.

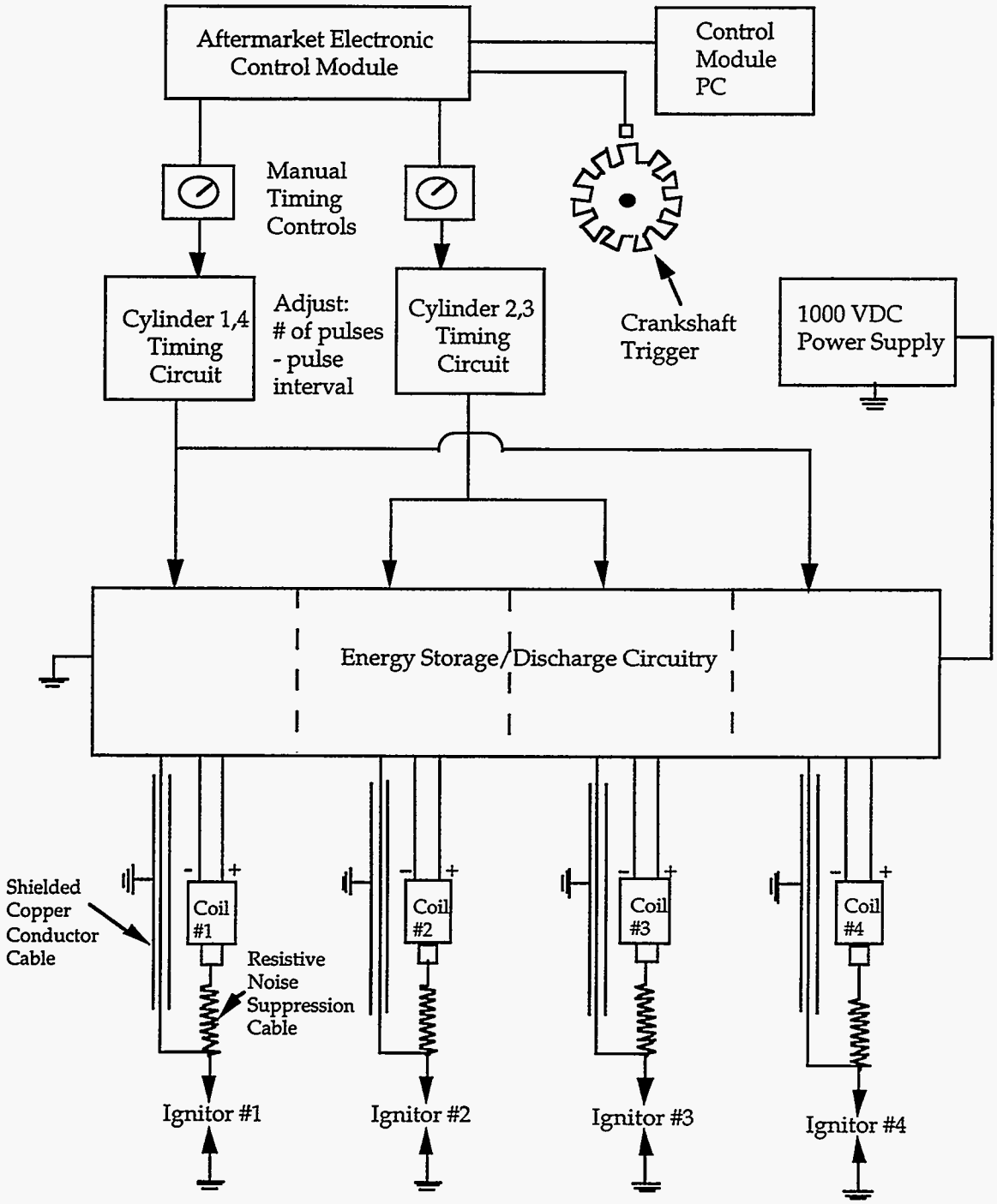

Figure 3.4: 4-Cylinder Enhanced Ignition Apparatus

During some experiments, manual ignition timing controls (ignition retard circuits) were used to extend the range of ignition timing beyond the range provided by the electronic control module. The timing signal was then used to trigger further ignition pulse timing circuits, which controlled the actual switching of the energy discharge circuitry of the ignition system. With these switching control circuits, it was possible to manually adjust the number of times that ignition energy was discharged during each spark "event" and the interval between pulses in each sequence of discharges.

The circuit details are proprietary and the relevant intellectual property is vested in Natural Resources Canada. However, it can be revealed that this circuit belongs to a general ignition circuit category in which capacitively stored electrical energy is discharged directly into the spark gap (bypassing the ignition coil) after gap ionization is achieved by a conventional coil ignition approach. This makes it possible to achieve much higher spark currents and shorter spark durations than would be possible in any case involving energy transfer to the spark gap through an ignition coil. Various embodiments of this category of circuit have been described in technical papers by the authors [14-19] and other researchers [20-28], as well as in a number of patents [14-20] that use terms such as "plasma jet", "low voltage add-on", "dual energy", and "low impedance" to describe this approach. For the remainder of this report we will refer to the system as plasma jet ignition (PJI), as this term is used most frequently in the literature when high-current, short-duration sparks are combined with recessed surface gap ignitors (the ignitor type used in this study). The principal advantages of the new circuit relative to earlier circuits include immunity to untimed plasma discharges (a common problem with earlier circuits where high voltage would be present at the ignitor prior to the intended spark timing and unintentional discharges of energy could result due to influences such as conductive carbon deposits), the ability to provide multiple sparks at very short intervals (as low as 60 μs for the system described in this report), and a reduction in the number of electronic components required.

3.3 Spark Plugs and Plasma Jet Ignitors

The spark plugs used in tests with standard inductive ignition were Champion prototypes (#AA24574912), which came with the preproduction engine test stand provided by GM of

Canada. These spark plugs were a conventional projected tip J-gap design with a 1.5 mm (0.06") specified gap width and platinum wear pins on both the centre and ground electrodes. They were equipped with an internal 40-kΩ resistor for radio frequency noise suppression. During limited testing in which standard spark plugs were used along with the enhanced ignition (plasma jet) circuit, the resistor was removed and replaced with a brass pellet to provide the low secondary resistance required for effective use with the plasma jet electrical discharges.

The plasma jet ignitors were fabricated by modifying standard automotive spark plugs. A recessed surface gap was created by machining away the high-voltage electrode to form a cavity within the ceramic insulator and welding a tip with an appropriate cavity orifice to the spark plug shell. The plasma jet ignitor design is depicted in Figure 3.5.

Steel tips were used for initial bench and engine testing because of ease of fabrication with this material. Tungsten was later evaluated as it is highly resistant to spark erosion. Tungsten had previously been used successfully in work with neat methanol (M100), but in the present work with E_d85, the use of this material lead to unacceptable increases in the voltage required for spark breakdown after only brief periods of engine running. It is believed that this behaviour was related to some form of surface corrosion (i.e., an incompatibility between tungsten and ethanol), but this was not investigated in detail. For the final engine tests, inconel, the standard centre electrode material for conventional spark plugs, was used; this provided good resistance to electrical erosion without the aforementioned voltage increase problems.

An orifice diameter equal to the cavity diameter (2.5 mm) was chosen for the final tests as small orifice sizes resulted in higher values of the coefficient of variation of indicated mean effective pressure. Surface gap lengths of 5.0 mm and 7.5 mm were tested during the project. Limited testing to determine the optimum distance for the ignitor tip to project into the combustion chamber was also carried out.

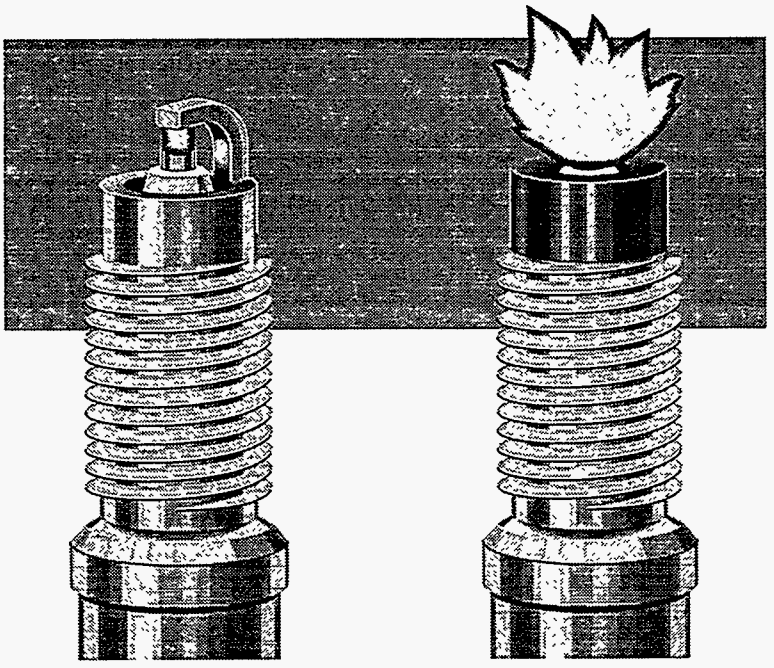

Figure 3.5: Recessed Surface Gap (Plasma Jet) Ignitor

3.4 Test Fuels

The ethanol fuels were supplied by Commercial Alcohols Inc., Toronto, Ontario. The fuel designated E_d85 in this report was blended to meet specifications supplied by GM for summer-grade fuel ethanol. It contained a total of 80% by volume ethanol and 20% nonleaded gasoline. The blend Reid Vapour Pressure for the GM specification was 38-59 kPa (5.5-8.5 psi). The fuel composition was not confirmed through any analysis at Thermotech Engineering. However, the final tests for both standard and enhanced ignition were performed using E_d85 from a single blend batch, so fuel composition would not have been responsible for any differences observed between the two ignition systems.

There was also a desire to perform some tests using a fuel that was nearly neat (pure) ethanol. In the United States, ethanol for fuel usage must contain a minimum of 5% by volume gasoline or other denaturant; therefore, E95 is the highest ethanol concentration available. However, in Canada, a denaturant concentration as low as 1% by volume is acceptable as a deterrent to voluntary ingestion. Thus, it was possible to test an E99 ethanol/gasoline blend during the project. Gasoline was also tested, which was a commercially available summer-grade 87 octane product.

3.5 Test Conditions and Procedures

All experiments described in this report were performed under steady-state, cold-idle conditions for which the engine was force-cooled by an external heat exchanger system. The setpoint of the cooling system was adjusted to 25°C, which resulted in actual engine coolant outlet temperatures of 23°-25°C depending on operating conditions. The highest coolant temperatures were observed when extreme spark retard was used.

Although it was possible to maintain a nearly constant engine coolant temperature during steady-state running, the engine did experience a warm-up phase following cold starting as the internal metal surfaces and oil warmed up to steady-state values. This had a noticeable effect on emission levels (which dropped during this phase), making it necessary to idle the engine for a "preconditioning period" sufficient to stabilize the hydrocarbon levels at their final (i.e., minimum) values. A preconditioning period of 30 minutes was found to be adequate for this purpose, which led to oil temperatures of 49°-50°C. The preconditioning was always carried out using the maximum spark advance setting for the test matrix. Oil temperatures as high as 55°C were observed when extreme spark retard was used.

The tests were carried out over the desired range of lambda and spark-timing values by conducting a series of "sweeps" at fixed spark timing points where lambda was varied in approximately 1% steps from rich to lean. For a given test run, spark-timing variations (usually in 5° steps) were always carried out in order of the most advanced to the most retarded settings. This was done because the higher exhaust temperatures that occurred as the spark timing was retarded would heat up the exhaust ports and manifold and influence hydrocarbon emissions. Thus, if the spark timing was advanced, the exhaust ports and manifold would have to cool down before true hydrocarbon measurements were achieved. By retarding the spark timing during the test run, the exhaust ports and manifold would become progressively hotter with each step change in spark timings, which caused the hydrocarbon emissions to stabilize more rapidly and produced more consistent test results.

At each test point, cylinder pressure data (recorded on a crank angle basis) and time-based measurements (emissions, flows, lambda, temperatures, etc.), were recorded simultaneously. To obtain combustion stability (COV%) values, 300 consecutive cylinder-pressure cycles were recorded from #1 cylinder along with a crankshaft position sensor signal to define an accurate TDC value for the calculations. The time-based measurements were recorded at 50 Hz during the same interval as the cylinder-pressure acquisition.

The FID was calibrated immediately before the test measurements (during the engine preconditioning period) and the calibration was rechecked immediately after engine shutdown at the end of each test run. The oil had to be changed frequently as fuel rapidly accumulated in the crankcase during sustained cold running. The engine was filled with fresh oil prior to the test runs used for the final data comparisons.

During the experiments described in Sections 4 to 7, a target idle speed of 1100 rpm was used. Actual idle speed could vary between 1050 rpm and 1150 rpm because a "deadband" of ±50 rpm was programmed into the controller to avoid idle-speed oscillations from control system overshoot or undershoot. During the experiments described in Section 9, the target idle speed was raised to 1450 rpm to make the engine less vulnerable to stalling. A deadband of ±50 rpm was used in this case as well.

4. SINGLE-CYLINDER MEASUREMENTS OF SPARK DISCHARGE CHARACTERISTICS AND COMBUSTION STABILITY

4.1 Comparison of Spark Characteristics of GM Inductive Ignition and Plasma Jet Ignition

Experiments to investigate the spark discharge characteristics of different ignition systems are commonly carried out using a bench-top pressure chamber apparatus. However, this does not duplicate the conditions that exist at the spark plug gap of a running engine, particularly a high-swirl design like the GM 2.2 litre where mixture velocities through the spark gap would be relatively high. High gap velocities tend to shorten the spark duration of inductive ignition systems, due to spark "stretch" and eventual "blowout" [37, 38, 39]. In this study, spark electrical measurements were carried out using the actual running engine at idle.

Figure 4.1 shows a comparison of spark current waveforms for the GM inductive ignition and a single discharge of the plasma jet system (as configured as a multistrike system with low-energy individual discharges). The GM system uses special "alcohol-compatible" coils that provide higher spark current, faster voltage rise rates (that improve the ability to fire alcohol-wetting spark plugs during cold starting), and slightly less spark duration than standard gasoline coils. The examples of current waveforms for the GM system illustrate how random cycle-to-cycle variations in spark current occurred in the high-swirl engine. With the exception of the brief current spike at the beginning of the waveforms, a peak current of about 120 mA can be observed along with a total spark duration of 550-700 μs. This duration is considerably shorter than the 1-2 ms typically expected from inductive ignition [27, 40] and is likely due to a combination of the high-current coils, the high spark gap velocities, and the relatively large 1.5-mm spark gap used (which also tends to shorten spark duration). The calculated ignition energy for the system (stored in the coil primary inductance) based on primary current measurements was 175-195 mJ.

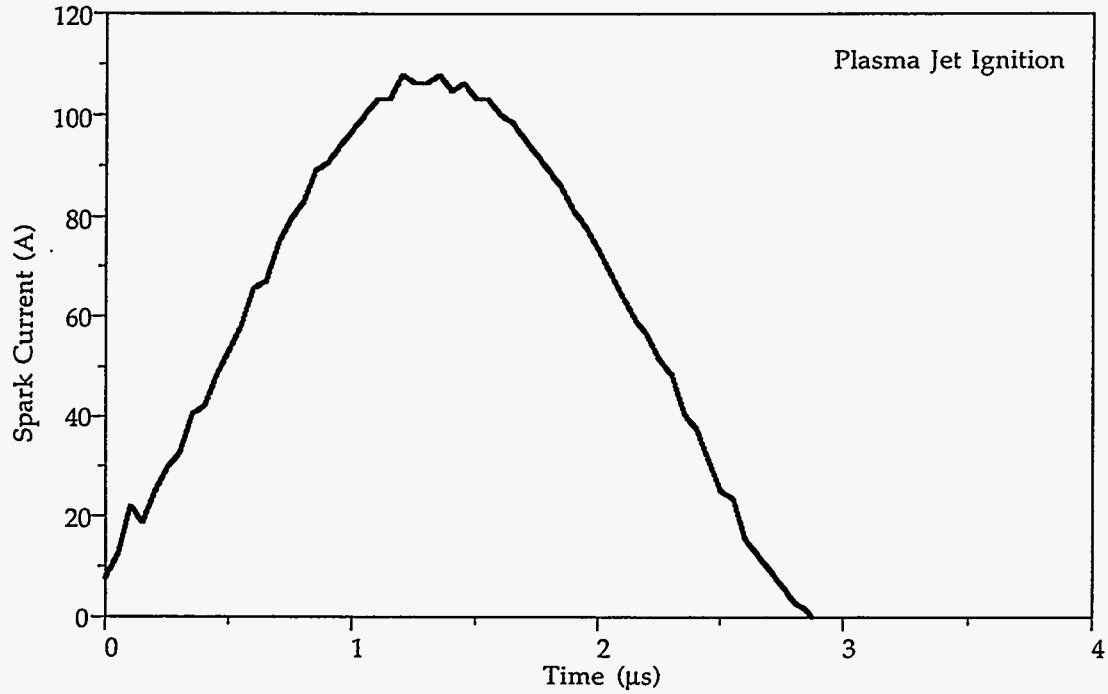

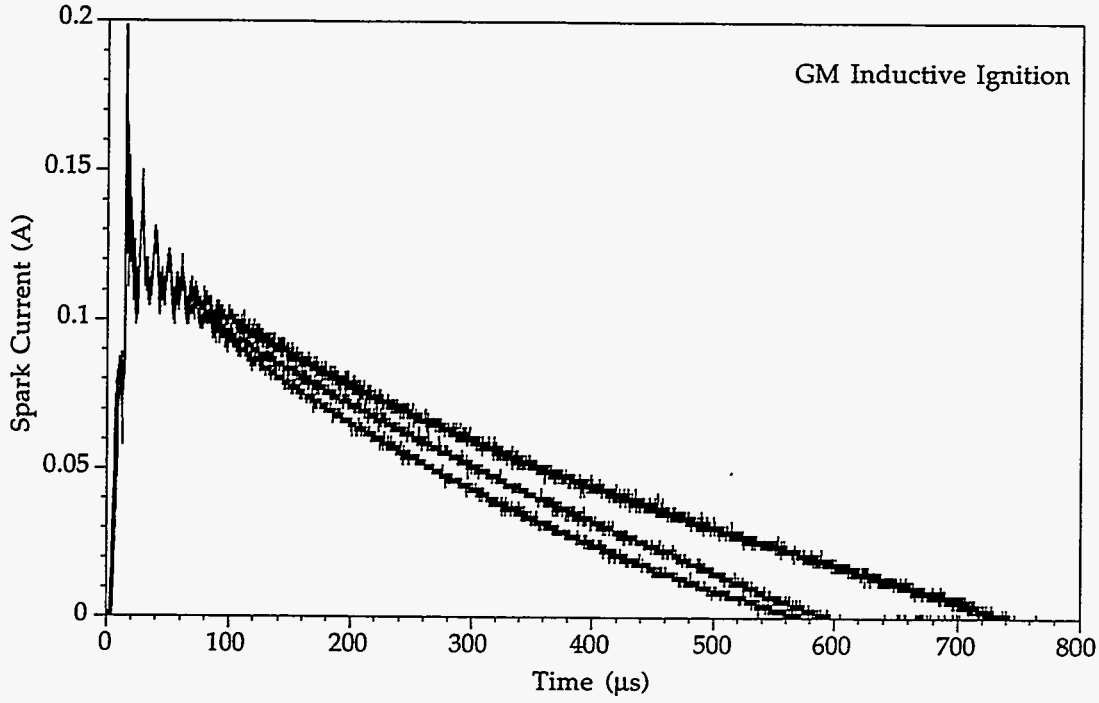

Figure 4.1: Comparison of Spark Current Waveforms for GM Inductive Ignition and PJI

In comparison, the spark current waveform for the plasma jet system shows extremely high spark current values and extremely short spark duration at over 100 A and under 5 μs, respectively. The total capacitively stored energy for the spark was 150 mJ, or slightly less than the GM system. In essence, the high current values are achieved with similar stored energy by compressing the time of energy transfer to the spark gap into a much shorter interval. This type of high-current/short-duration spark is desirable for use with recessed surface gap ignitors, as the sudden discharge of electrical energy within the ceramic cavity of the ignitor leads to shock heating of the air/fuel mixture in the cavity (which can be considered as a small precombustion chamber) and a turbulent, fast-growing initial flame kernel. This in turn causes the pressure inside the cavity to rise abruptly such that a turbulent plasma jet is ejected from the ignitor orifice to provide an enhanced ignition source for the main air/fuel mixture in the engine combustion chamber.

The plasma jet ignition circuit used in this study can be configured to provide multiple spark discharges. Conventional capacitor discharge ignition systems with multistrike capability are available but the interval between sparks is typically greater than 1 ms. The plasma jet ignition circuit was operated at restrike intervals as low as 60 μs during this study, which would ensure that the total 900 mJ of energy in a typical six-strike sequence would be delivered within about 300 μs. This behaviour can be seen in Figure 4.2, which shows spark current and voltage waveforms for the plasma jet system in multistrike mode under engine idle conditions. As shown by the voltage waveforms, the peak or "breakdown" voltage requirement for the additional sparks tended to be lower than that of the first spark. This was likely due to residual ionization in the spark gap, which would have been present after the first spark discharge took place.

4.1

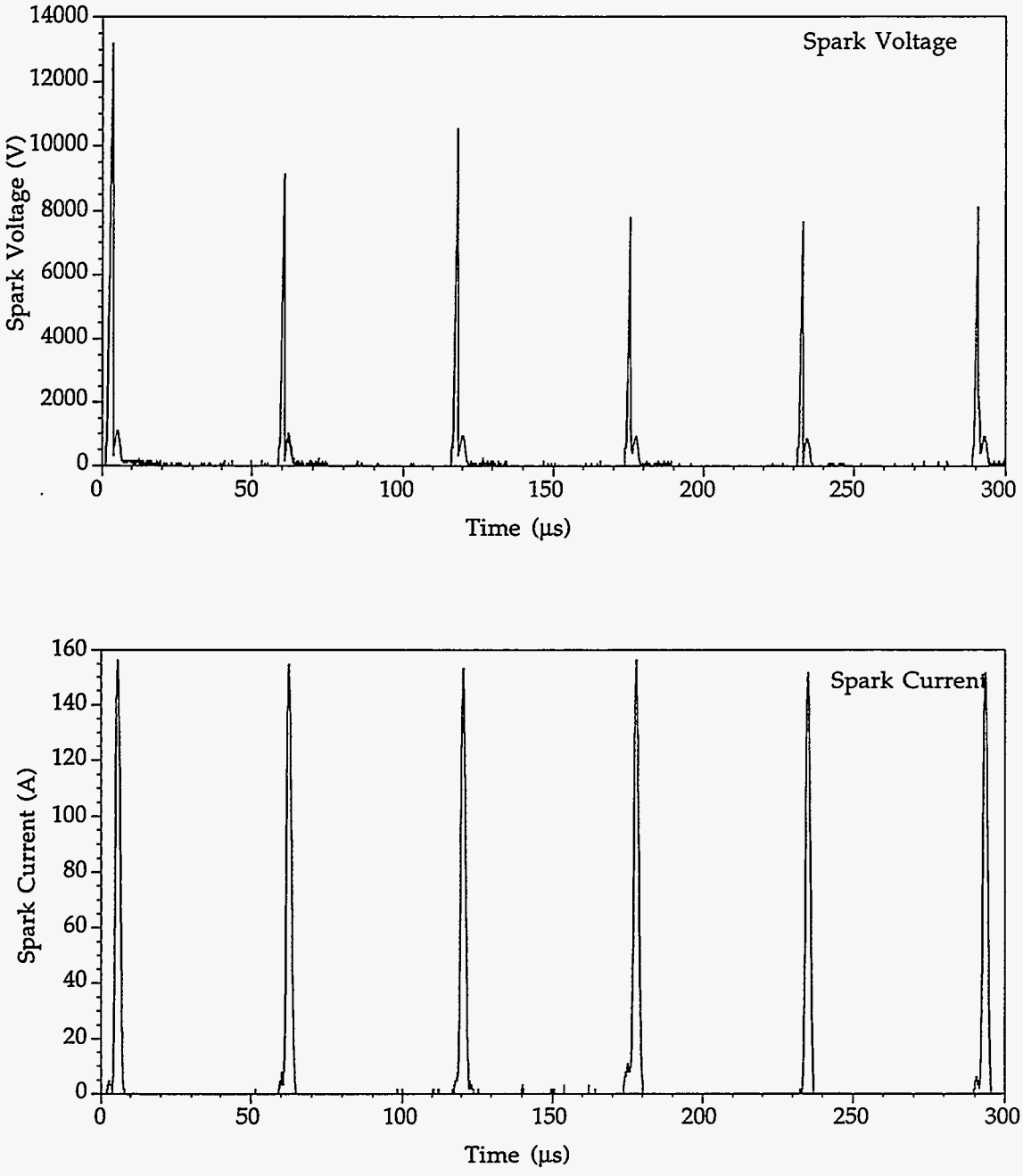

Figure 4.2: Spark Current and Voltage Waveforms for Multistrike PJI During Engine Idle

Continuous use of high ignition energy levels would be expected to cause unacceptably rapid electrode wear. The strategy for using plasma jet ignition would be to temporarily boost the ignition energy during cold starting and early cold running to allow the hydrocarbon emissions to be reduced and to lower the ignition energy to levels similar to those of a conventional ignition system during normal warm running.

4.2 Initial Combustion Startability Experiments

The initial experiments to examine the effects of ignition system changes in combustion stability were carried out by equipping a single cylinder of the engine with the plasma jet ignition system, while the remaining three cylinders operated using conventional ignition. These experiments were intended to provide the information necessary to select appropriate energy and restrike interval configurations for the 4-cylinder plasma jet system. For a comparison test point, the engine was operated under steady-state, cold-idle conditions (25°C coolant) under closed-loop stoichiometric fuel control (lambda = 1.0) using the standard value of spark advance (13° bottom top dead centre [BTDC]) in the original GM controller calibration. For the plasma jet ignition system, a gap width for the recessed surface gap ignitor of 7.5 mm was used, as this had been found to provide a good compromise between ignition performance and breakdown voltage requirements in earlier studies using methanol fuel [19].

As shown in Figure 4.3, the initial results were very encouraging as the plasma jet system provided a substantial reduction in COV values relative to the standard inductive ignition even when a single 150 mJ discharge was used. It was also evident that the degree to which benefits could be realized through additional discharges was strongly influenced by the discharge interval. A shorter interval was obviously better and with the system originally configured to allow a minimum interval of 100 μs, minimum COV values were obtained with three discharges. The system was later modified to decrease the minimum interval to 60 μs, which lowered COV values further and produced reductions in COV for up to six discharges. The observation that COV values tended to increase with higher numbers of discharges is believed to be related to the additional electrical noise that was created. This was detrimental to the stability of the closed-loop fuel control system (a subject discussed in more detail further in this report) and would have led to a net deterioration in combustion stability.

Based on these test results, further experiments using the multistrike plasma jet ignition configuration were carried out using one, three, or six discharges with a 60-μs discharge interval and 150 mJ of stored energy per discharge.

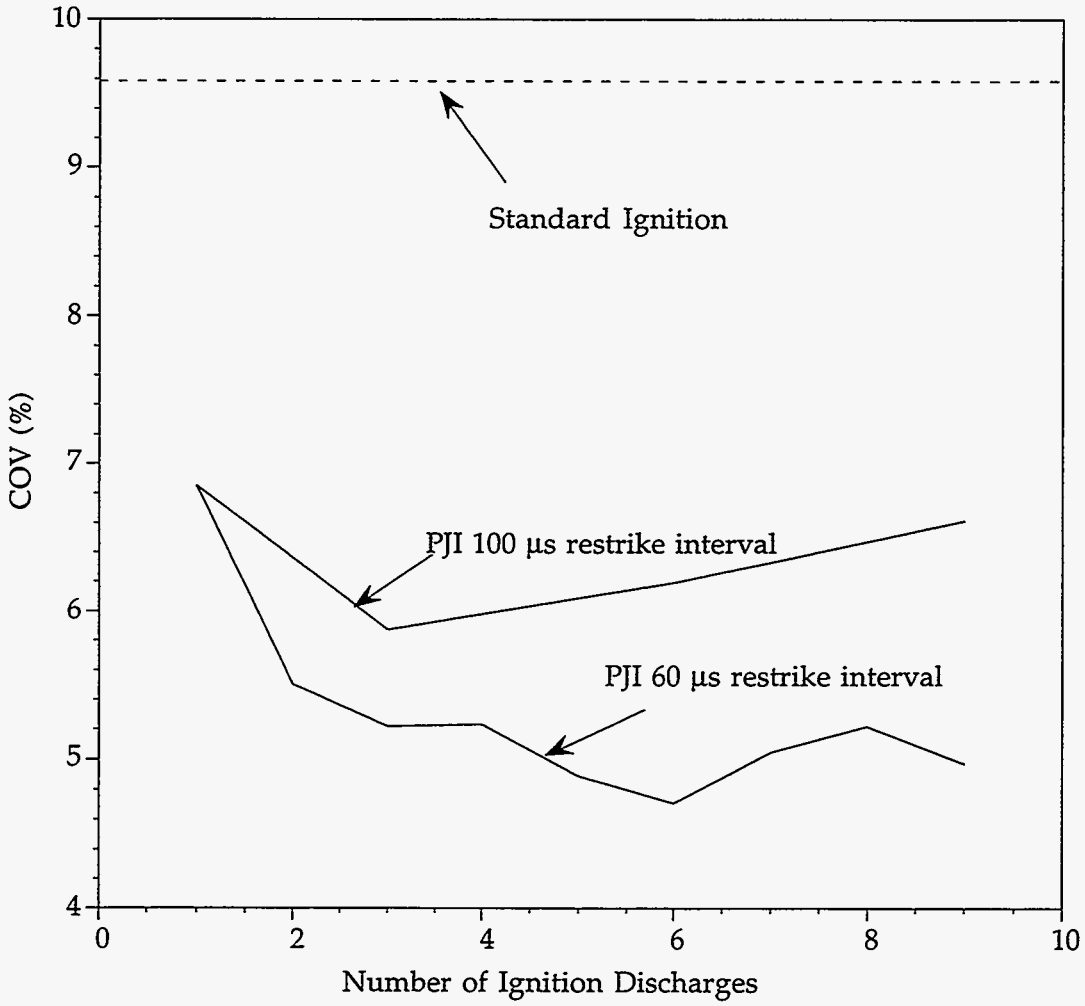

Figure 4.3: Effect of Multistrike PJI Ignition Parameters on COV of IMEP During Cold Idle (Closed-Loop Stoichiometric Operation, 13° Spark Advance)

5. FUEL ETHANOL (E_d85) STEADY-STATE, COLD-EMISSION EXPERIMENTS USING THE GM POWERTRAIN CONTROL MODULE

5.1 Effects of Excess Air Ratio and Spark Advance Using Standard Ignition

Initial emission testing was carried out to characterize the response of the test engine to changes in excess air ratio and spark advance while using the standard inductive ignition system. Figures 5.1 and 5.2 show the effects of these calibration variables on exhaust hydrocarbon concentration, calculated hydrocarbon mass flow rate, COV of IMEP, and exhaust temperature. The excess air ratio ranged from 0.9 to 1.05-1.06 (i.e., approximately 10% rich to 5%-6% lean). The spark advance values included 0° (the most retarded timing possible with the standard PCM), 10° (which was close to the standard calibration value of 13), and 20°.

The hydrocarbon concentration results shown in Figure 5.1 follow the expected trends of lowering concentrations with either greater excess air ratio or reduced spark advance. The fact that a "knee" in the concentration curves appears at near lambda=1 is also normal, as bringing the air/fuel mixture from a rich condition to a stoichiometric condition would be expected to have a greater effect on hydrocarbon concentrations than further enleanment from stoichiometric conditions would have. And, although the effect of spark retard on hydrocarbon concentration is fairly linear when the mixture is 5%-10% rich, the incremental reduction from the 10° to the 0° setting becomes much less than that from the 20° to 10° change when stoichiometric or lean mixtures are used. Also, in the work of Nakayama et al. [2] described earlier, in which 20° advance was the most retarded ignition timing setting used and the air/fuel mixture was 10% rich, an approximately linear relationship was shown between spark advance and hydrocarbon emissions (see Figure 2.4).

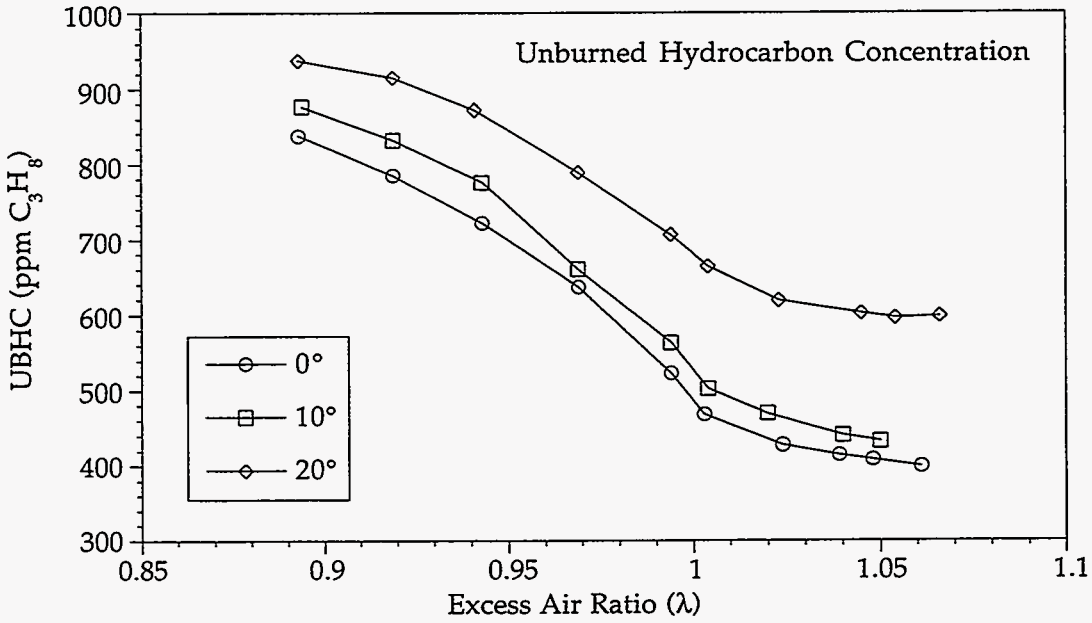

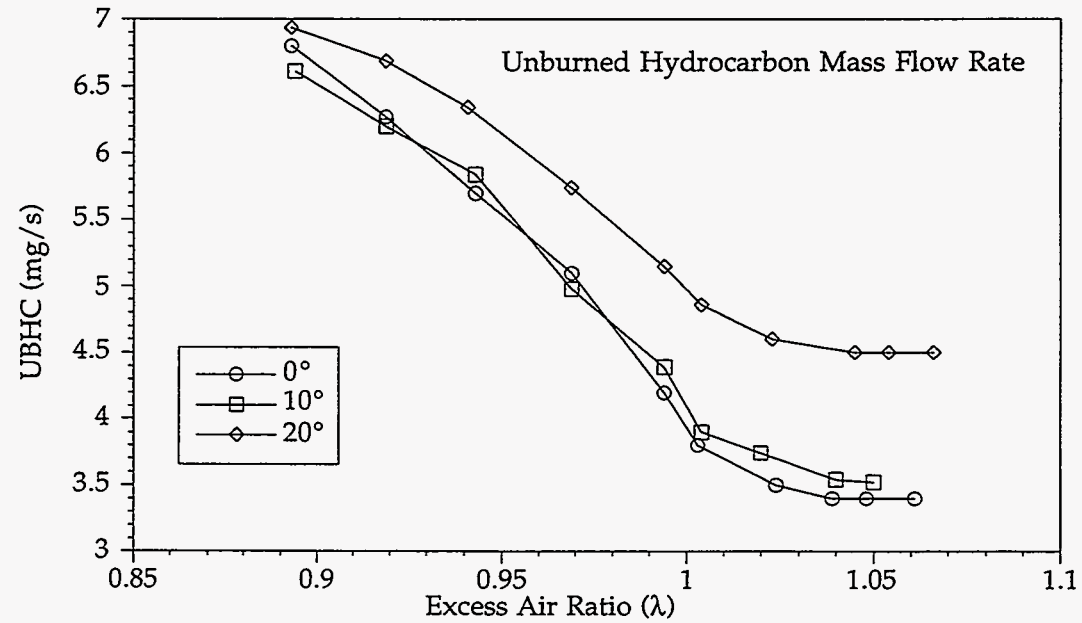

Figure 5.1: Effect of Spark Advance and Excess Air Ratio on Exhaust Unburned Hydrocarbon Emissions (Standard Ignition, E_d85 Fuel)

In cases when either spark timing is retarded or the mixture becomes leaner, the IMEP for a given air flow rate will be reduced. Consequently, the engine's idle air control (IAC) valve will open to provide additional air such that the mass flow rate of air/fuel mixture into the engine increases until a sufficient IMEP is developed to maintain the engine's target idle speed. Increased mixture mass flow into the engine will result in increased exhaust mass flow out of the engine, which will have a detrimental effect on the mass flow rate of unburned hydrocarbons at a given exhaust hydrocarbon concentration. Because it is the cumulative mass of unburned hydrocarbons that ultimately affect the results of the FTP emission test procedure, hydrocarbon mass flow rates were calculated for the tests in this project using measured values of hydrocarbon concentration, air/fuel ratio, and inlet air mass flow.

As shown in Figure 5.1, the detrimental influence of increased air/fuel mixture mass flow requirements caused the relationship between the hydrocarbon mass flow rate curves to differ significantly from those of the concentration curves. Most noticeable is overlap between the 0° and 10° mass flow rate curves for rich mixtures. However, it is clear that a net benefit from spark retard and enleanment was still obtained for stoichiometric and leaner mixtures.

The COV results shown in Figure 5.2 departed from the expected trends in that COV values using 10° spark advance were higher than those at 0°. In addition, the 10° test results showed a much more scattered relationship with excess air ratio. The cause of this behaviour is uncertain but it may have been related to control loop stability problems experienced in tests where the GM PCM was interfaced with the wide-range air/fuel ratio sensor system. (This is discussed in detail later in the report.) Normal COV spark timing behaviour (i.e., COV inversely proportional to spark advance) was recorded in later tests with conventional inductive ignition where improved control loop behaviour was obtained using an aftermarket electronic control system (see Section 8).

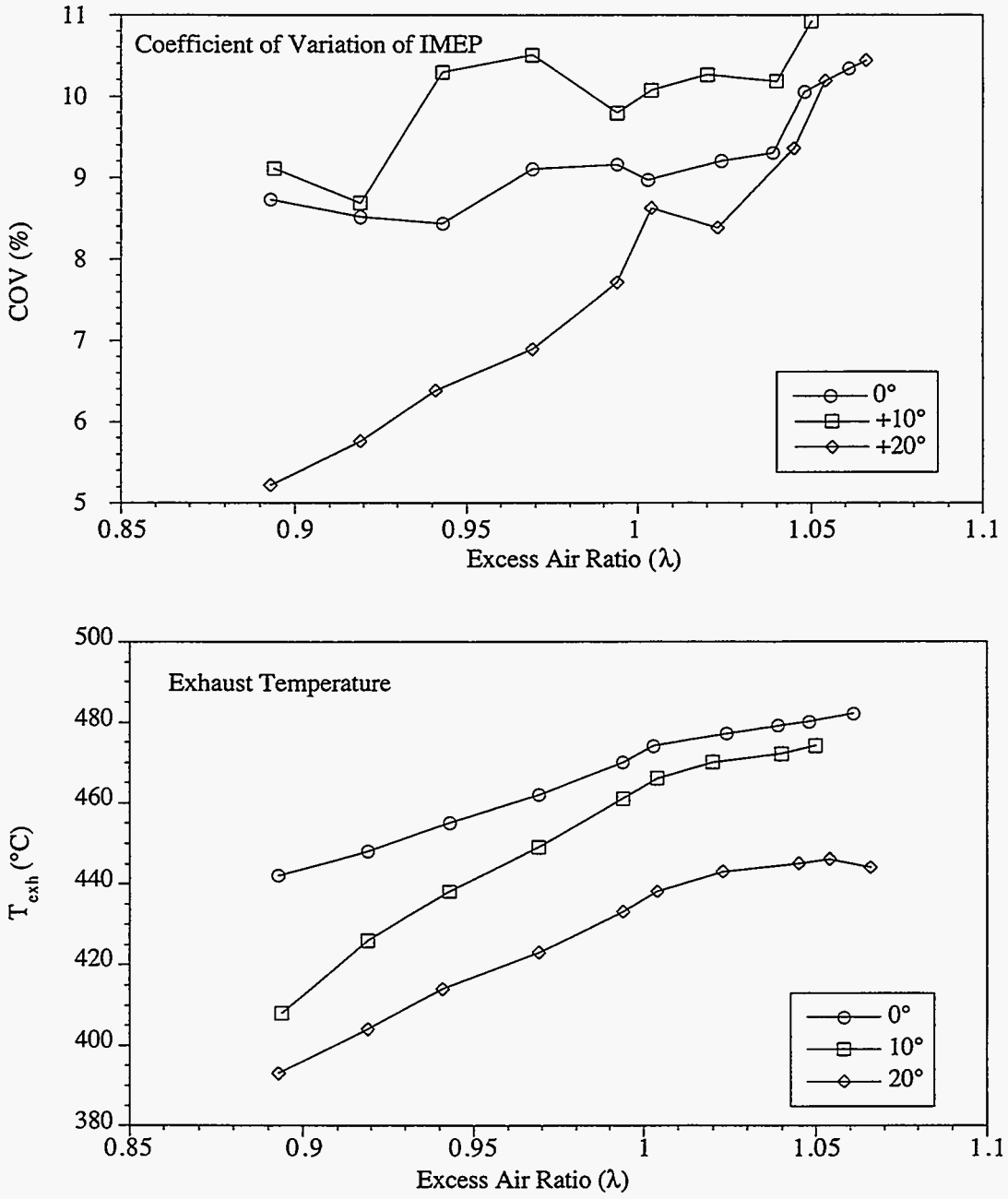

Figure 5.2: Effect of Spark Advance and Excess Air Ratio on COV of IMEP and Exhaust Temperature (Standard Ignition, E_d85 Fuel)

It was only at 20° advance that a pronounced COV versus lambda trend similar to that described by Nakayama et al. [2] was seen. In addition, only the combination of 20° advance and approximately 10% enrichment produced COV values approaching 5%. COV values for all three spark advance settings converged at over 10% at near lambda=1.05.

Reductions in spark advance and increased excess air ratios produced higher exhaust temperatures, as expected. The effect of excess air ratio was smaller at lambda=1 and leaner, where a pronounced change in the slope of the exhaust temperature curves can be seen. The relationship between the curves for each ignition timing reflects that seen earlier for hydrocarbon concentration, with the 0° and 10° values moving closer together as the mixture becomes leaner. In fact, it is probable that exhaust temperature was the "cause" and hydrocarbon concentration was the "effect", as the strong relationship between exhaust temperature and the post-combustion oxidation of unburned hydrocarbons is well documented [41].

5.2 Experimental Difficulties with the Plasma Jet Ignition System

As described earlier, single-cylinder testing of the plasma jet ignition system had previously produced substantial reductions in COV relative to the standard ignition system. However, the initial testing of the 4-cylinder version of the plasma jet system revealed two problems that prevented similar improvements from being achieved in these experiments. These problems involved ignitor breakdown voltage requirements and electrical noise interference with the air/fuel ratio control system.

In the single-cylinder experiments, recessed surface gap ignitors with 7.5-mm gap lengths were used. This gap size was selected based on our earlier research with methanol-fuelled engines [19] and had been used successfully for some time in our neat methanol (M100) engine program. However, it was found that in testing with fuel ethanol, the ignitors rapidly experienced increases in the voltage required for spark breakdown. This problem was worst with

ignitors fabricated using a tungsten alloy ground electrode, but was experienced to an unacceptable degree by ignitors with steel and inconel electrodes as well.

The greatest difficulties occurred while the engine was being started, when spark breakdown voltage requirements are normally highest. Although the ignitors would normally break down at 16-20 kV under this condition, ignitors used with fuel ethanol developed breakdown voltage requirements that frequently exceeded the 27-28 kV available from the ignition system. Even when the engine could be started, breakdown voltages in excess of 20 kV could be required at idle; this sustained operation at high breakdown voltage caused severe electrical noise problems.

The reasons why such problems were experienced with fuel ethanol but not previously with methanol are uncertain at this time. It is believed to be related to the fuel ethanol's effects both on the surfaces of the metal electrodes (as indicated by the influence of electrode material charges) and on the surface discharge path of the ceramic cavity of the recessed gap ignitors. Methanol has relatively high electrical conductivity and tends to "short circuit" spark plugs or ignitors [4]. This can be overcome by supplying high currents to the ignitor prior to breakdown, thereby achieving a fast voltage risetime at the gap so that breakdown voltage is reached before excessive energy is lost via the short-circuit path [4]. We have used this approach successfully in earlier M100 subzero cold-starting work in which severe ignitor wetting would take place [15,17] and the ≈2-μs, 0-20 kV risetime of the plasma jet circuit used in this study should have been more than adequate to deal with that type of problem.

In contrast, ethanol is usually not significantly conductive unless badly contaminated with ionic material [4]. This avoids spark plug shorting problems, but in the case of surface gap ignitors, may lead to a gap insulating effect if the ceramic surface becomes wetted with ethanol; that is, additional voltage is required to arc through the insulating layer of ethanol on the ceramic surface between the high-voltage and ground electrodes. Gasoline also has low conductivity, but the lower required fuel quantities (which would reduce wetting effects) and the tendency to create conductive carbon deposits on the ceramic surface may avoid a problematic insulating effect. Too few gasoline tests were carried out in this project to reach any conclusions regarding

its relative compatibility with surface gap ignitors compared with that of methanol and ethanol. We have, however, used gasoline and a different plasma jet ignition apparatus in earlier work without experiencing such problems [18].

In order to reduce ignitor breakdown voltage requirements to acceptable values for fuel ethanol tests, new ignitors were fabricated, with the gap length reduced to 5.0 mm from 7.5 mm. It was known from previous work that this would reduce the effectiveness of the ignitor at a given energy level [19], but substantial improvements over standard ignition could still be expected if sufficient energy was used. However, this expectation was based on experience using single, high-energy discharges rather than low-energy, multistrike approaches.

Even with the 5.0-mm ignitors, electrical noise (electromagnetic and radio frequency interference, EMI and RFI) from the 4-cylinder plasma jet ignition system was found to affect the air/fuel ratio control loop of the GM PCM. This was due in part to a failure to implement adequate noise suppression measures with the plasma jet system. A contributing factor was likely the unusually high EMI/RFI susceptibility of the test bed control module setup where the removable EPROM module was mounted remotely from the main PCM circuit and connected via an unshielded ribbon cable.

In addition, even the baseline control loop stability of the apparatus while using the standard ignition system was not good under cold-idle conditions. The GM control system has a highly sophisticated proprietary EGO sensor closed-loop control algorithm. However, this algorithm is "tuned" to the complex waveform characteristics normally produced by conventional EGO sensors. The simulated EGO signal produced by the wide-range air/fuel ratio sensor apparatus was a much simpler high/low switching waveform (i.e., essentially digital rather than analog like a true EGO signal) with which the GM control algorithm did not function well. The GM algorithm was also intended to make rapid corrections in air/fuel ratio to maintain stoichiometric mixtures during transient driving conditions. Under cold-idle conditions in which the engine stability is extremely sensitive to small air/fuel ratio variations, a slower, more stability-oriented control loop strategy would likely be required.

The differences in control loop characteristics between the standard and plasma jet ignition systems are shown in Figures 5.3 and 5.4. For the examples for closed-loop stoichiometric operation in Figure 5.3, the lambda value for the standard ignition system fluctuates approximately ±2.5% about lambda=1.0. With the plasma jet ignition system, excursions of up to about ±4% occur. The fluctuations are reflected in variations in IMEP and engine speed.

In Figure 5.4, it can be seen that the situation for plasma jet ignition worsened when lean, closed-loop operation was used. Whereas the control loop widened slightly to about ±3% with the standard ignition, excursions of up to 8% could occur with the plasma jet system. These differences in control loop behaviour were likely to have strongly influenced the results of the experiments that were carried out using the GM PCM for fuel control.

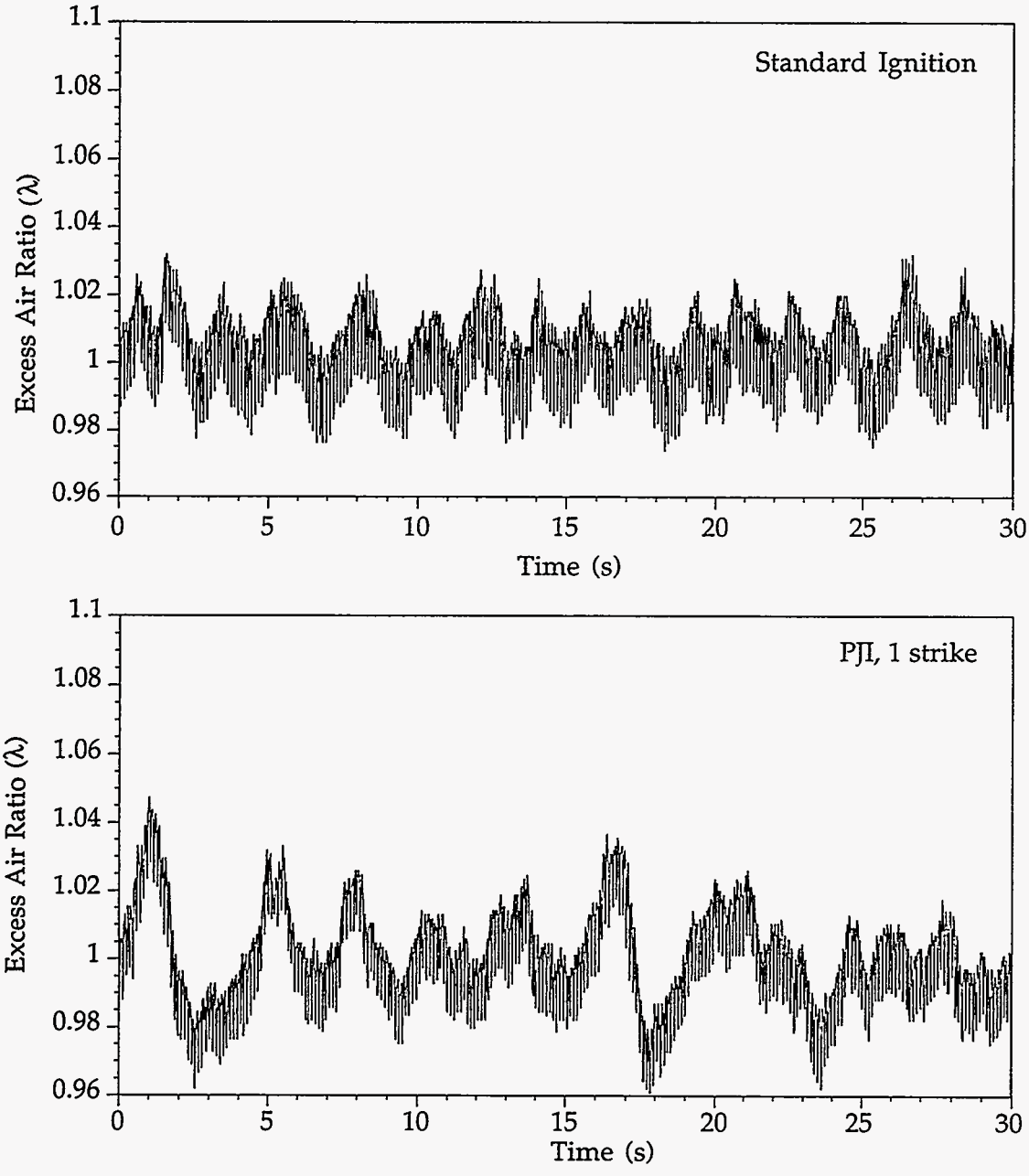

Figure 5.3: Comparison of UEGO Sensor λ Waveforms During Closed-Loop Stoichiometric Operation

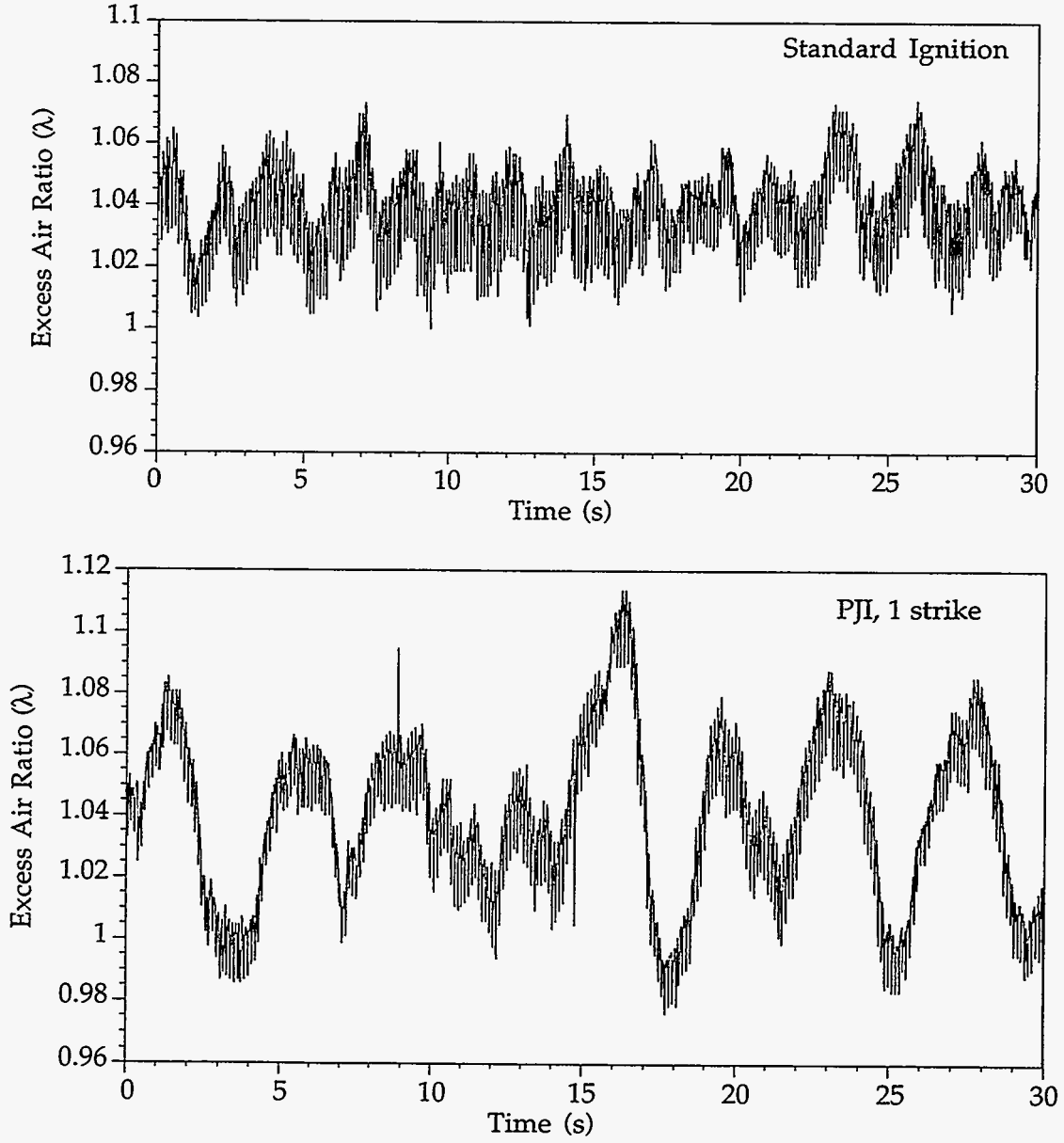

Figure 5.4: Comparison of UEGO Sensor λ Waveforms During Closed-Loop Lean Operation

5.3 Ignition System Comparison at 0° Spark Advance

Because the standard inductive ignition system had produced its lowest hydrocarbon emissions when its minimum spark advance value was used, this spark advance value was selected for detailed comparisons between the standard and plasma jet ignition systems. The results of these experiments are shown in Figures 5.5 and 5.6. For the plasma jet ignition system, only lambda values of 1.0 or leaner were tested, as avoiding the use of rich mixtures was a key part of the emission reduction strategy. Plasma jet ignition settings of one strike (150 mJ), three strikes (450 mJ), and six strikes (900 mJ) were used.

As shown in Figure 5.5, all ignition setups showed similar trends with increasing lambda values. Reductions in both unburned hydrocarbon concentrations and mass flow rates were shown for the plasma jet ignition system. This was not expected because provided that the standard ignition did not experience misfiring (no misfiring was observed), a stronger ignition source would be expected to offer little reduction of hydrocarbon emissions and would serve mainly to reduce the COV levels. In fact, a stronger ignition source would tend to encourage earlier burning of the mixture (similar to advancing the spark timing) and lead to some increase in hydrocarbon emissions at a given lambda and spark-timing setting.

This trend can be seen when the three plasma jet energy levels are compared, as hydrocarbon emissions were slightly higher with three or six strikes than with a single discharge. The fact that all of the plasma jet hydrocarbon results were lower than the standard ignition results may have been related to the differences in air/fuel ratio control loop characteristics discussed earlier. The greatest hydrocarbon reductions relative to the standard ignition occurred as the mixture became leaner; this is consistent with the relatively wider control loop fluctuations experienced while using plasma jet ignition under lean control loop control.

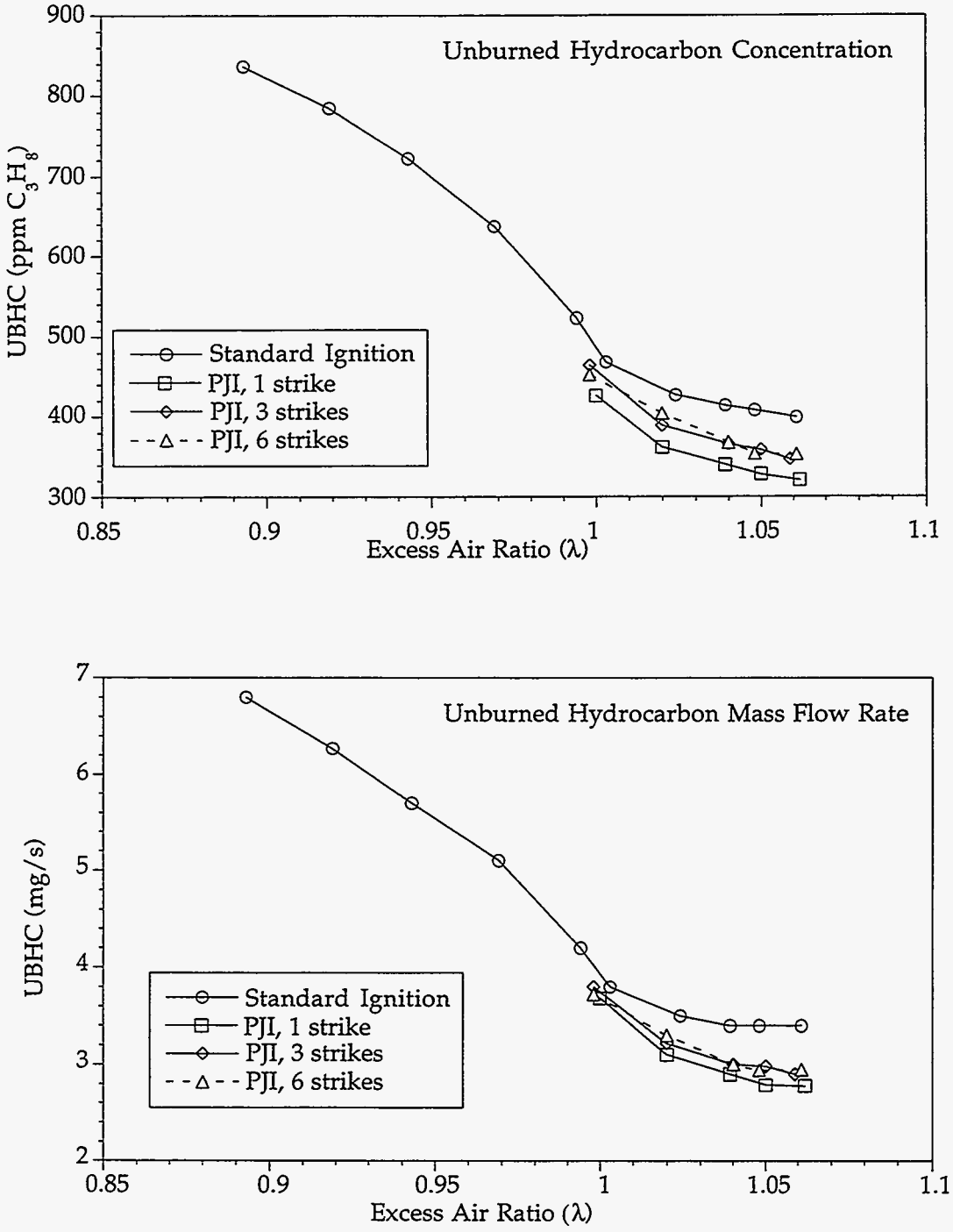

Figure 5.5: Ignition System Comparison at 0° Spark Advance Using E85 Fuel - Effects of Excess Air Ratio on Exhaust Unburned Hydrocarbon Emissions

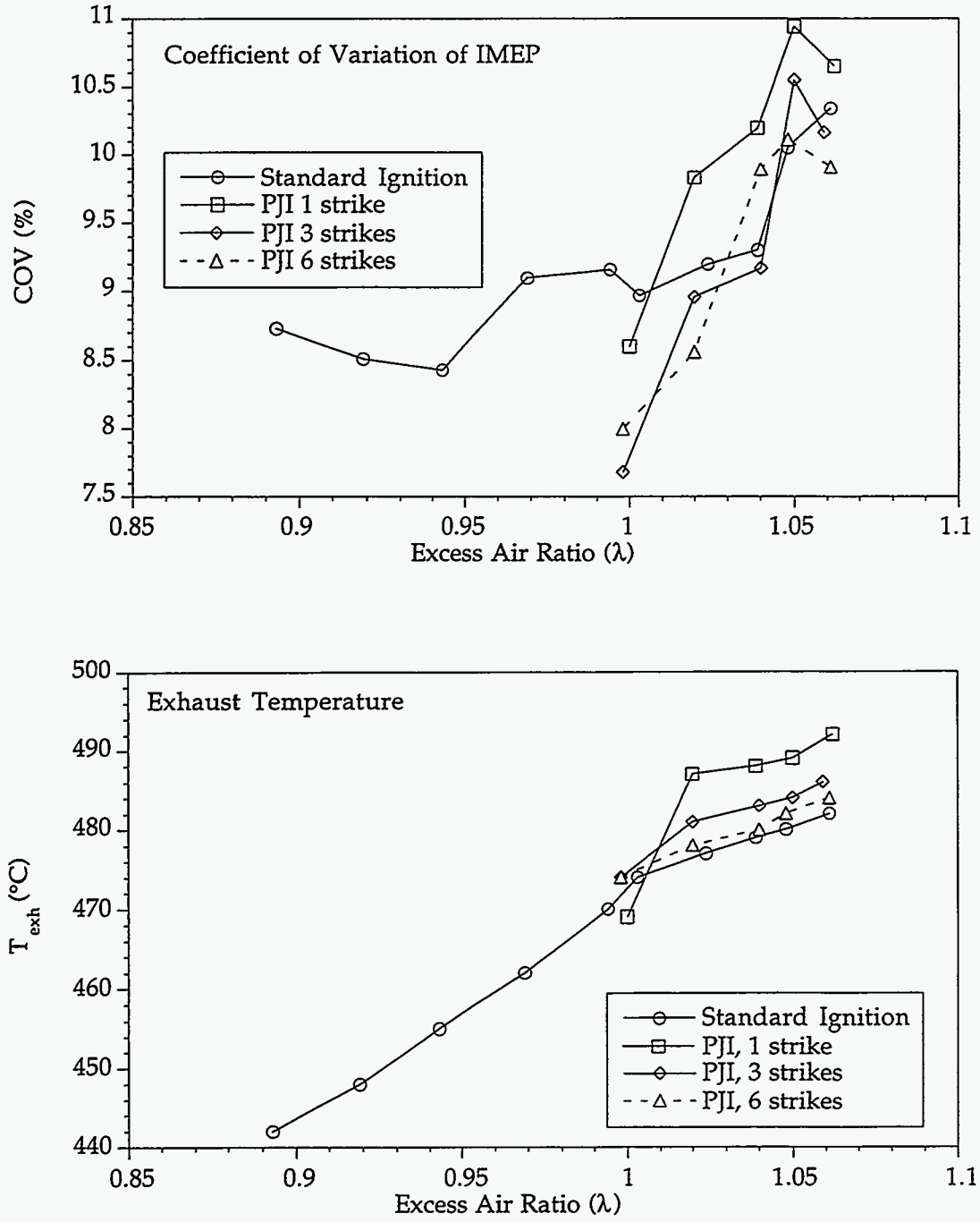

Figure 5.6: Ignition System Comparison at 0° Spark Advance Using E_d85 Fuel - Effects of Excess Air Ratio on COV of IMEP and Exhaust Temperature

The greater air/fuel fluctuations may have had a positive effect on hydrocarbon emissions with plasma jet ignition, but were also probably responsible for increasing COV levels. As shown in Figure 5.6 at lambda=1.0, the plasma jet system produced reductions in COV levels relative to the standard ignition system, but the improvements were much less than the earlier single-cylinder results using larger ignitor gaps. The fact that COV improvements were obtained despite a degraded air/fuel ratio control loop is significant. However, at leaner excess air ratios where further control loop degradation occurred, the single-discharge PJI results became inferior to standard ignition, while the three- and six-strike results were similar to standard ignition values.

The exhaust temperature results in Figure 5.6 are somewhat unusual, as almost all of the plasma jet results were higher than the corresponding standard ignition values. Earlier burning from an enhanced ignition source would be expected to produce lower exhaust temperatures. Whereas the hydrocarbon results using three and six-strikes with PJI were almost identical, exhaust temperatures with six strike PJI were closer to the standard ignition values than to the three-strike PJI values. This would indicate that factors in addition to exhaust temperature had influenced the hydrocarbon results. Again, variations in the air/fuel ratio control loop may offer the most likely explanation.

5.4 Effects of Excess Air Ratio and Extreme Spark Retard Using Plasma Jet Ignition

Despite the control loop stability problems experienced while using plasma jet ignition, it was apparent that the engine was not operating at or near its misfiring or stalling limit with 0° spark advance. Additional circuitry was added to the apparatus to delay the trigger pulse from the GM coil drivers that provided the spark timing signal for the plasma jet system. With this setup, spark-timing values as late as 30° after top dead centre (ATDC) could be explored. We have called the region of spark timing settings after TDC (i.e., during the expansion stroke while the piston is descending) "extreme spark retard." Because the normal way of defining spark timing is as spark advance BTDC, the extreme spark retard settings have negative advance values. Thus, for the remainder of this report, spark-timing values occurring during the compression stroke are identified as a positive value indicating degrees before TDC, whereas spark timing values occurring during the expansion stroke are identified as negative values indicating degrees after TDC.

Figures 5.7 to 5.10 show experimental results for the plasma jet ignition system using six strikes over a spark timing range of 0° to -30° and a lambda range of 1.0-1.05. Results from the standard ignition system with 0° spark timing are also shown for comparison. The experiments were conducted as lambda "sweeps" at fixed spark-timing settings and are plotted in this manner (i.e., as a function of lambda) in the upper graph of each figure. In the lower graph of each figure, the results were replotted as a function of spark timing, which provides a clearer picture of trends resulting from varying lambda and spark-timing combinations.

As shown by the hydrocarbon concentration and mass flow results in Figures 5.7 and 5.8, the use of extreme spark retard proved to be a highly effective strategy for reducing hydrocarbon emissions. For both the hydrocarbon concentration results and the hydrocarbon mass flow results, the lowest levels observed were under 10% of their respective values for 0° spark timing. From the plots showing the effects of spark timing, it can be seen that emissions dropped rapidly as the spark was retarded up to a value of -20° to -25°, depending on the excess air ratio. When the increased mixture mass flow requirements from spark retard are accounted for, hydrocarbon mass flow is determined (Figure 5.8), and the same trends remain. The hydrocarbon mass flow rates showed the same trends as the hydrocarbon concentrations, despite the fact that the spark retard increased mixture mass flow requirements.

In analyzing the results shown as a function of spark timing in Figure 5.8, several features are apparent that relate to the selection of optimum lambda and spark-timing combinations. For these tests, providing a small amount of excess air (lambda=1.02) caused a substantial drop in emissions, whereas enleanment from lambda=1.04 to 1.05 yielded little further benefit. In practice, one strategy might be to select calibration values that did not produce the potential minimum hydrocarbon emission values, but rather allowed a slightly higher hydrocarbon value so that less spark retard or enleanment could be used. In this particular case, it can be seen that similar results could be obtained with combinations of either lambda=1.02/-30° or lambda=1.04/-20°. The selection would depend on whether it was desirable to minimize either lambda or spark retard to provide a stalling or driveability safety margin.

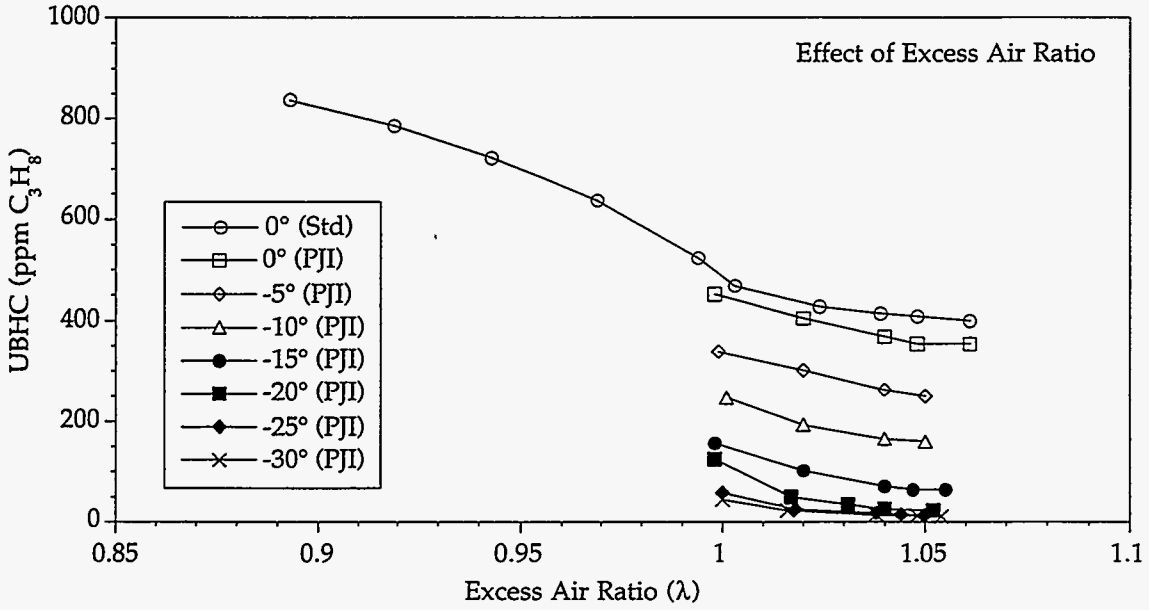

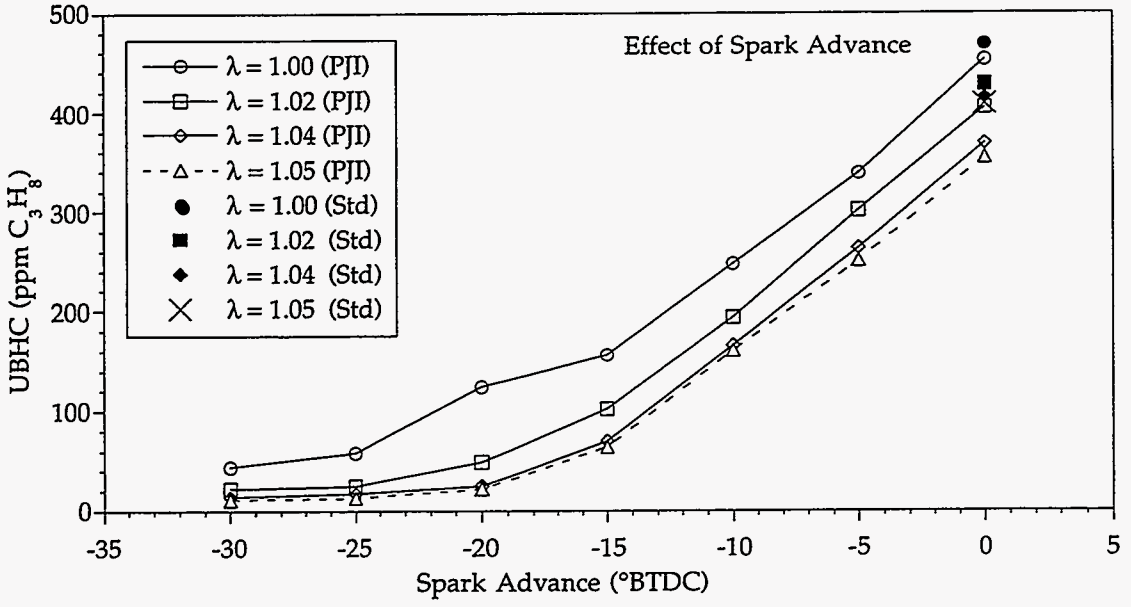

Figure 5.7: Effects of Spark Advance and Excess Air Ratio on Unburned Hydrocarbon Concentration (Standard Ignition, PJI with six strikes, E_d85 Fuel)

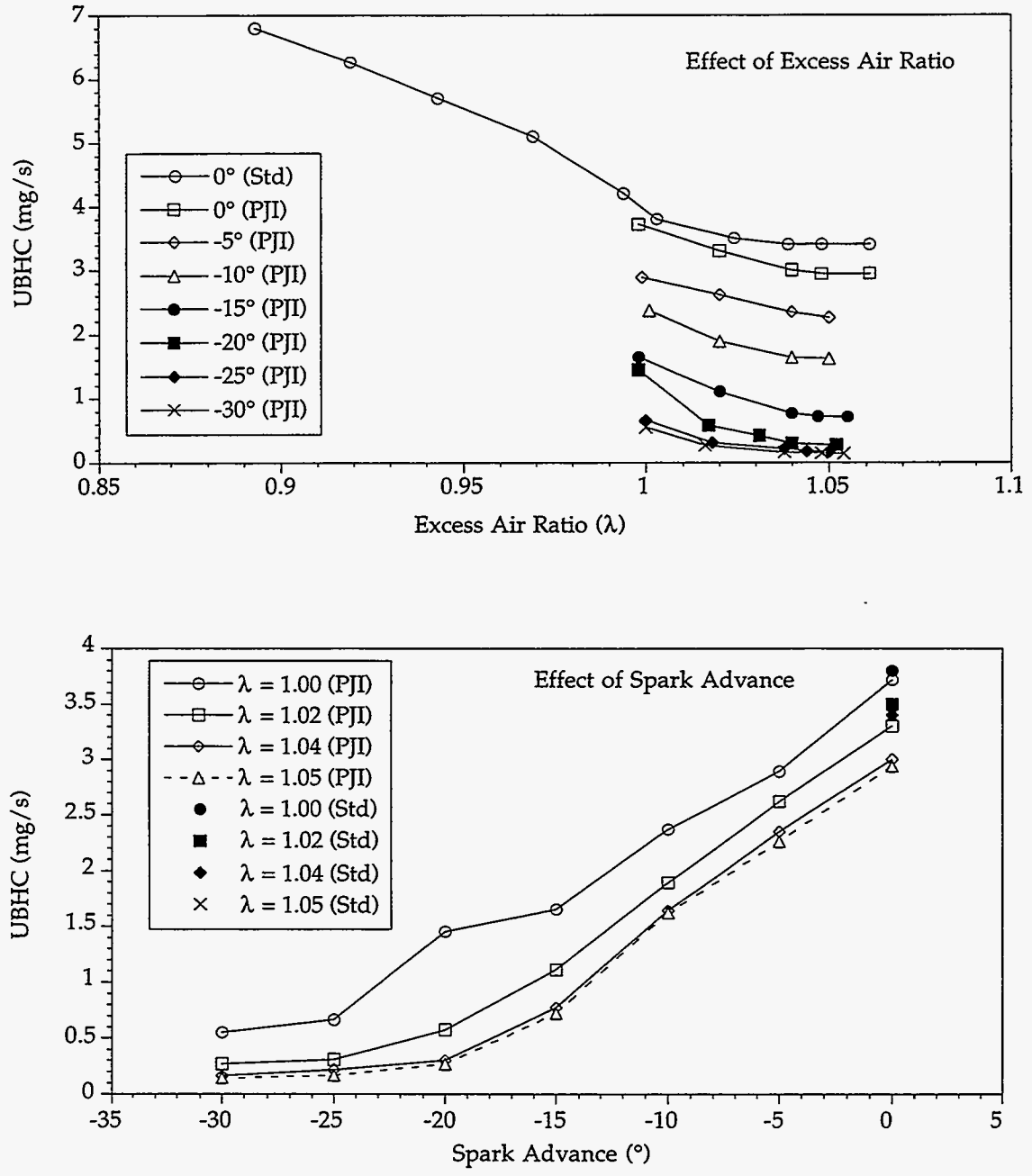

Figure 5.8: Effects of Spark Advance and Excess Air Ratio on Unburned Hydrocarbon Mass Flow Rate (Standard Ignition, PJI with six strikes, E_d85 Fuel)

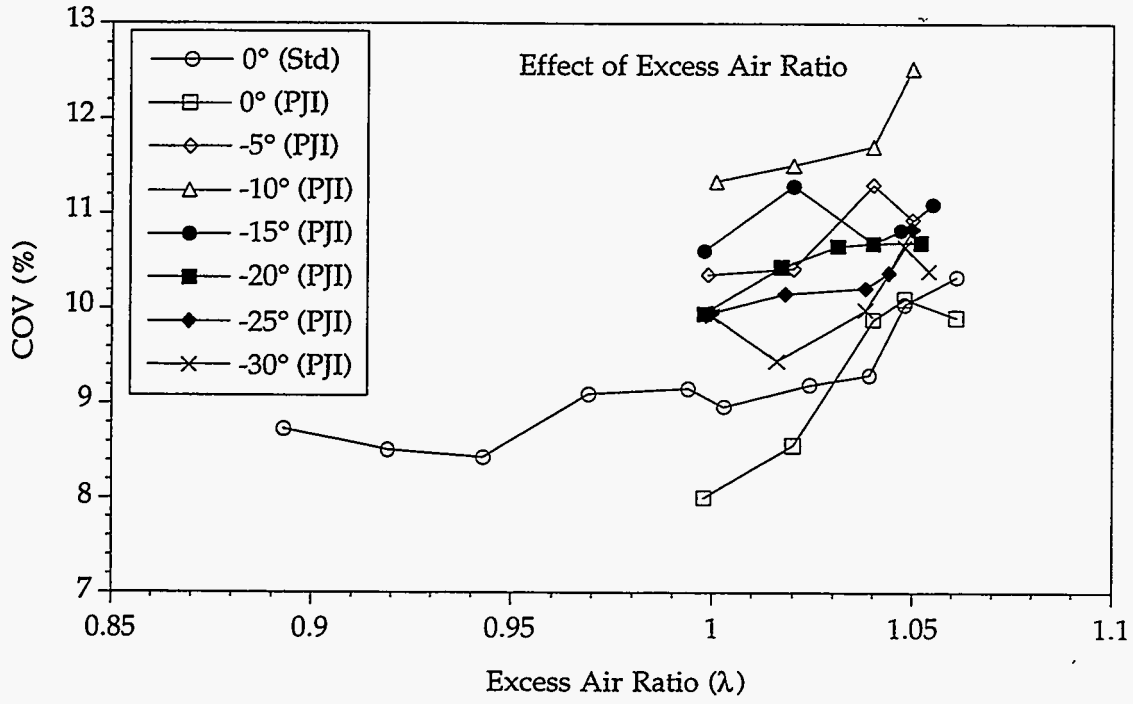

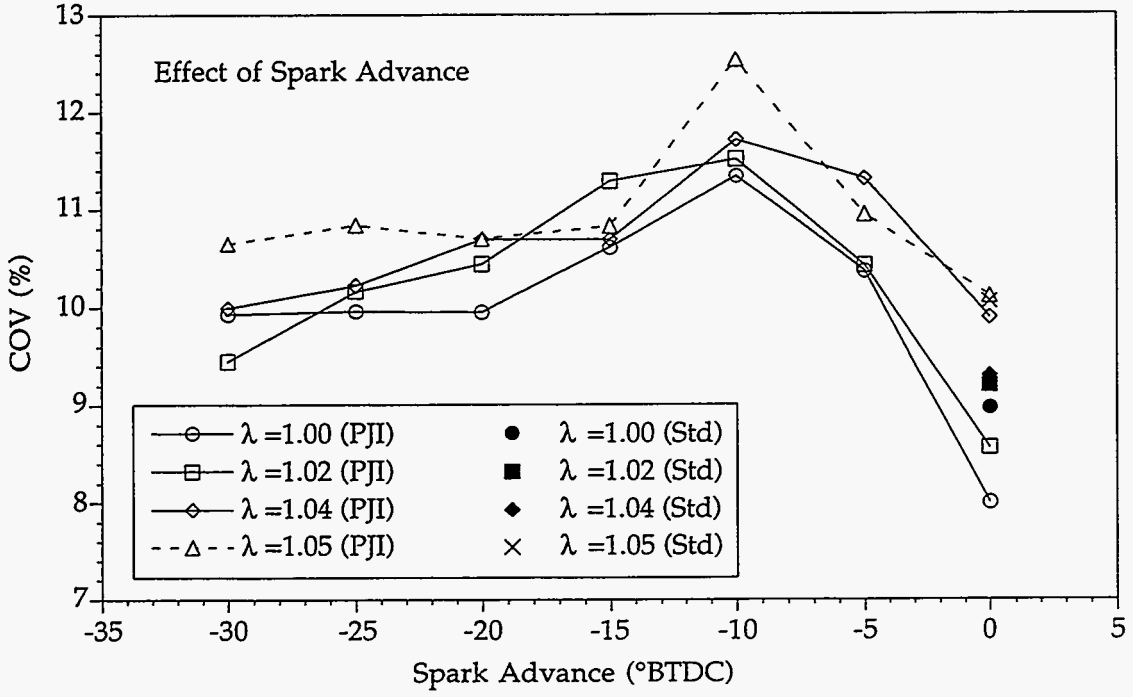

Figure 5.9: Effects of Spark Advance and Excess Air Ratio on COV of IMEP (Standard Ignition, PJI with six strikes, E_d85 Fuel)

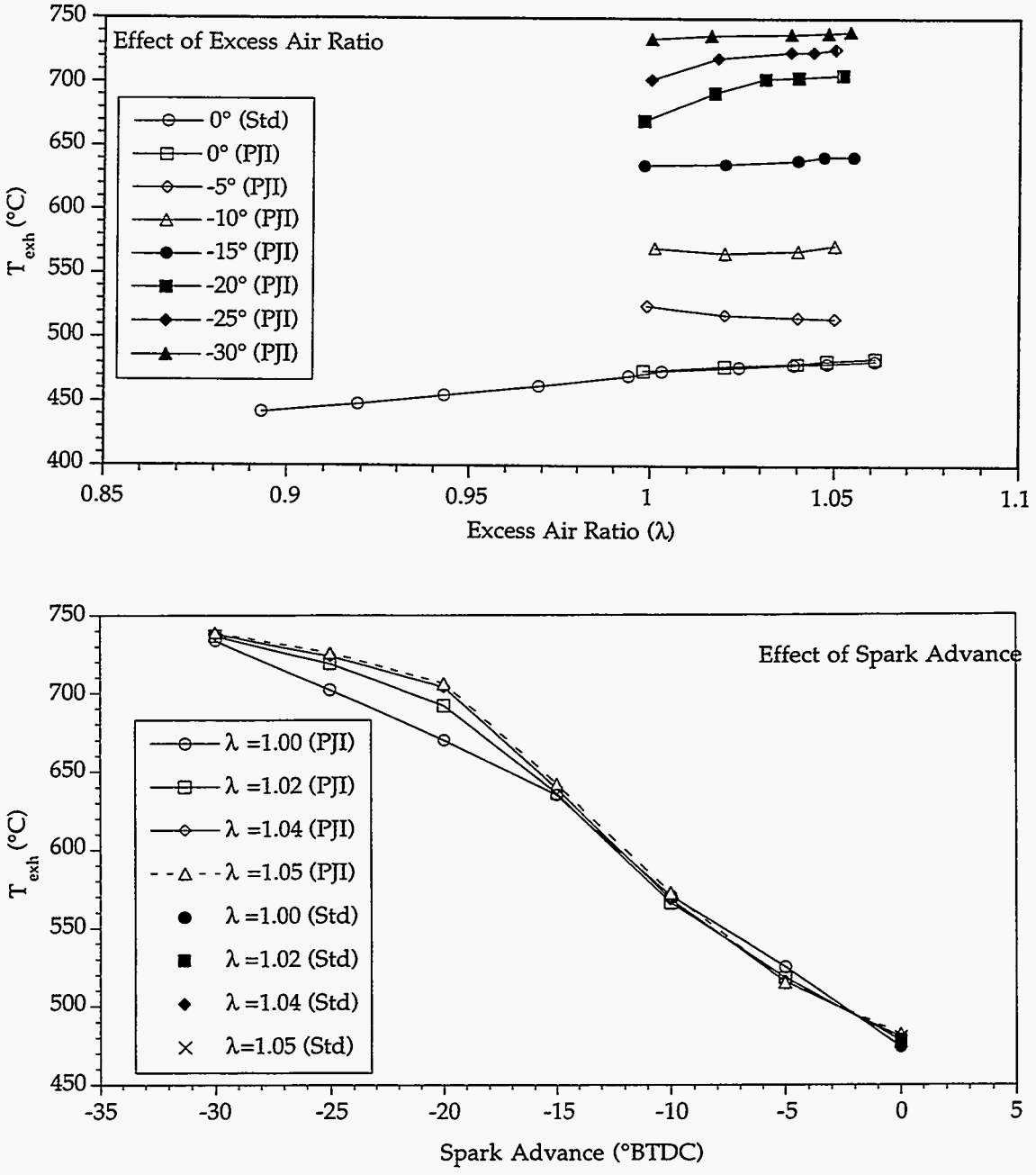

Figure 5.10: Effects of Spark Advance and Excess Air Ratio on Exhaust Temperature (Standard Ignition, PJI with six strikes, E_d85 Fuel)

In the COV comparison of Figure 5.9, the trends are unclear when the results are plotted as a function of lambda, due to overlap between all results except those at 0° and -10° spark timing. However, an interesting trend emerges when the results are replotted as a function of spark timing. Rather than the COV always rising with the spark timing retard as expected, a rise in COV was observed only until -10°. Further spark retard to -15° caused a drop in COV in all cases, whereas changing the spark timing between -15° and -30° appears to have had relatively little effect on COV. In this region, COV values were still about 10% or greater and so were much higher than desirable.

At the time this report was written, the authors were aware of no published cold-emission test data using such highly retarded spark timings. One recent reference [42] that includes no COV results describes reductions in catalyst light-off time using spark-timing settings as retarded as -8° to -9°. Perhaps earlier researchers were deterred from exploring the spark-timing region beyond -10° by the rising COV values experienced up until that point and the assumption that COV values would continue to rise with further spark retard. A recent patent assigned to Ford [43] describes an adaptive learning system for controlling the spark advance and air/fuel ratio of an engine immediately after cold starting but does not specify the range of spark-timing values being used. This may indicate that Ford's proprietary research in this area has explored extreme spark retard settings.

In the exhaust temperature comparisons of Figure 5.10, it can be seen that the use of extreme spark retard could increase exhaust temperatures by over 250°C relative to the 0° timing values. This would be expected to shorten catalyst light-off time considerably. As clearly shown in the results plotted as a function of spark timing, lambda values had little effect compared with spark timing in the range from 0° to -15°. The use of stoichiometric mixtures resulted in significantly lower exhaust temperatures at -20° and -25° spark timing. For all lambda values except stoichiometric, the reduction in the slope of the exhaust temperature curve (i.e., the onset of diminishing returns in exhaust temperature for further amounts of spark retard) occurred at about -20°. Thus, taking into account the earlier hydrocarbon emission values, a spark-timing

setting at least as retarded as -20° appeared to be necessary to approach the potential minimum hydrocarbon and maximum exhaust temperature values.

6. DENATURED ETHANOL (E99) STEADY-STATE, COLD-EMISSION EXPERIMENTS USING THE GM POWERTRAIN CONTROL MODULE

Limited experiments were carried out with ethanol denatured with 1% gasoline (E99) in order to provide a preliminary assessment of the effects of ignition system and calibration changes while using neat alcohol fuel. The experiments included a comparison of the standard and plasma jet ignition systems at 0° spark timing and testing of the plasma jet ignition system at -20° spark timing. The results of these experiments are shown in Figures 6.1 and 6.2.

In the 0° timing comparison, the emission trends with respect to lambda were similar to those observed using E_d85, as hydrocarbon emissions fell gradually with increasing lambda values. The relative ranking of the different ignition setups was slightly different. Whereas all the PJI setups had produced lower hydrocarbon emissions at a given lambda value while using E_d85, while using E99, the three- and six-strike PJI setups produced slightly higher hydrocarbon mass flow rates compared with the standard ignition system. These differences between fuels may not be significant in light of the control loop stability variations discussed earlier. With E99, the combination of -20° spark timing, PJI and lean lambda values resulted in a large reduction in hydrocarbon emissions as with E_d85, although the minimum concentration and mass flow rates reached were higher with E99 versus E_d85. This may simply be related to the lower volatility (therefore, poorer vaporization) of the near-neat ethanol fuel.

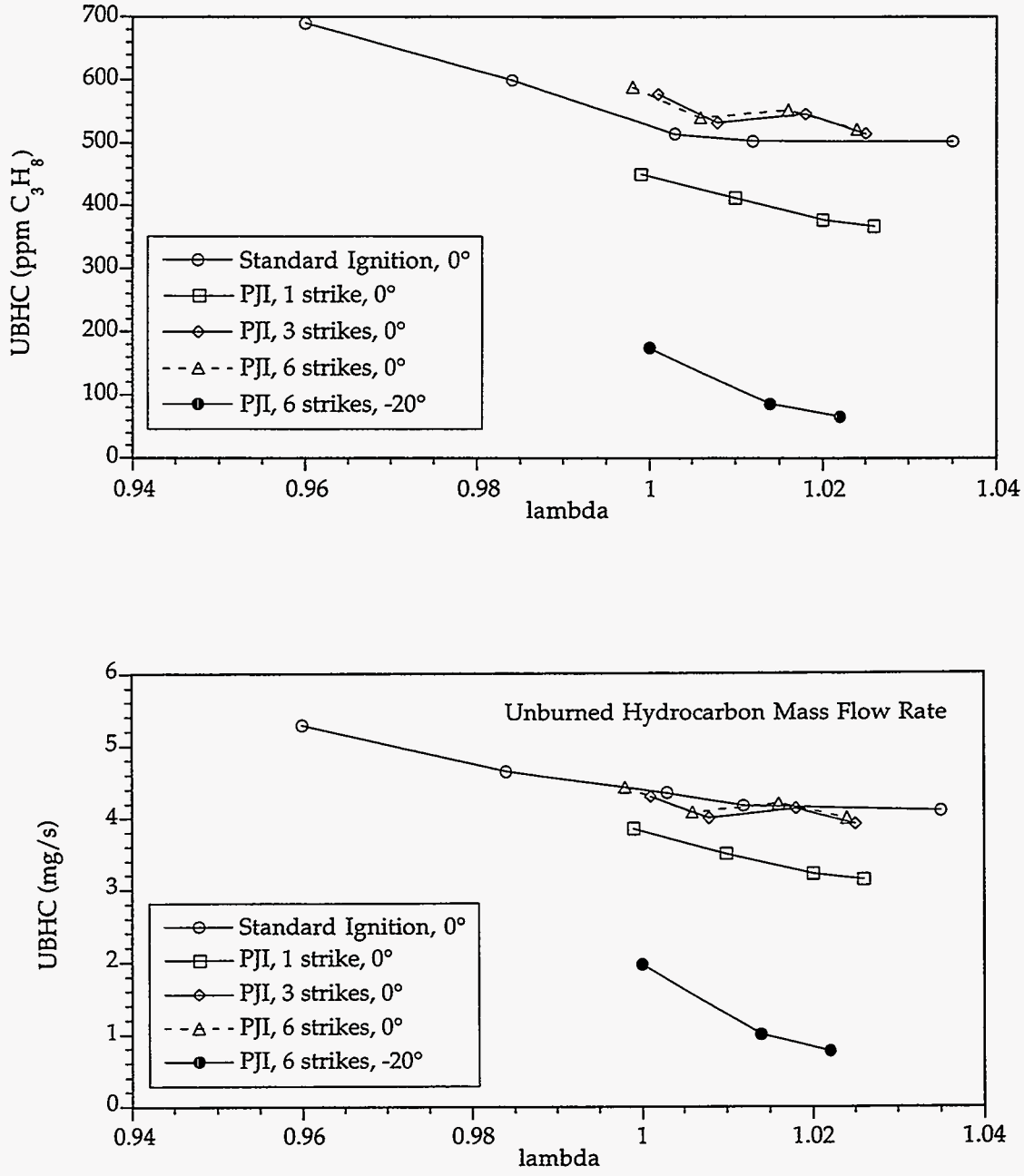

Figure 6.1: Ignition System Comparison Using E99 Fuel - Effects of Excess Air Ratio and Spark Advance on Exhaust Unburned Hydrocarbon Emissions

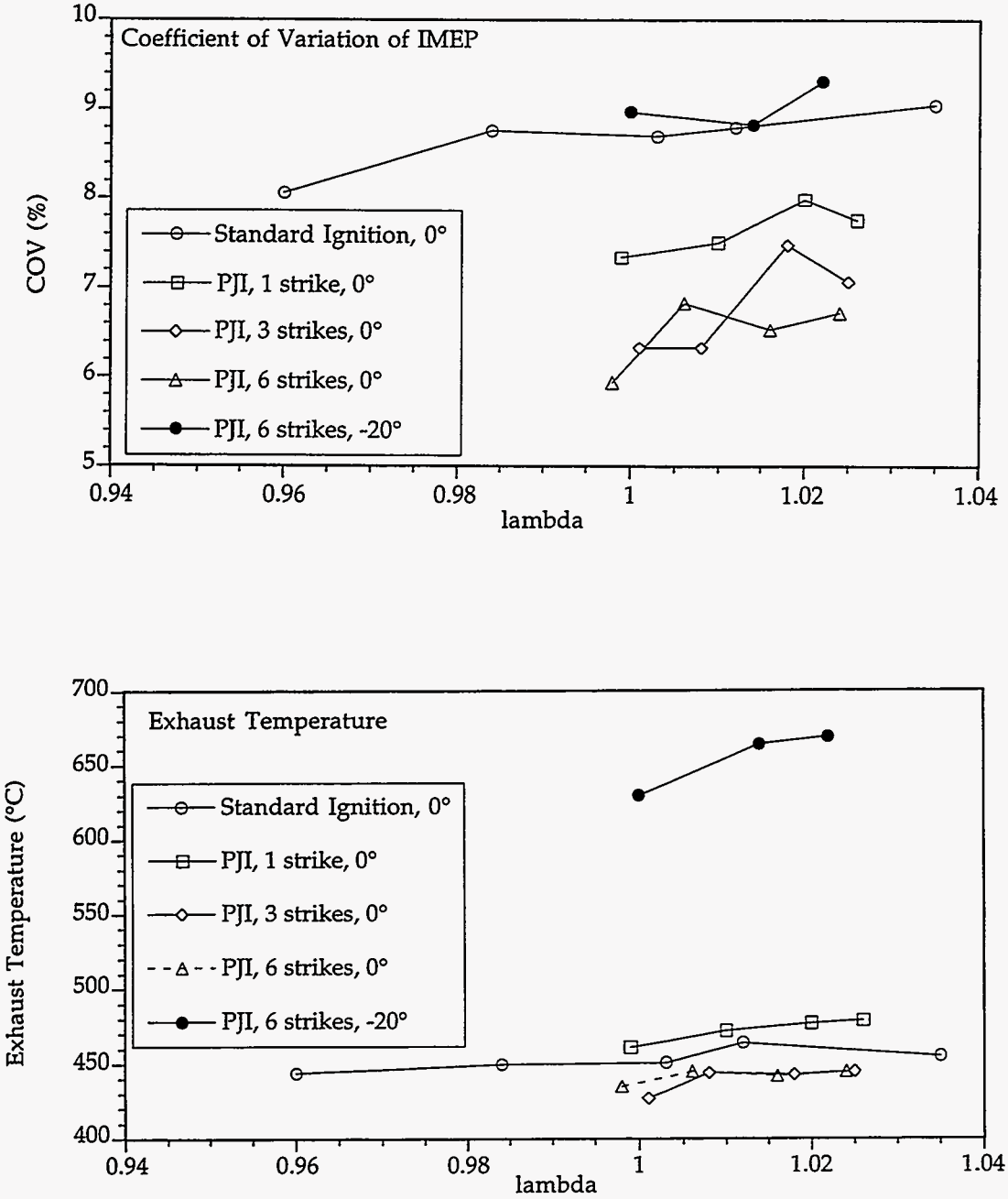

Figure 6.2: Ignition System Comparison Using E99 Fuel - Effects of Excess Air Ratio and Spark Advance on COV of IMEP and Exhaust Temperature

The COV results while using E99 showed an advantage for the plasma jet system, as COV values were lower than standard ignition values while using one, three, or six discharges. As in the earlier work, the three- and six-strike settings gave similar COV values that were lower than with the single-strike setting. It is interesting to note that the PJI/six-strike COV values using -20° spark-timing were similar to the standard ignition, 0° spark timing values. That is, as the spark timing was retarded from 0° to -20° with six-strike PJI, the COV deteriorated to about the standard ignition values at 0° timing.

The exhaust temperature results for E99 showed a more consistent ranking between ignition setups with respect to the hydrocarbon concentration results than the earlier E_d85 results, as higher exhaust temperatures correlated with lower hydrocarbon concentrations in each case. With the spark timing retarded to -20°, while using PJI and six strikes, the exhaust temperature increased by over 200°C over the range of 0° spark-timing values, which was similar to the case with E_d85.

In summary, while using E99, by employing plasma jet ignition in combination with spark timing well after TDC and slightly lean lambda values, it was possible to obtain large decreases in hydrocarbon emissions and increases in exhaust temperature while maintaining COV levels at or near standard ignition values using TDC spark timing.

7. GASOLINE STEADY-STATE, COLD-EMISSION EXPERIMENTS USING THE GM POWERTRAIN CONTROL MODULE

Limited experiments were also carried out with commercially available, summer-grade, regular octane gasoline. This was of relevance because E_d85 variable-fuel vehicles could use gasoline frequently and in addition, the degree to which the ignition hardware and calibration changes could benefit conventional gasoline vehicles was also of interest. As was the case with E99, the experiments included a comparison of the standard and plasma jet ignition systems at 0° spark timing and testing of the plasma jet ignition system at -20° spark timing. The results of these experiments are shown in Figures 7.1 and 7.2.

The hydrocarbon emission results with gasoline differed substantially from those of either E_d85 or E99 in several ways. The hydrocarbon concentration and mass flow curves for all of the ignition setups exhibited a more consistent and pronounced drop with increasing lambda values than had been the case for the ethanol fuels. That is, the curves were more linear and had a greater negative slope. Hydrocarbon emission values for the one-, three- and six-strike PJI setups were almost identical, whereas with the ethanol fuels, the three- and six-strike setups had produced higher emissions than the single-strike setup. All of the PJI setups produced higher hydrocarbon emissions than the standard ignition system, although the difference was less in the case of hydrocarbon mass flow rates as the reduced inlet flow of air/fuel mixture using plasma jet ignition (i.e., lower specific fuel consumption) partially offset the higher exhaust hydrocarbon concentration levels.

As shown in Figure 7.1, when six strike PJI and -20° spark timing was used, tests were run with lambda values of over 1.09. The extended lambda range was tested with gasoline because during the experiments, it was evident that hydrocarbon concentrations were continuing to drop while the engine did not experience stalling or severe instability problems. Although the incremental reductions in hydrocarbon emissions were modest beyond about lambda 1.04 - 1.05, the excess oxygen provided by further enleanment would be beneficial for further hydrocarbon oxidation by the exhaust catalyst. The relatively wide lambda range over which the hydrocarbon emissions could be minimized would also be advantageous in practice, as the engine's fuel-

injection control system (which would likely be operating open loop immediately after startup) would have less difficulty in providing an appropriate lambda value than if a narrow lambda target range was necessary.

As shown in Figure 7.2, the COV and exhaust temperature results with gasoline also differed from the trends observed while using E_d85 and E99. COV values using plasma jet ignition were all below those for standard ignition. This was largely due to the fact that the standard-ignition COV values were higher with gasoline than with the ethanol fuels and showed a pronounced increase with mixtures leaner than lambda = 1.0. When -20° spark timing was used with six-strike PJI, the COV increased only to the levels observed using single-strike PJI at 0° and remained well below the standard ignition 0° values. One aspect which was similar to the ethanol results was the ranking of the PJI setups, with the three- and six-strike setups giving similar COV values that were significantly lower than the single-strike values.

As also shown in Figure 7.2 at 0° spark timing, the PJI setups produced similar exhaust temperatures (with the single-strike setup being slightly higher) that were all well below the standard ignition values. This is consistent with the higher hydrocarbon emissions for PJI and gasoline discussed earlier. The overall combination of lower COV, higher hydrocarbon emissions, and lower exhaust temperature with PJI is behaviour that would be expected if the PJI system reduced the time required (following the spark timing) for the mixture to be burned. Using -20° spark timing, the exhaust temperature was about 175°C higher than the standard ignition, 0° values, and rose slightly at the leanest lambda values tested.

Comparisons between the experimental results using E_d85, E99, and gasoline must be made with caution because of the limited nature of the testing and the experimental difficulties described previously. However, the available evidence suggests that significant differences exist for different fuel formulations in their response to changes in ignition system characteristics and control system calibration strategies.

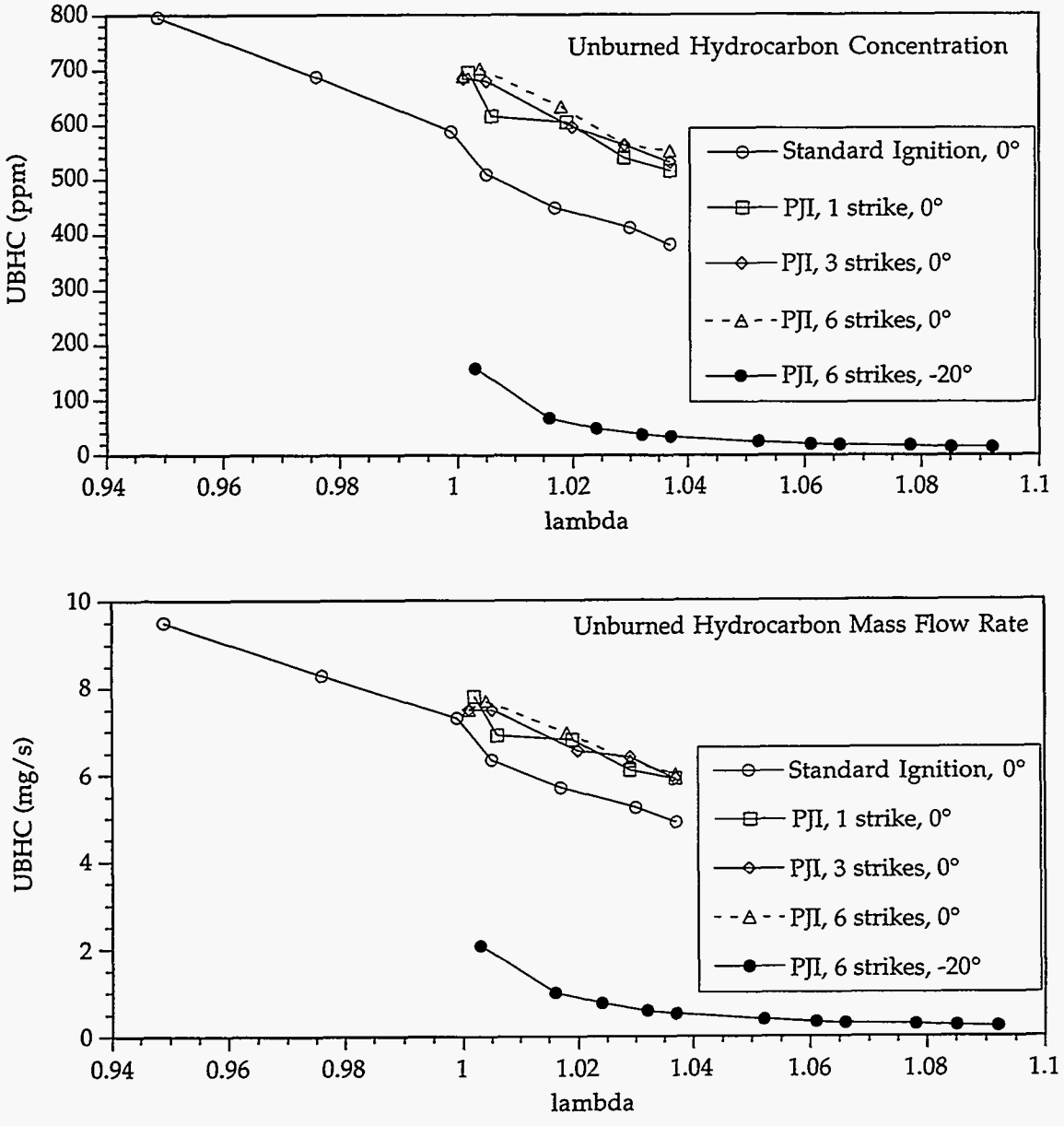

Figure 7.1: Ignition System Comparison Using Gasoline - Effects of Excess Air Ratio and Spark Advance on Exhaust Unburned Hydrocarbon Emissions

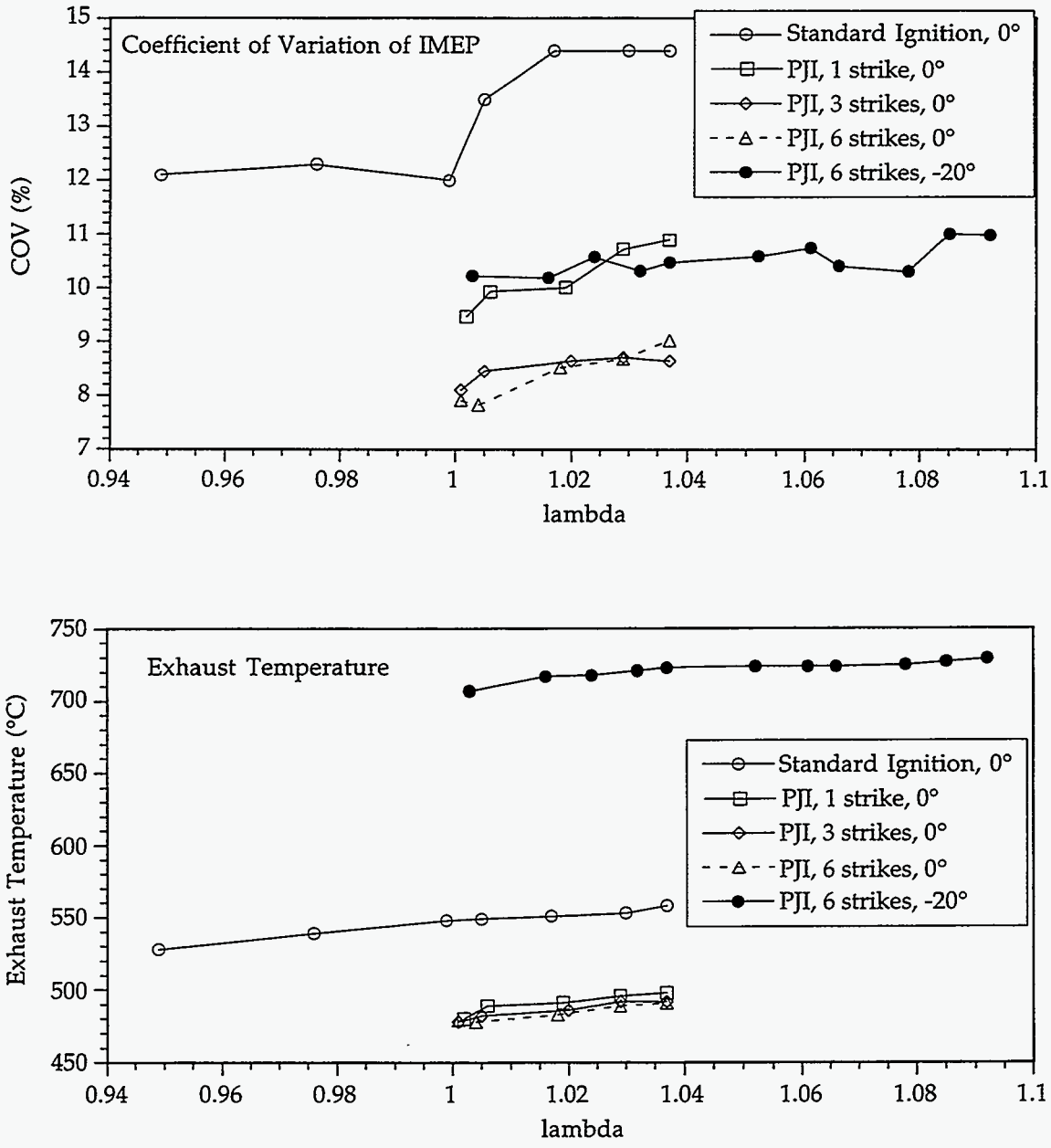

Figure 7.2: Ignition System Comparison Using Gasoline - Effects of Excess Air Ratio and Spark Advance on COV of IMEP and Exhaust Temperature

8. MODIFICATIONS TO THE ENGINE TEST BED APPARATUS

For the experiments described thus far in which the GM PCM was used, a number of serious problems existed. The stability of the air/fuel ratio control loop degraded (because of electrical noise) when plasma jet ignition was used. This influence acted to increase COV values, thus partially or completely offsetting the ability of the plasma jet ignition to lower the COV. Even while using standard ignition, the control system stability was problematic during lean closed-loop running with the GM PCM interfaced with the wide-range air/fuel ratio system.

It was shown that large reductions in hydrocarbon emissions could be achieved when the plasma jet ignition system was used in combination with extreme spark retard (circa -20°) and slightly lean mixtures. However, it was impossible to retard the spark timing of the standard GM inductive ignition system beyond 0°. Thus, the potential for hydrocarbon emission reductions and accompanying COV and exhaust temperature behaviour for standard ignition remained unknown for the region of negative spark-timing values.

In order to overcome these problems, the apparatus was modified to improve the air/fuel ratio control loop stability and to provide an extended range of spark timing settings for standard inductive ignition comparisons. The main change was the replacement of the GM PCM by a programmable aftermarket electronic control system (Electromotive TEC2) capable of controlling the fuel-injection system and providing distributorless inductive ignition. This control system was much less susceptible to electrical noise than the previous test bed setup of the GM PCM and remote EPROM assembly. The plasma jet ignition system was also modified to improve shielding and grounding in order to reduce electrical noise emissions at the source.

For fuel-injection control, the aftermarket control system was configured so that its injector driver outputs provided pulsewidth triggering to the standard GM remote injector driver module. The injection was eventually timed to provide sequential injector firing (like the GM system) with injection taking place (for each cylinder) while the intake valve was closed. In preliminary experiments where open-valve injection took place for some cylinders, combustion

stability was found to degrade markedly. Consultations with GM of Canada staff revealed that this particular engine design is unusually sensitive to injector timing, as the intake port design and injector targeting permits fuel to be injected through the inlet valve opening and impinge upon the opposite cylinder wall.

The aftermarket control system had a very simple closed-loop control algorithm (interpreting whether to increase or decrease injection based on whether the EGO signal was above or below a fixed setpoint) compared with the GM system, but this made it possible to interface the aftermarket system with the digital sensor signal of the wide-range air/fuel ratio sensor system successfully. The closed-loop control parameters were calibrated to produce a very slow, stable control loop with pulsewidth incremental changes of 0.4% being implemented every four engine cycles. In practice, a much more sophisticated control approach would be required to provide both rapid initial air/fuel ratio corrections when the air/fuel ratio was far from the target value, followed by a slow correction approach once the target was approached or reached.

The crankshaft magnetic position sensor assembly that provides baseline ignition timing information for the aftermarket control system was re-indexed so that the signal timing that would normally indicate 0° actually occurred at -28°. Using this setup, the system's electronic spark advance could be used to provide ignition timing from -28° to +32° for the inductive ignition coil drivers. The GM high-current alcohol coils were used. Because of differences in peak primary current and dwell characteristics between the GM coil drivers and the Electromotive drivers, the spark current profiles from the two systems were not identical. As shown by the comparison in Figure 8.1, use of the aftermarket inductive ignition system resulted in more consistent spark current characteristics with about the same duration as the maximum values with the GM system but with slightly lower peak current values.

Following the installation of the new control system setup, a series of combustion stability tests were run with the plasma jet ignition installed in only one cylinder. This was done to examine the effects of ignitor design and in particular, to compare performance with the

original 7.5-mm, recessed-gap ignitors and the 5.0-mm, recessed-gap ignitors that had been adopted to maintain acceptable breakdown voltage levels. The plasma jet ignition circuit was also combined with a standard spark plug (with the resistor removed) for some tests.

As shown in Figure 8.2, the 5.0-mm ignitor was markedly inferior to the 7.5-mm ignitor. Whereas the 7.5-mm ignitor produced progressively lower COV values when additional ignition strikes were used, minimum COV values were obtained using three strikes with the 5.0-mm ignitor. The advantages of a larger surface gap were shown by the authors in earlier work [19], as the greater voltage drop across a larger gap increases the peak power and total energy dissipated in the gap versus the losses in the circuit components.

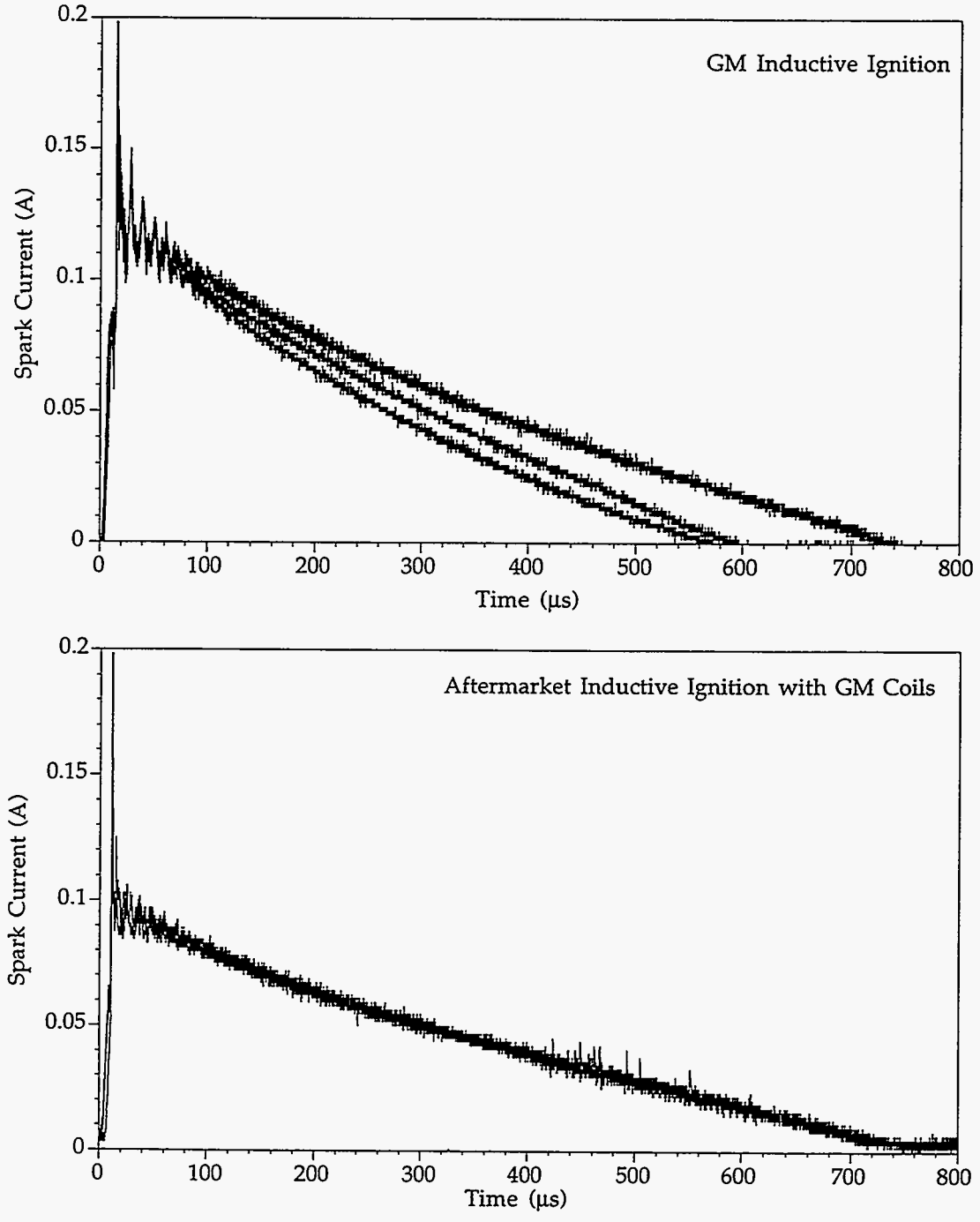

Figure 8.1: Comparison of Three Typical Spark Current Waveforms for the GM and Aftermarket Inductive Ignition

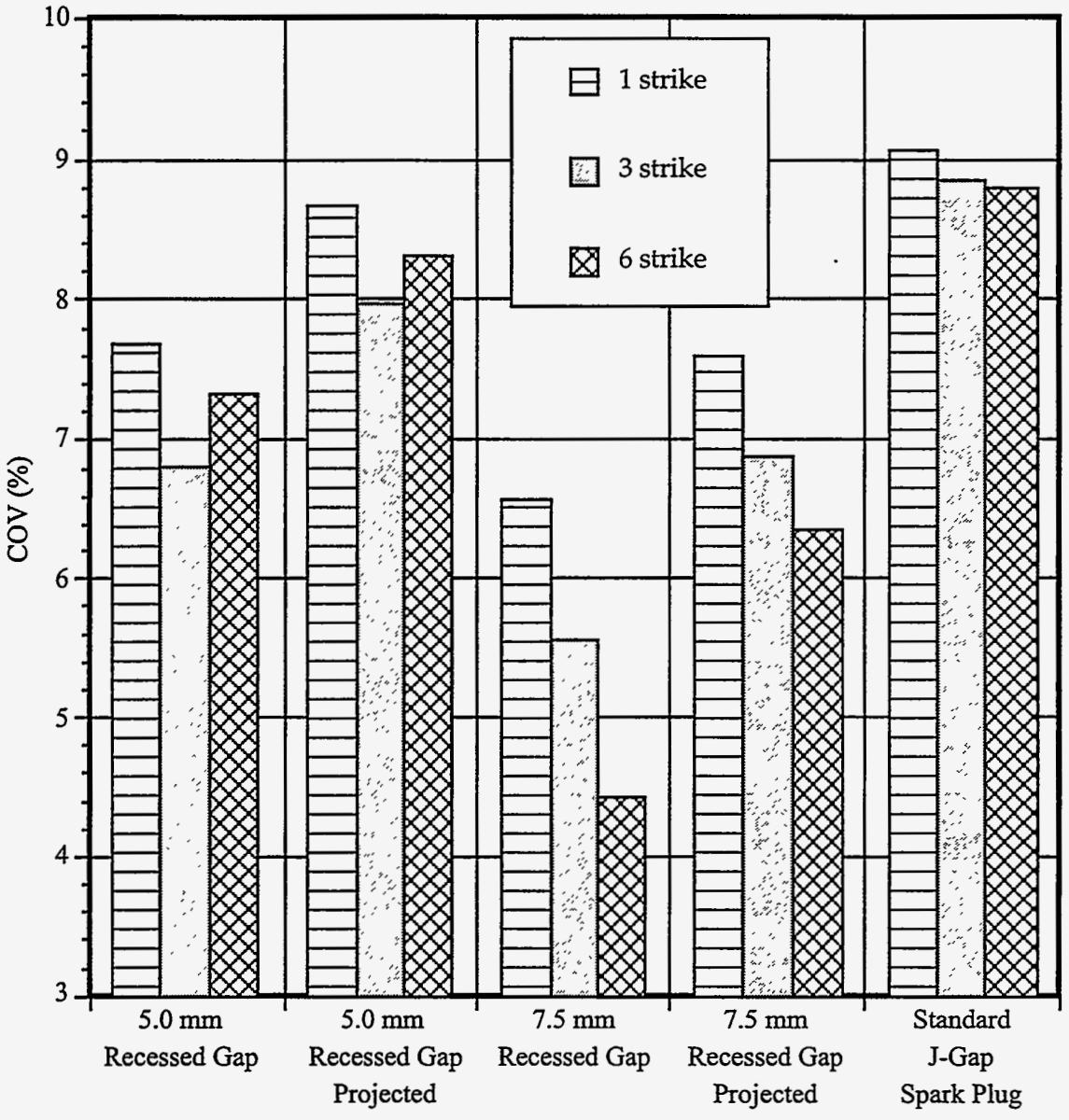

Figure 8.2: Single-Cylinder Comparison of COV Values for Different Ignitors using PJI (25° Coolant, 0° Spark Advance, lambda = 1.0)

The reasons for the observed effects of gap width on performance with multistrike plasma jet ignition are not certain at this time, but may be related to residual ionization effects following the first discharge. The fuel/air mixture in the spark gap is ionized by the initial spark breakdown and energy discharge and some ionized mixture will remain in the spark gap after the discharge is completed. This so-called "residual ionization" changes the electrical characteristics of spark gap (in effect lowering its electrical resistance), such that the voltage drop across the gap (therefore the power and energy dissipation) would be lower during any subsequent spark discharges. The influence could be greater with a small gap length as there would be a relatively low initial voltage drop (during the first discharge) that would degrade to still lower levels if residual ionization effects were present.

7.5-mm and 5.0-mm ignitors that projected 3.0 mm further into the combustion chamber were also tested, as it was thought that adjustments to the ignitor tip projection might improve the COV results. In both cases, additional projection produced higher COV values, but the 7.5-mm and 5.0-mm ignitors exhibited the same differences in their response to the number of ignition strikes as in the case with the original projection values. The standard J-gap spark plug had higher COV values with plasma jet ignition than any of the recessed surface gap ignitors and also showed the least response to the number of ignition strikes. The relatively poor performance of the J-gap/plasma jet ignition combination observed in this project is consistent with earlier work by the authors [19] in which short-duration, high-current discharges were found to provide no significant improvements in COV (relative to standard inductive or capacitor discharge ignition) when J-gap spark plugs were used along with neat methanol (M100) fuel.

As previously discussed, 7.5-mm recessed surface gap ignitors had been used successfully with methanol in the earlier work, but in this work with fuel ethanol it was necessary to reduce the gap to 5.0 mm to maintain acceptable breakdown voltage requirements. However, as shown in the COV results in Figure 8.2, much of the benefit from the additional discharges of the multistrike plasma jet ignition was lost by the reduction in gap length. In light of these circumstances, it was decided that supplying high-ignition energy in the form of a single discharge would likely yield better results for this application. Varying the energy of a single discharge is possible with the new plasma jet ignition circuit as an alternative to multiple discharges. For the remaining plasma jet experiments, the circuit was reconfigured to provide 440 mJ for a single discharge. This was similar to the 450-mJ energy level for three discharges with the multistrike system.

9. FUEL ETHANOL (E_d85) STEADY-STATE, COLD-EMISSION EXPERIMENTS USING THE AFTERMARKET ENGINE CONTROL MODULE AND MODIFIED IGNITION SYSTEMS

During the initial experiments with the aftermarket control module and inductive ignition, the engine tended to suffer from extreme instability or stalling when retarded spark timing was used. It was later recognized that the onset of stalling was related to the engine speed. Any time the engine speed dropped much below 1000 rpm, misfiring would begin and the engine would eventually stall. Because the target idle speed was only 1100 rpm, the engine speed fluctuations encountered as the COV worsened with inductive ignition would cause the engine speed to drop below this critical speed for stalling. In practice, the engine could not be operated at COV levels above about 10%. This made it impossible to operate with inductive ignition and retarded spark timing unless rich air/fuel mixtures were used.

In order to allow a wider test matrix with inductive ignition so that comparisons with plasma jet ignition could be made for retarded timing and lean mixtures, a revised engine calibration strategy was developed. The target idle speed was raised to 1450 rpm and a "deadband" of ±50 rpm was used for the idle speed control algorithm to avoid speed oscillations from the idle control loop oscillations. Having a fast idle speed this high following startup is common; for example, 1500 rpm was used in the work done at Honda by Nakayama et al. [2]. In addition, the open-loop parameters for the control system were modified so that the air/fuel ratio would become progressively richer if the engine speed dropped below 1300 rpm. This ensured that if there were any random fluctuations in engine speed, the engine would not experience low speed and lean mixtures simultaneously, and would thus be saved from stalling. With these changes, the engine would not experience misfiring or stalling even as COV levels approached 15%. This permitted the testing of the inductive ignition system over the full range of extreme spark retard and lean lambda values used for the plasma jet ignition system. The inductive ignition system was also tested using richer lambda values and more advanced spark timing than the plasma jet ignition system so that the additional enrichment or spark advance required to match the COV levels of the plasma jet system could be determined.

In the following figures, the results for a given measurement (hydrocarbon concentration, hydrocarbon mass flow, indicated specific fuel consumption [ISFC], COV, and exhaust temperature) have been plotted two different ways. In the first figure of each set, all of the

results have been plotted versus lambda. This reflects the way the experiments were actually run, as lambda sweeps at fixed spark-timing settings. The results for each ignition system are plotted separately, so that the behaviour of each system may be examined in detail.

In the second figure of each set, the results have been replotted versus spark timing. In the interest of clarity, only lambda values of 1.0 and leaner are shown. With the results replotted in this form, it is possible to overplot the inductive ignition and plasma jet ignition data without excessive overlap so that the characteristics of the two ignition systems may be compared.

The hydrocarbon concentration results are shown in Figures 9.1 and 9.2. For a given spark-timing and lambda combination, exhaust hydrocarbon concentrations were always lower for the inductive ignition system. For both systems, the minimum UBHC concentration values shown were under 1% of the calibration range for the FID, so the absolute value of these particular measurements would be uncertain. The FID had originally been set up in anticipation of rather high UBHC values and the minimum values observed were much lower than expected.

As shown in Figure 9.2, while using inductive ignition it was possible to approach the minimum UBHC concentration values with the spark timing retarded to only -5° if the mixture was lean enough (i.e., lambda=1.02 or greater). Retarding the spark timing beyond -10° provided no further improvements. With the plasma jet ignition system, minimum UBHC concentration values were not reached until the timing was retarded to between -15° and -20°. In the case of inductive ignition, the minimum UBHC concentration values were achieved at the expense of COV values in excess of 10% (as discussed later).

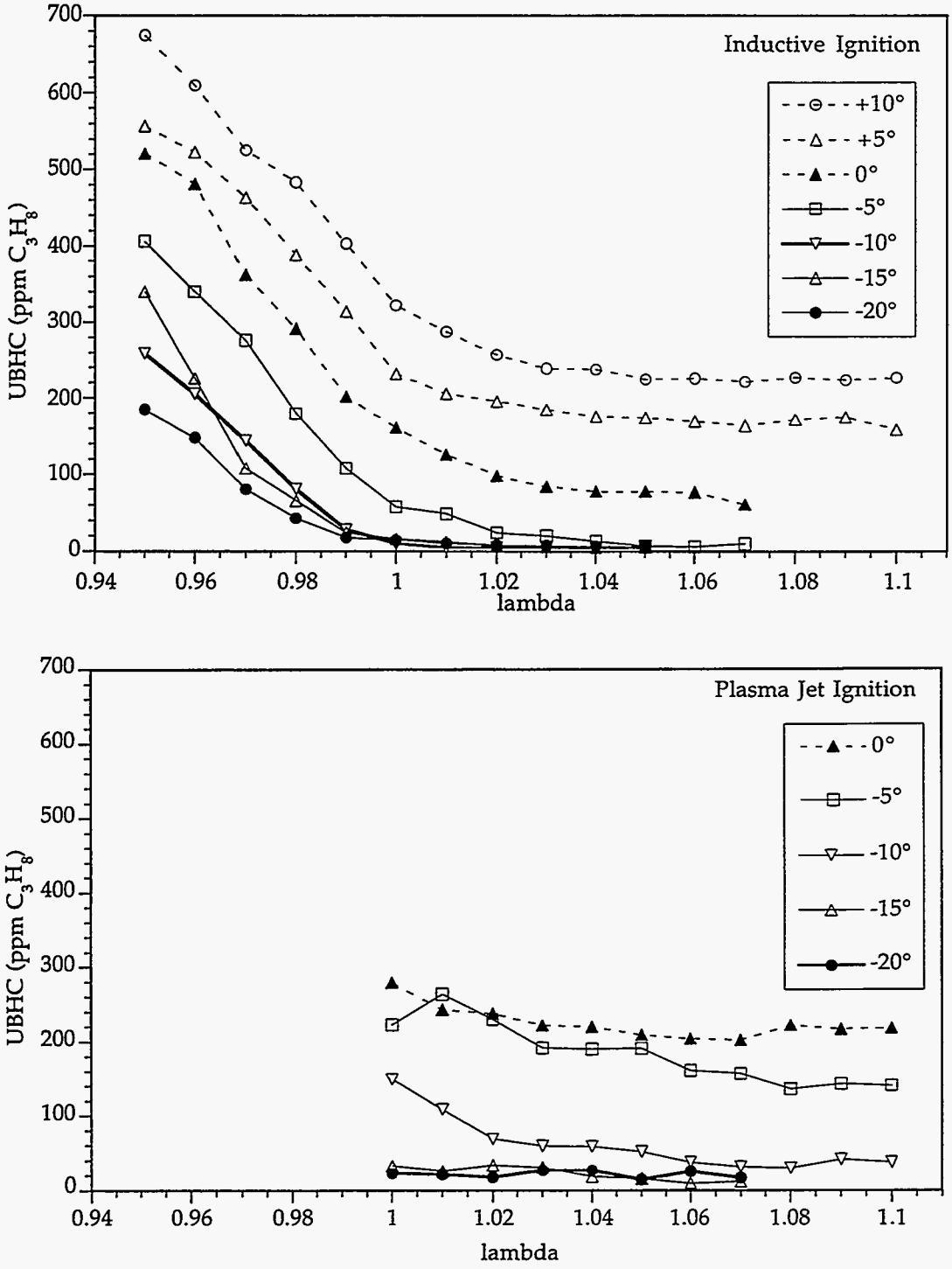

Figure 9.1: Comparison of Exhaust Hydrocarbon Concentration versus Lambda

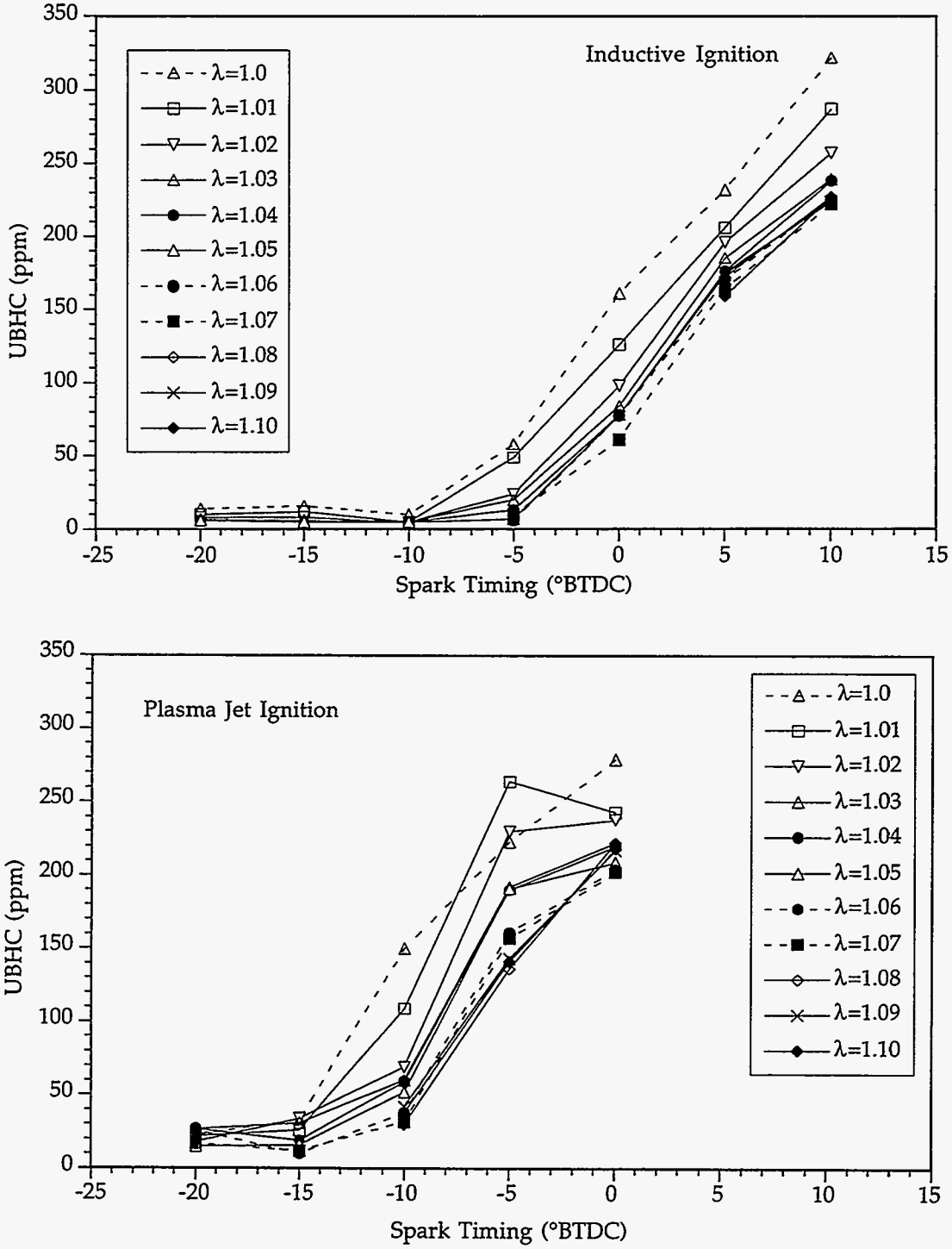

Figure 9.2: Comparison of Exhaust Hydrocarbon Concentration versus Spark Timing

The hydrocarbon mass flow rate results are shown in Figures 9.3 and 9.4. Although retarding the spark timing caused increases in the mass flow rate of air/fuel mixture entering the engine (and therefore the mass flow rate of exhaust leaving the engine), this had a small effect on calculated hydrocarbon mass flow rates in comparison with the large reductions in hydrocarbon concentration that the retarded timing accomplished. Consequently, the UBHC mass flow trends observed for the two ignition systems were the same as the trends in UBHC concentration discussed earlier. Although not readily apparent in the figures, the hydrocarbon mass flow comparison favoured the plasma jet ignition system slightly relative to the hydrocarbon concentration comparison because for a given combination of spark timing and lambda, lower air/fuel mixture flow rates were required to maintain the idle speed. Because similarly indicated power was required to maintain idle speed with either ignition system, the lower mixture flow rates with plasma jet ignition led to lower ISFC values.

ISFC trends for the two ignition systems are shown in Figures 9.5 and 9.6. As shown in Figure 9.5, the effect of lambda on ISFC was small in comparison with the effect on spark timing. Although leaner lambda values would be expected to lower specific fuel consumption by improving the cycle efficiency and (in the case of increasing lambda up to 1.0 to eliminate enrichment) by ensuring that there was enough oxygen available for complete combustion of the fuel, the competing influences of higher cyclic variation (as indicated by higher COV values) and slower burning would tend to raise specific fuel consumption. In most cases, the net effect was evidently a nearly even trade-off between these positive and negative influences. However, close inspection of Figure 9.5 reveals that for most spark-timing values, ISFC tended to lower slightly with increasing lambda when plasma jet ignition was used and raise slightly with increasing lambda when inductive ignition was used.

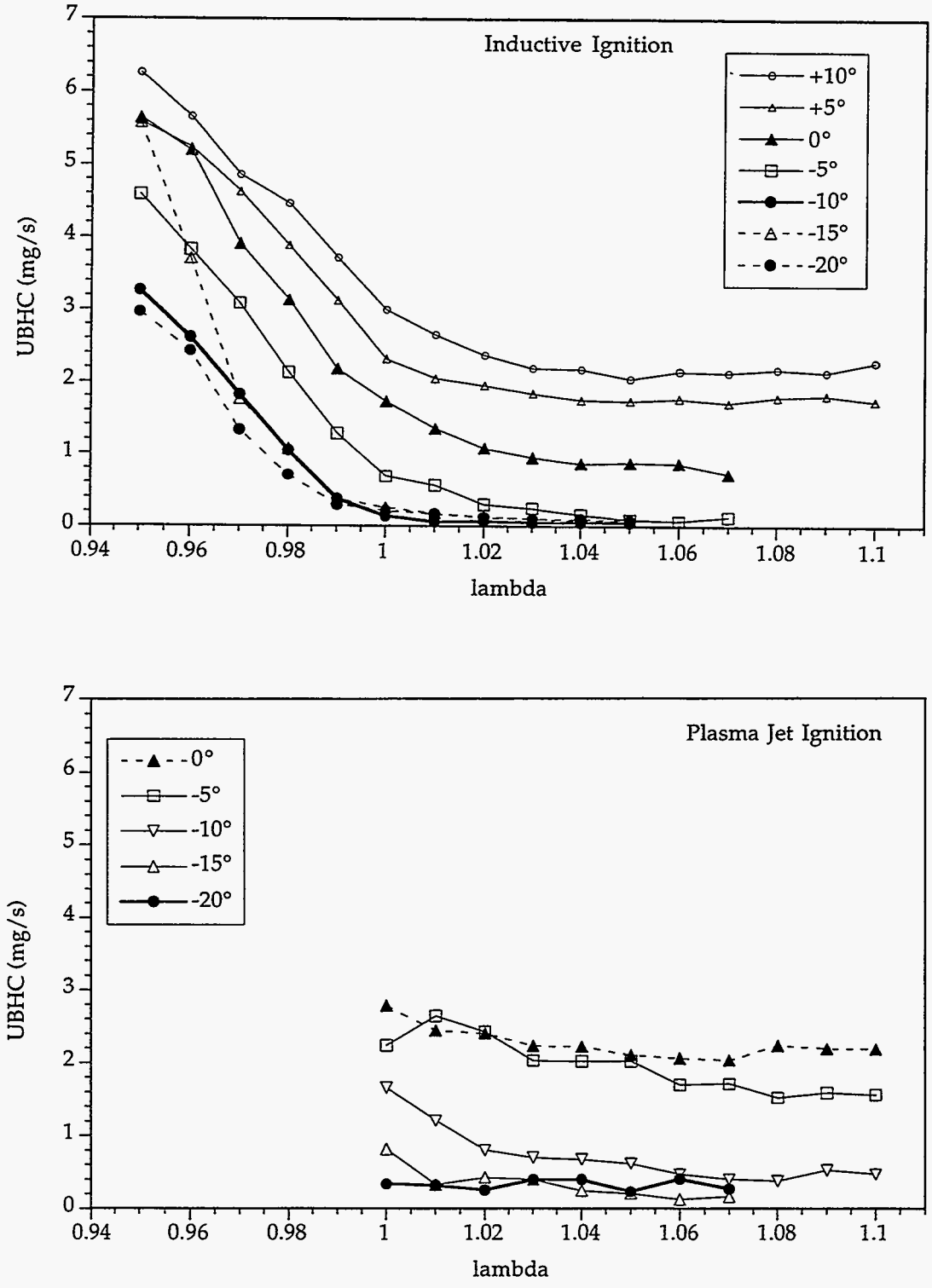

Figure 9.3: Comparison of Exhaust Hydrocarbon Mass Flow Rate versus Lambda

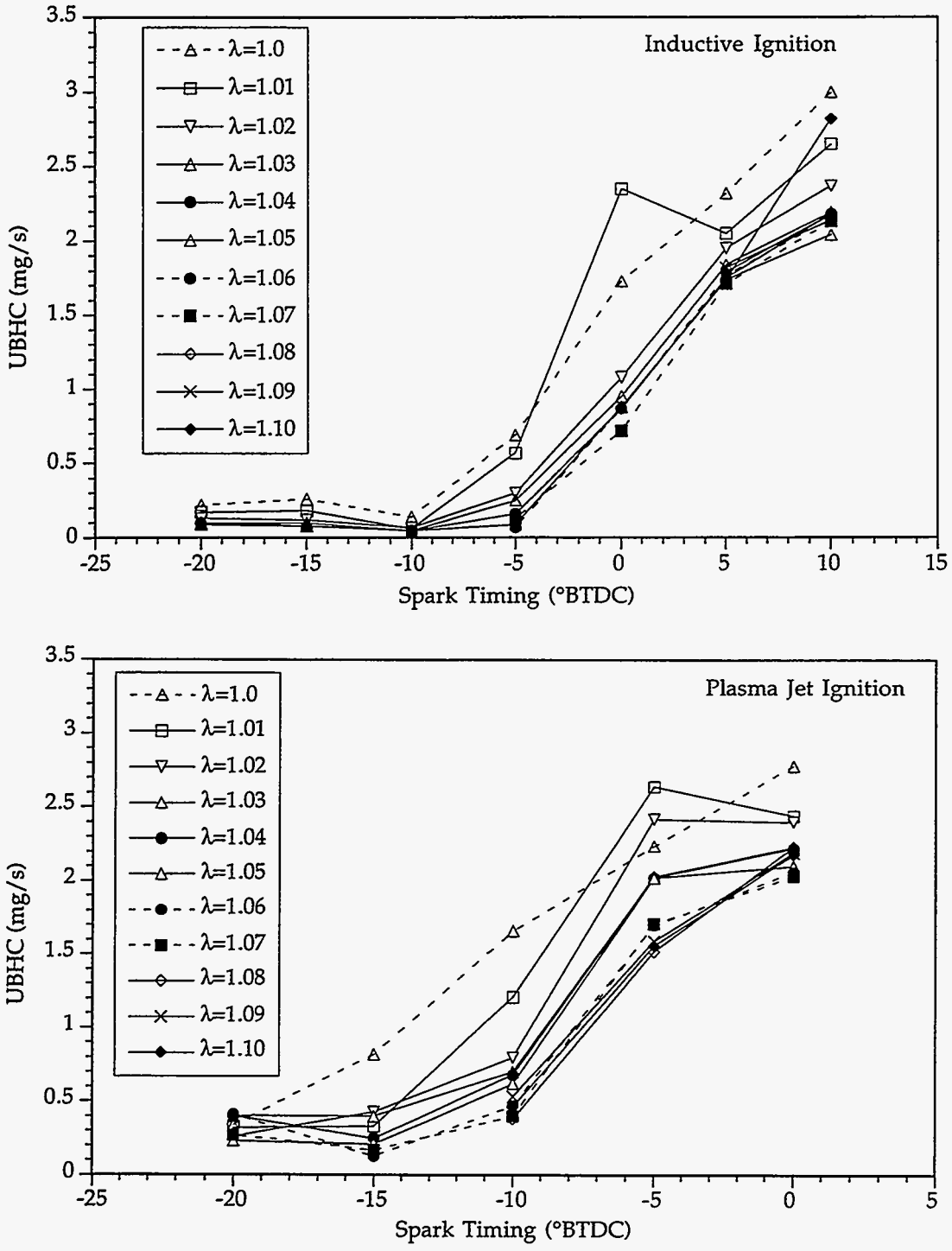

Figure 9.4: Comparison of Exhaust Hydrocarbon Mass Flow Rate versus Spark Timing

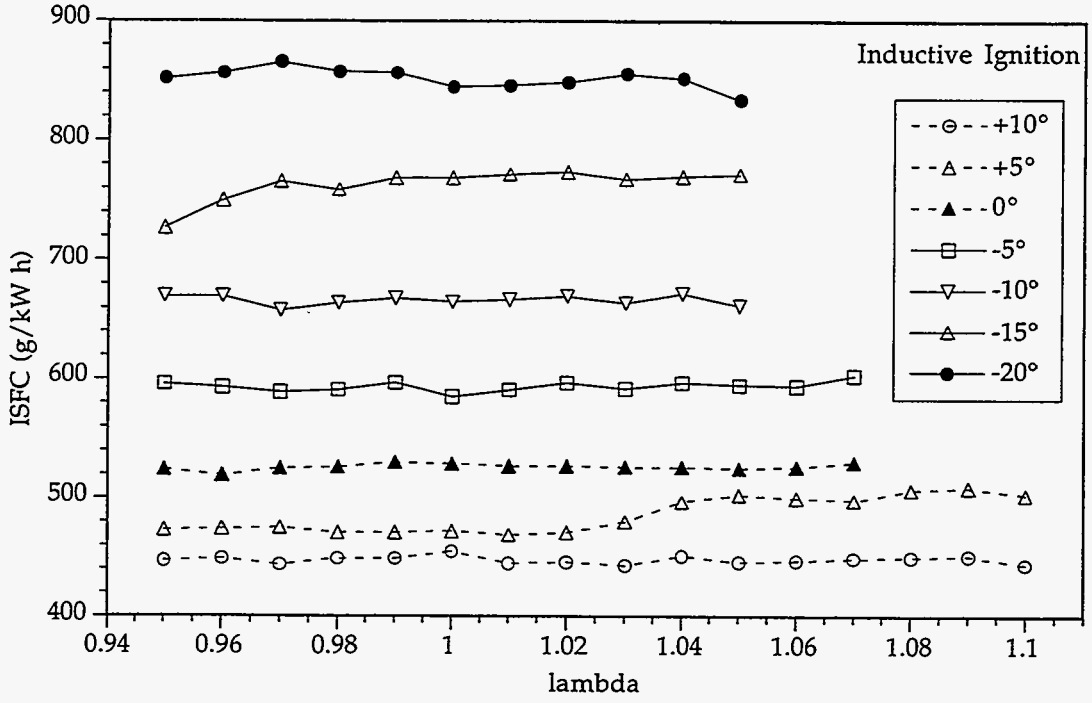

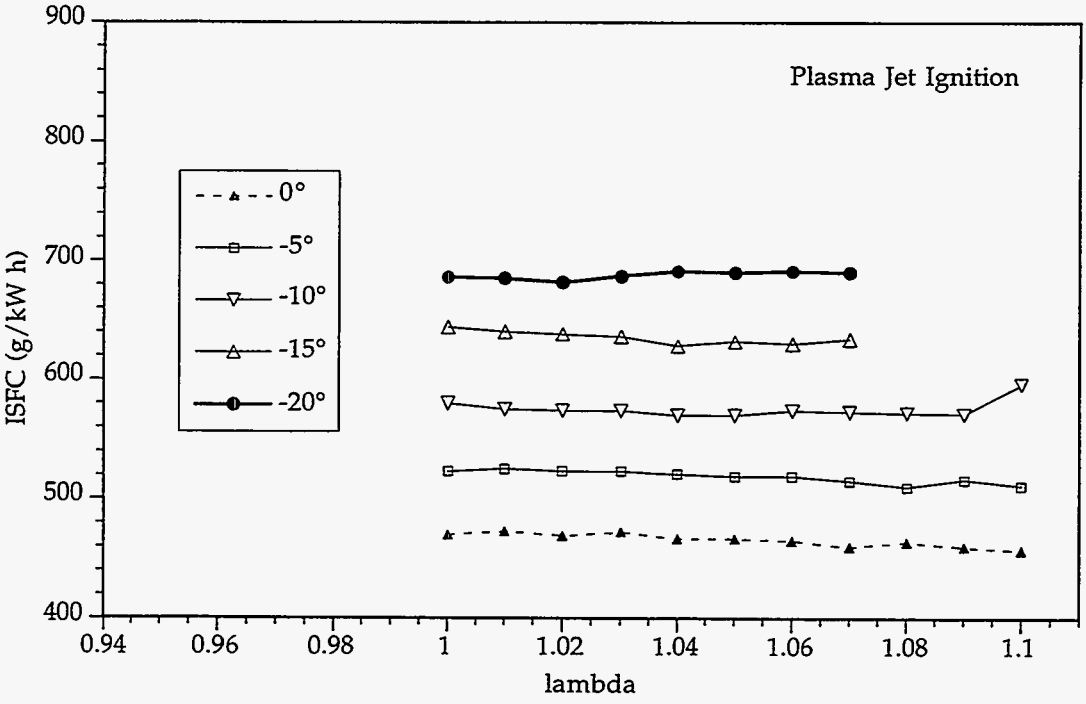

Figure 9.5: Comparison of Indicated Specific Fuel Consumption versus Lambda

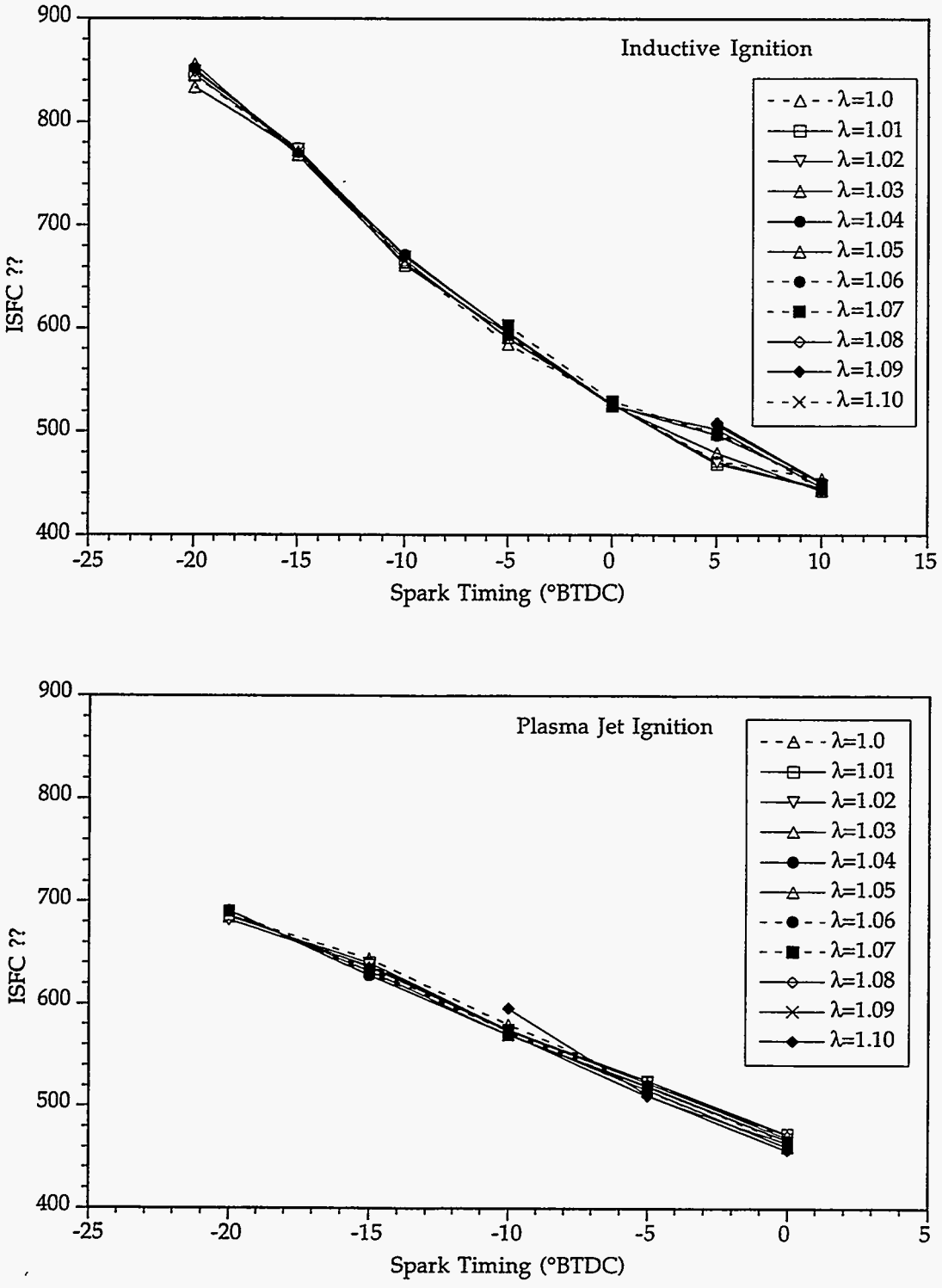

Figure 9.6: Comparison of Indicated Specific Fuel Consumption versus Spark Timing

The relatively small effect of lambda on ISFC is emphasized in Figure 9.6 as the results for different lambda values form a single curve for each ignition system when plotted versus spark timing. In comparing these curves, it is evident that the relative improvement with plasma jet ignition became greater as the spark timing was retarded. As a percentage of the inductive ignition ISFC, the reductions in ISFC with plasma jet ignition ranged from ≈11% at 0° spark timing to ≈19% at -20° spark timing. Comparison of the curves for the two ignition systems also shows that the use of plasma jet ignition provided an effect that was roughly equal to advancing the spark timing of the inductive ignition by 7°-10°.

A comparison of the coefficient of variation of indicated mean effective pressure is shown in the two ignition systems in Figures 9.7 and 9.8. Although the curves for different spark-timing values all exhibited some inconsistency with respect to changes in lambda (i.e., both increases and decreases in COV could occur for a given step change in lambda), the overall trend with inductive ignition was that COV increased as the mixture became leaner, as expected. This trend was not apparent with plasma jet ignition. With both ignition systems, there was overlap between the COV values at a given lambda value for post-TDC spark-timing settings (-5° to -20°).

The reason for this overlap can be seen in Figure 9.8, as COV values tended to increase consistently with spark retard only up to -5° and remain relatively constant with further spark retard. The practical implication of this result is that retarding the spark timing beyond -5° could provide lower hydrocarbon emissions and (as described later) higher exhaust temperatures without necessarily causing any further increases in COV. The superiority of the plasma jet ignition system with regard to COV behaviour is also clearly shown in this figure. Note that for most of the plasma jet results at lambda values up to 1.05, it was possible to limit COV values to 10% at all spark-timing settings.

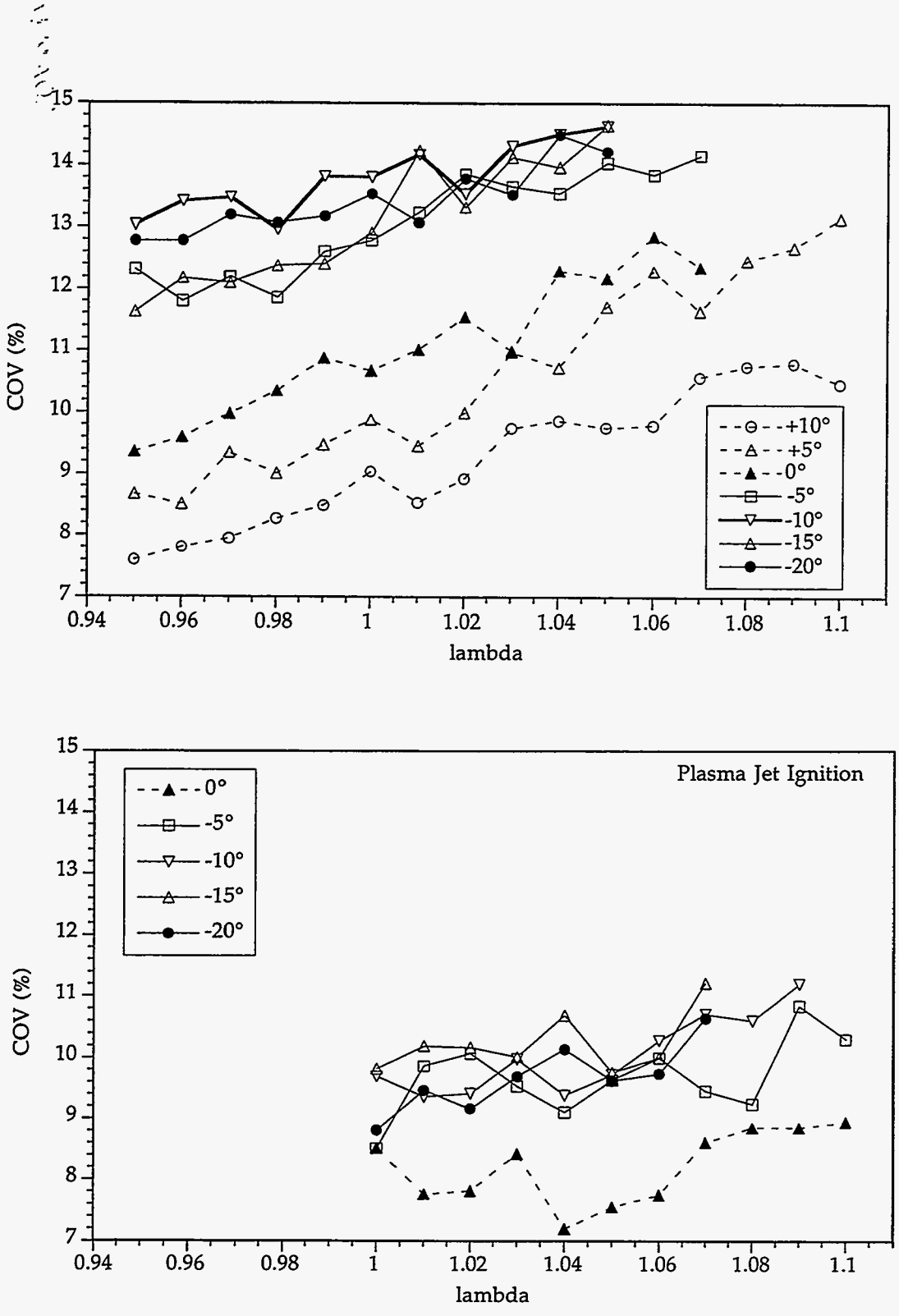

Figure 9.7: Comparison of COV of IMEP versus Lambda

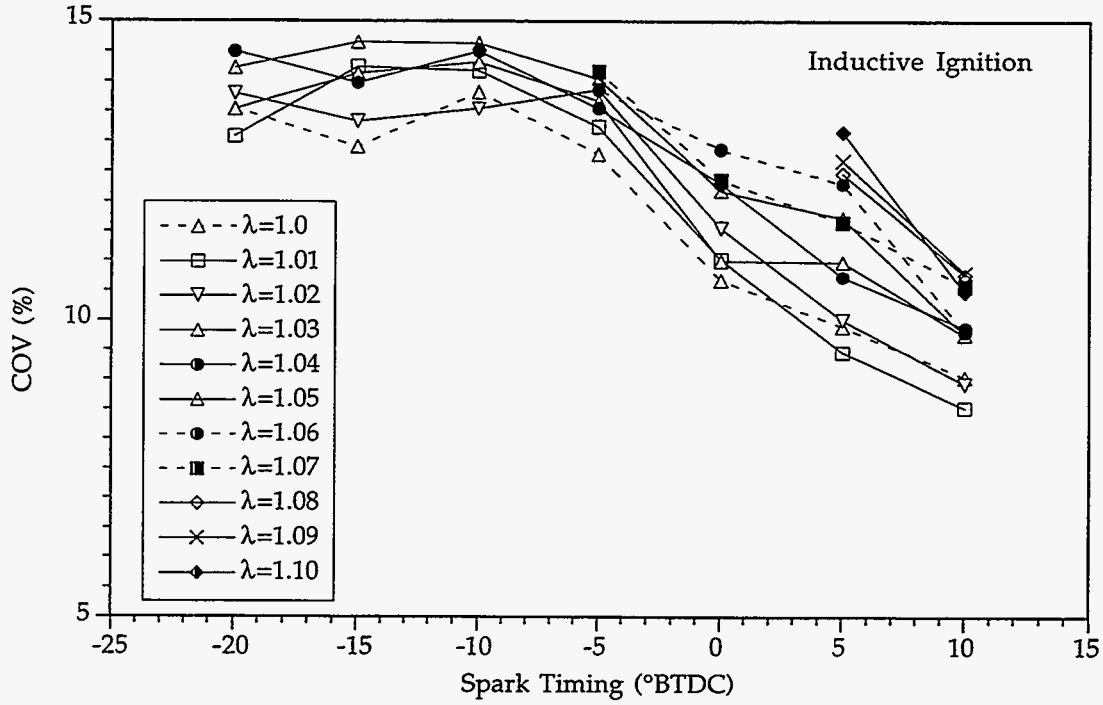

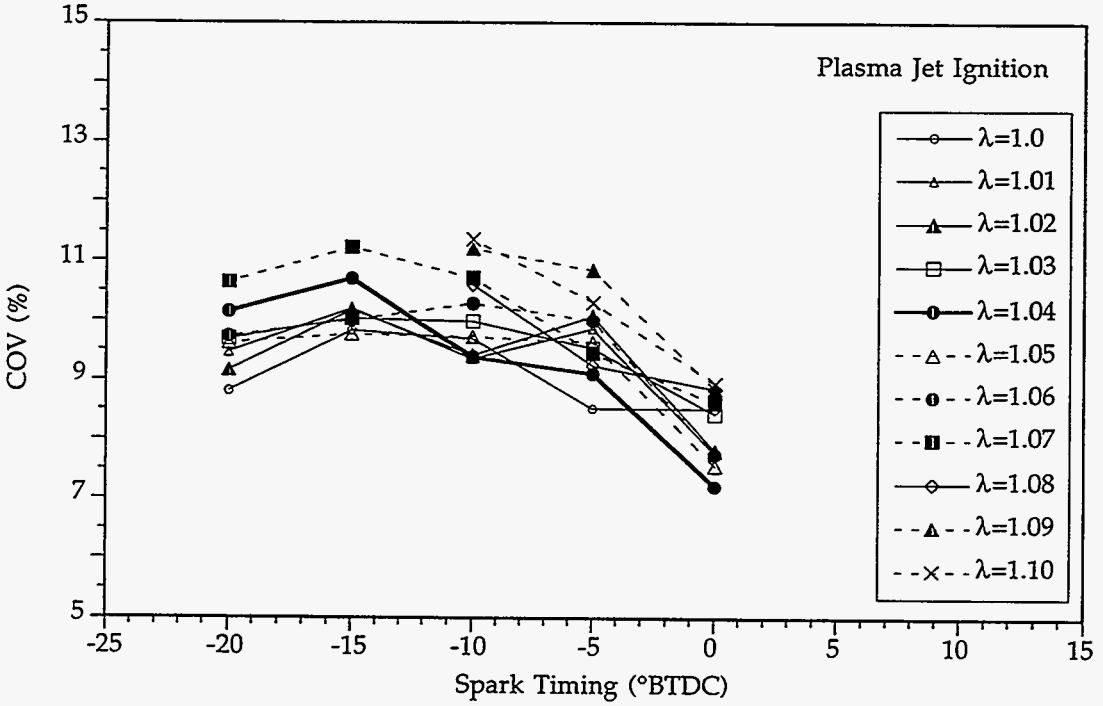

Figure 9.8: Comparison of COV of IMEP versus Spark Timing

The exhaust temperature results for the two ignition systems are compared in Figures 9.9 and 9.10. Because a greater lambda value means that the mixture is diluted with excess air, lowering of exhaust temperatures is possible. In practice, leaner mixtures usually burn more slowly; thus, the combustion products in the cylinder are at a higher temperature when the exhaust valve opens and exhaust gas temperatures become higher. In almost all of the results shown in Figure 9.9, exhaust temperatures become higher with increasing lambda or (in some cases for lambda values above 1.0) remained relatively constant. The exception is the curve for plasma jet ignition at 0° spark timing, where a trend of lowering exhaust temperature with increasing lambda was observed. This likely occurred in this case because the ability of the plasma jet ignition to enable the mixture to be burned earlier to partially offset the slower burning characteristics of the leaner mixtures, thus allowing the influence of excess air dilution to dominate and cause lower exhaust temperatures. We have observed similar trends in earlier work comparing plasma jet and conventional ignition where the mixture was diluted with exhaust gas recirculation (EGR) [18]. In this work, increased EGR rates sometimes caused exhaust temperatures to rise with conventional ignition, whereas they became lower with plasma jet ignition.

As shown in Figure 9.10, the effect of lambda on exhaust temperature was small in comparison with the effect of spark timing. At a given spark-timing value, exhaust temperatures with plasma jet ignition were approximately 50°-100°C lower than with inductive ignition. These lower exhaust temperatures would be expected with earlier burning of the mixture, but would also cause increased hydrocarbon emissions because post-combustion oxidation of unburned hydrocarbons would be worse at lower temperatures. The effect on exhaust temperature using the plasma jet ignition system was similar to a 6°-8° advance in spark timing with inductive ignition. Based on this difference, it is apparent that lower exhaust temperatures were not solely responsible for the higher hydrocarbon emissions with plasma jet ignition at a given test point.

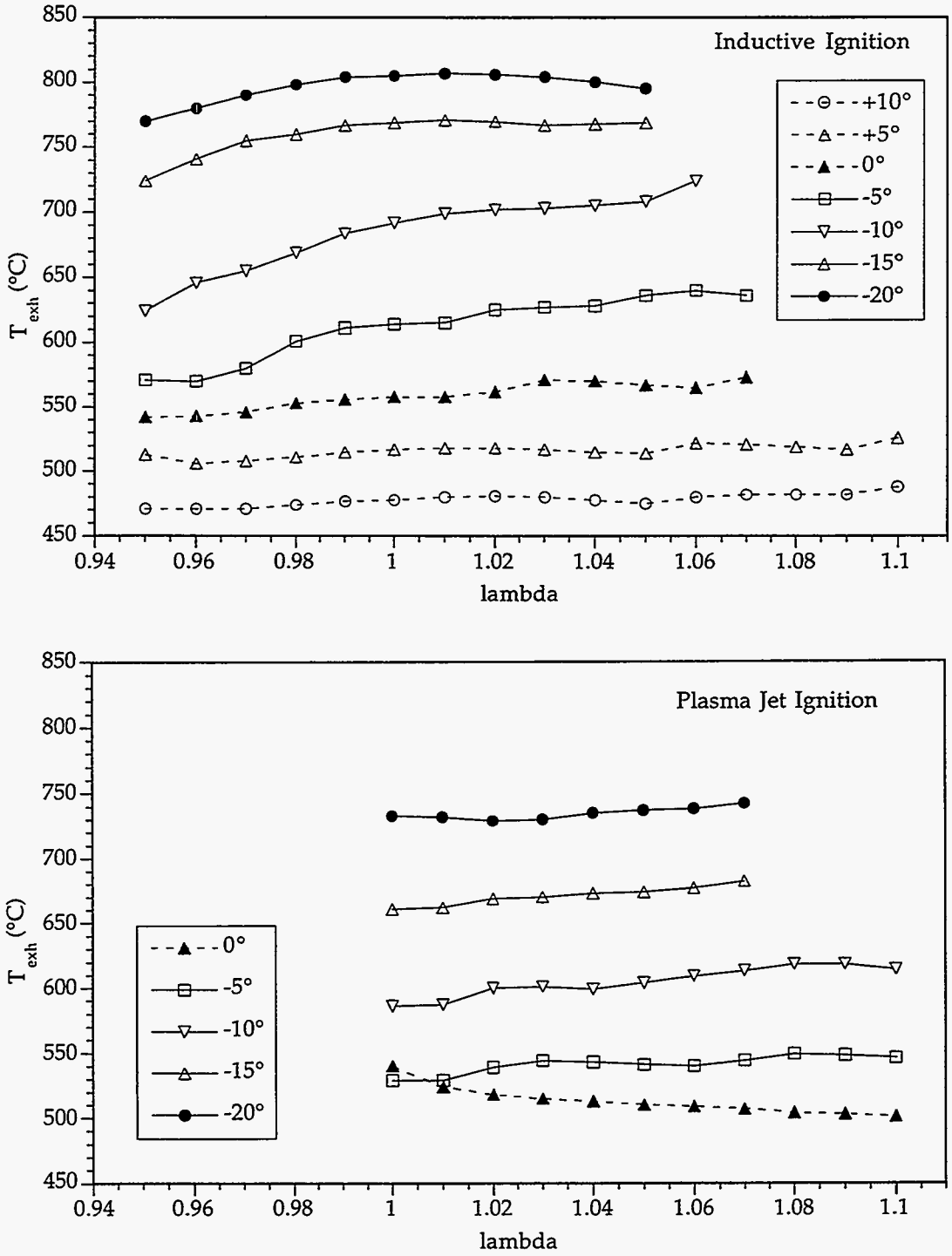

Figure 9.9: Comparison of Exhaust Temperature versus Lambda

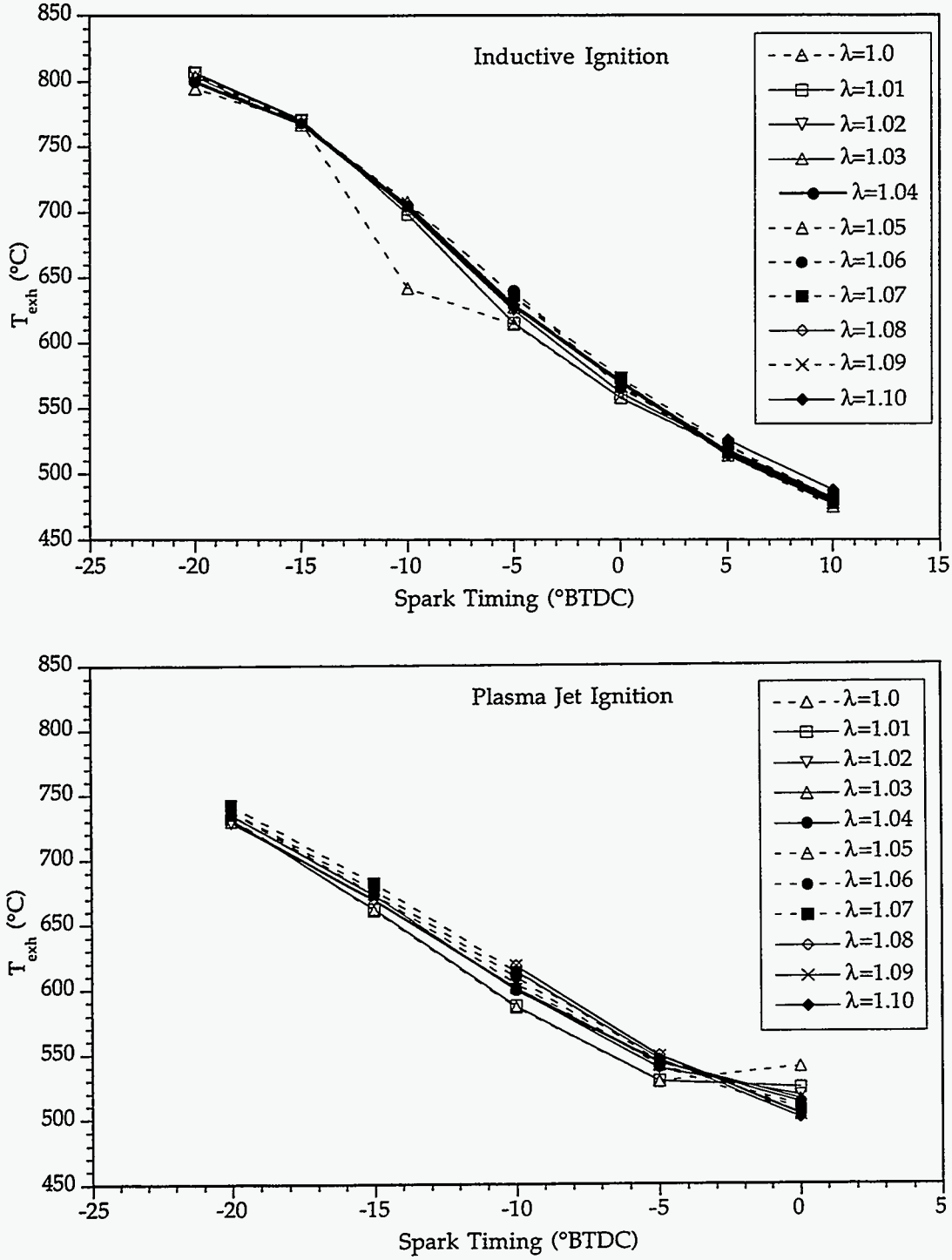

Figure 9.10: Comparison of Exhaust Temperature versus Spark Timing

As shown earlier in Figures 9.2 and 9.4, spark timing with plasma jet ignition had to be retarded (relative to inductive ignition) by more than this amount before the hydrocarbon values for the two systems were equal. Factors other than exhaust temperatures that could have contributed to hydrocarbon increases with plasma jet ignition include differences in the "packing" of in-cylinder crevices with unburned hydrocarbons (because of different cylinder pressure development during combustion) and higher residual gas fractions in the cylinder (because the reduced air flow requirements with plasma jet ignition led to lower intake manifold pressures, which would have caused more exhaust gas to back-flow into the intake during valve overlap and reenter the cylinder along with the fresh air/fuel mixture—commonly referred to as "internal EGR").

In summary, at equal lambda and spark-timing settings, results using plasma jet ignition differed from those with inductive ignition in the following ways:

- Higher exhaust unburned hydrocarbon concentrations and mass flow rates
- Lower indicated specific fuel consumption
- Lower coefficient of variation of indicated mean effective pressure
- Lower exhaust temperatures.

These differences are all consistent with the earlier burning of the mixture (i.e., a given fraction of the mixture being burned at an earlier crank angle than with inductive ignition), which has been established by the authors and other researchers as an essential characteristic of plasma jet ignition [19,22]. In this study, the rationale for using plasma jet ignition was that the anticipated improvements in COV would allow combinations of mixture enleanment and spark retard to be used that would not be feasible with standard ignition systems, thereby lowering hydrocarbon emissions. Whether or not a given lambda/spark-timing calibration is feasible depends on the COV level that is acceptable. Thus, the relationship of interest is that between the selected COV threshold and the minimum hydrocarbon mass flow possible, using calibration values that do not cause the COV to exceed this threshold.

In Figure 9.11, the COV and hydrocarbon mass flow results for inductive and plasma jet ignition have been plotted in this form by selecting the lowest UBHC mass flow results attainable at a given COV level (in increments of 0.5% COV). The lambda/spark-timing calibration for each point has been shown. Clearly, the plasma jet ignition system provided a better trade-off between reductions in mass hydrocarbon emissions and accompanying rises in COV levels. Because COV levels using plasma jet ignition rose little or not at all as the spark timing was retarded between -5° and -20° while emissions dropped substantially, optimum spark timing with plasma jet ignition shifted from 0° to -20° at a COV level of 9%.

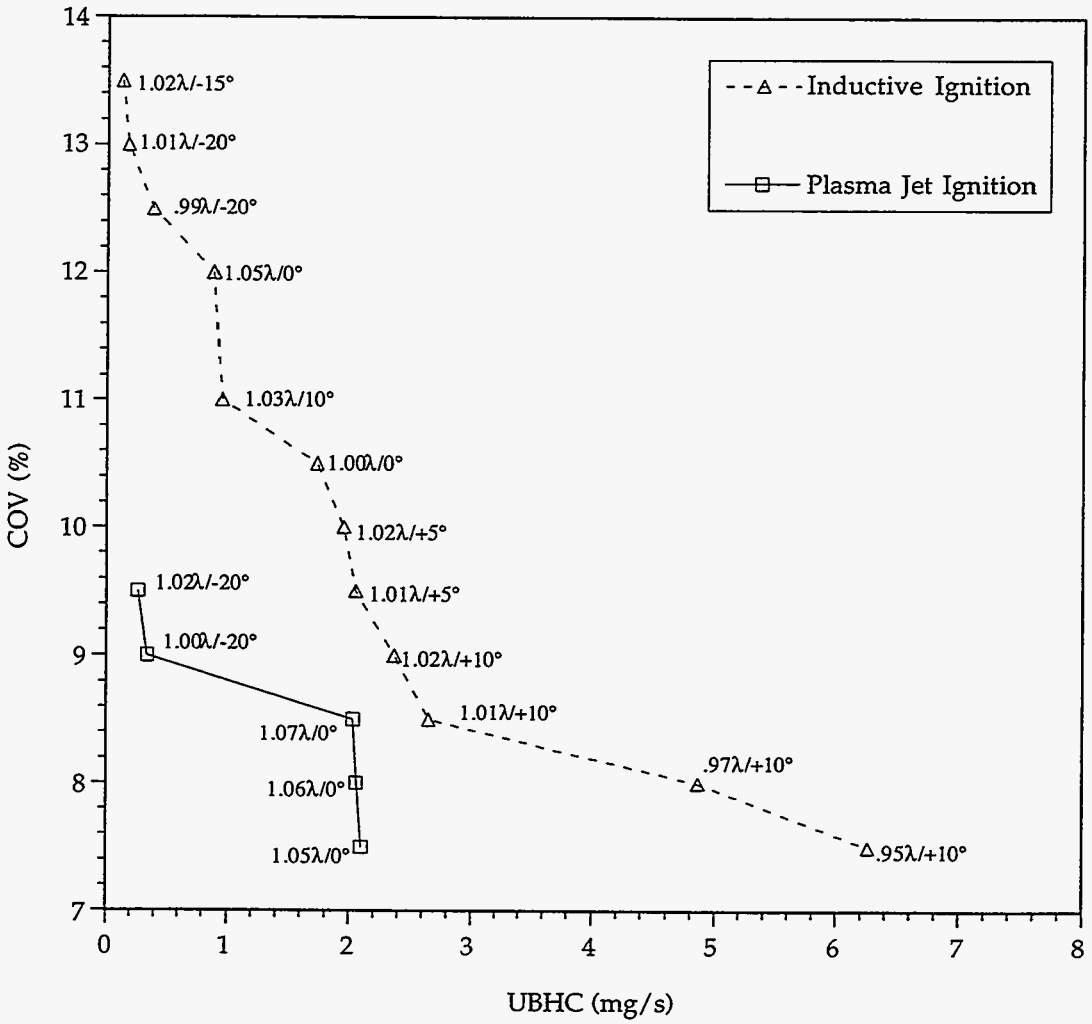

Figure 9.11: Comparison of COV versus Hydrocarbon Mass Flow Rate

The degree of improvement offered by the plasma jet ignition system depends on the maximum COV threshold that is selected. As described earlier, a COV level of 5% or less is usually desired for modern engines under normal operating conditions. However, a higher COV level would likely be acceptable temporarily during the period following cold starting. For a 4-cylinder engine, Kuroda et al. [44] proposed that a COV level of 10% corresponds with "acceptable" engine stability as judged by both human sensing and a stability meter that detected the engine's transverse displacement. This is consistent with our observations for the engine used in this study, as special measures had to be taken to prevent the engine from encountering speed oscillations and eventually stalling once COV levels exceeded about 10%.

If the results of Figure 9.11 are compared using a COV threshold of 10%, the use of plasma jet ignition would reduce UBHC mass flow to about 13% of the value obtained using the inductive ignition system. This would also be accompanied by higher exhaust temperatures, because -20° spark timing could be used with plasma jet ignition while +5° spark timing would be required with inductive ignition to remain below the 10% COV threshold. If a COV level of up to 12% was tolerated with inductive ignition, plasma jet ignition at a COV level less than 10% would still reduce UBHC mass flow to about 30% of the respective inductive ignition value.

10. CONCLUSIONS

The final conclusions of this report are based on the experimental results described in Section 9 that were obtained after the apparatus had been improved and that provide an unambiguous comparison between the inductive and plasma jet ignition systems using E_d85. These results were obtained using a steady-state, force-cooled, cold-idle experimental technique, and actual transient cold-starting conditions would be expected to yield somewhat different results primarily to colder combustion chamber and cylinder wall temperatures. Nevertheless, the steady-state tests provided a valid means of comparing the essential characteristics of the two ignition systems. The main conclusions of the study are as follows:

1. For both inductive and plasma jet ignition, the use of extreme spark retard (spark timing after top dead centre) and slightly lean mixtures was a highly effective means of reducing hydrocarbon emissions with fuel ethanol (E_d85). The higher exhaust temperatures that resulted from the use of extreme spark retard would be an additional benefit, as exhaust catalyst light-off would be accelerated. With inductive ignition, the coefficient of variation of indicated mean effective pressure would exceed 10% if the spark timing was retarded beyond 0°, whereas with plasma jet ignition it was possible to retard the spark timing up to -20° without exceeding 10% COV.

2. In summary, at equal lambda and spark-timing settings, results using plasma jet ignition differed from those with inductive ignition in the following ways:
   - Higher exhaust unburned hydrocarbon concentrations and mass flow rates
   - Lower indicated specific fuel consumption
   - Lower coefficient of variation of indicated mean effective pressure
   - Lower exhaust temperatures.

These differences are all consistent with earlier burning of the air/fuel mixture, which is behaviour normally associated with plasma jet ignition.

3. When lambda and spark timing values were selected separately for each ignition system to provide the best trade-off between mass hydrocarbon emissions and COV levels, it was possible to achieve lower hydrocarbon emissions for a given COV limit with plasma jet ignition. For a maximum COV threshold of 10% (considered to be a practical limit for the engine to avoid the risk of stalling), minimum hydrocarbon mass emission flow rates with plasma jet ignition were about 13% of those using inductive ignition.

ACKNOWLEDGEMENTS

The engine testing described in this report was funded by NREL. The support of technical monitors, Peg Whalen and Chris Colucci, is gratefully acknowledged. The development of the enhanced ignition system described in this report was funded by Natural Resources Canada under the guidance of Research Advisor René Pigeon. The engine test stand and related components were donated by General Motors of Canada Ltd., thanks to the efforts of John Christie and Norman Brinkman. We also wish to thank Richard Gibson of GM Canada Ltd., Experimental Engineering, for his continuing technical advice and support of our work.

The ethanol fuels were donated by Commercial Alcohols Inc., Toronto, Ontario, through the efforts of Bob MacKenzie. Power semiconductor components were donated by Harris Corporation and the technical support provided by Jim Azotea of Harris Power R&D is gratefully acknowledged. Prototype ignition coils and technical advice were provided by Andover Inc., Lafayette, Indiana, through Harry Minns. The engineering graphics and manuscript for the report were prepared by our colleague, D. Fisher.

BIBLIOGRAPHY

1. Nakamura, H., Motoyama, H., and Kiyota, Y., "Passenger Car Engines for the 21st Century", SAE Paper #911908, Society of Automotive Engineers, Warrendale, PA, 1991.

2. Nakayama, Y., Maruya, T., Oikawa, T., Fujiwara, M., and Kawamata, M., "Reduction of HC Emission from VTEC Engine During Cold-Start Condition", SAE Paper #940481, Society of Automotive Engineers, Warrendale, PA, 1994.

3. Quader, A.A., "Single-Cylinder Engine Facility to Study Cold Starting-Results with Propane and Gasoline", SAE Paper #92001, Society of Automotive Engineers, Warrendale, PA, 1992.

4. Dasch, C.J., Brinkman, N.D., and Hopper, D.H., "Cold Starts Using M-85 (85% Methanol): Coping with Low Fuel Volatility and Spark Plug Wetting", SAE Paper #910865, Society of Automotive Engineers, Warrendale, PA, 1991.

5. Kirwan, J.E. and Brinkman, N.D., "Fuel Methanol Composition Effects on Cold Starting", SAE Paper #912416, Society of Automotive Engineers, Warrendale, PA, 1991.

6. Kaiser, E.W., Siegel, W.O., Baidas, L.M., Lawson, G.P., Cramer, C.F., Dobbins, K.L., Roth, P.W., and Smokovitz, M., "Time-Resolved Measurement of Speciated Hydrocarbon Emissions During Cold Start of a Spark-Ignited Engine", SAE Paper #940963, Society of Automotive Engineers, Warrendale, PA, 1994.

7. Guillemot, P., Gatellier, B., and Rouveirolles, P., "The Influence of Coolant Temperature on Unburned Hydrocarbon Emissions from Spark Ignition Engines", SAE Paper #941962, Society of Automotive Engineers, Warrendale, PA, 1994.

8. Russ, S.G., Kaiser, E.W., Siegl, W.O., Podsiadik, D.H., and Barret, K.M., "Compression Ratio and Coolant Temperature Effects on HC Emissions from a Spark-Ignition Engine", SAE Paper #950163, Society of Automotive Engineers, Warrendale, PA, 1995.

9. Russ, S., Kaiser, E.W., and Siegl, W.O., "Effect of Cylinder Head and Engine Block Temperature on HC Emissions from a Single Cylinder Spark Ignition Engine", SAE Paper #952536, Society of Automotive Engineers, Warrendale, PA, 1995.

10. Alkidas, A.C. and Drews, R.J., "Effects of Mixture Preparation on HC Emissions of a S.I. Engine Operating Under Steady-State Cold Conditions", SAE Paper #961958, Society of Automotive Engineers, Warrendale, PA, 1995.

11. Drake, M.C., Sinkevitch, R.M., Quader, A.A., Olson, K.L., and Chapaton , T.J., "Effect of Fuel/Air Ratio Variations on Catalyst Performance and Hydrocarbon Emissions

During Cold-Start and Warm-Up", SAE Paper #962075, Society of Automotive Engineers, Warrendale, PA, 1996.

12. Alkidas, A.C., Drews, R.J., and Miller, W.F., "Effects of Piston Crevice Geometry on the Steady-State Engine-Out Hydrocarbons Emissions of a S.I. Engine", SAE Paper #952537, Society of Automotive Engineers, Warrendale, PA, 1995.

13. Manz, P., "Operating a Gasoline Engine at Constant Low Temperature Conditions. The Influence of Different Fuel Droplet Sizes", SAE Paper #961999, Society of Automotive Engineers, Warrendale, PA, 1996.

14. Gardiner, D.P., Rao, V.K., Bardon, M.F., Dale, J.D., Smy, P.R., and Haley, R.F., "Improving the Operation of Gasoline and Methanol Fuelled Spark Ignition Engines Under Canadian Winter Conditions", SAE Paper #920011, Society of Automotive Engineers, Warrendale, PA, 1992.

15. Gardiner, D.P., Rao, V.K., Bardon, M.F., Dale, J.D., Smy, P.R., Haley, R.F., Dawe, J.R., and Battista, V., "Sub-Zero Cold Starting of a Port-Injected M100 Engine Using Plasma Jet Ignition and Prompt EGR", SAE Paper #930331, Society of Automotive Engineers, Warrendale, PA, 1993.

16. Dawe, J.R., Smy, P.R., Haley, R.F., Dale, J.D., Bardon, M.F., and Gardiner, D.P., "Plasma Jet Ignition of Methanol at Subzero Temperature", *Proc. Instn. Mech. Engrs.*, Vol. 208, Part D: *J. Automobile Engineering,* 1994.

17. Gardiner, D.P., Mallory, R.W., Rao, V.K., Bardon, M.F. and Battista, V., "Vehicle Implementation and Cold Start Calibration of a Port Injected M100 Engine Using Plasma Jet Ignition and Prompt EGR", SAE Paper #952375, Society of Automotive Engineers, Warrendale, PA, 1995.

18. Neame, G.R., Gardiner, D.P., Mallory, R.W., Rao, V.K., Bardon, M.F., and Battista, V., "Improving the Fuel Economy of Stoichiometrically Fuelled S.I. Engines by Means of EGR and Enhanced Ignition - A Comparison of Gasoline, Methanol and Natural Gas", SAE Paper #952365, Society of Automotive Engineers, Warrendale, PA, 1995.

19. Gardiner, D.P., Mallory, R.W., Pucher, G.R., Todesco, M.K., Bardon, M.F., and Battista, V., "Experimental Studies Aimed at Lowering the Electrical Energy Requirements of a Plasma Jet Ignition System for M100 Fuelled Engines", SAE Paper #961989, Society of Automotive Engineers, Warrendale, PA, 1996.

20. Topham, D.R., Smy, P.R., and Clements, R.M., "An Investigation of a Coaxial Spark Ignitor with Emphasis on its Practical Use", *Combustion and Flame,* 25, 187.

21. Asik, J.R., Piatkowski, P., Foucher, M.J., and Rado, W.G., "Design of a Plasma Jet Ignition System for Automotive Application", SAE Paper #770355, Society of Automotive Engineers, Warrendale, PA, 1977.

22. Edwards, C.F., Oppenheim, A.K., and Dale, J.D., "A Comparative Study of Plasma Jet Ignition Systems", SAE Paper #830479, Society of Automotive Engineers, Warrendale, PA, 1983.

23. Dale, J.D., Wilson, J.P., Santiago, J., Smy, P., and Clements, R., "Low Temperature Starting of Diesel Engines Using Timed Spark Discharge", SAE Paper #850049, Society of Automotive Engineers, Warrendale, PA, 1985.

24. Cavolowsky, J.A., Paris, D.W., Oppenheim, A.K., and Smy, P.R., "Formation of a Plasma Puff", SAE Paper #870609, Society of Automotive Engineers, Warrendale, PA, 1987.

25. Murase, E., Ono, S., Hanada, K., and Nakahara, S., 'Plasma Jet Ignition in Turbulent Lean Mixtures", SAE Paper #890155, Society of Automotive Engineers, Warrendale, PA, 1989.

26. Anderson, R. and Asik, J., "Lean Air Fuel Ignition System Comparison in a Fast Burn Engine", SAE Paper #850076, Society of Automotive Engineers, Warrendale, PA, 1985.

27. Teets, R.E. and Sell, J.A., "Calorimetry of Ignition Sparks", SAE Paper #880204, Society of Automotive Engineers, Warrendale, PA, 1988.

28. VanDuyne, E. and Porreca, P., "Performance Improvement from Dual Energy Ignition on a Methanol Injected Cosworth Engine", SAE Paper #940150, Society of Automotive Engineers, Warrendale, PA, 1994.

29. Anderson, H.E., "Low Impedance Capacitor Discharge System and Method", U.S. Patent No. 3,788,293, Jan. 26, 1974.

30. Hamley, J.P., "High Energy Spark Ignition System", U.S. Patent No. 4,223,656, Sept. 23, 1980.

31. Imai, I. and Yukitsuga, H., "Plasma Jet Ignition System", U.S. Patent No. 4,308,488, Dec. 29, 1981.

32. Imai, I. and Some, M., "Plasma Jet Ignition System with Noise Suppressing Arrangement", U.S. Patent No. 4,327,702, May 4, 1982.

34. Ezoe, M., "Plasma Jet Ignition System for Internal Combustion Engine", U.S. Patent No. 4,369,756, Jan. 24, 1983.

35. Anzai, M., "Plasma Jet Ignition System", U.S. Patent No. 4,369,757, Jan. 25, 1983.

36. VanDuyne, E. and Porreca, P., "Dual Energy Ignition System", U.S. Patent No. 5,197,448, 1993.

37. Kuwahara, K., Watanabe, T., Takemura, J., Omori, S., Kume, T., and Ando, H., "Optimization of In-Cylinder Flow and Mixing for a Center-Spark Four-Valve Engine Employing the Concept of Barrel-Stratification", SAE Paper #940986, Society of Automotive Engineers, Warrendale, PA, 1994.

38. Canup, R.E., "The Texaco Ignition System - A New Concept for Automotive Engines", SAE Paper #750347, Society of Automotive Engineers, Warrendale, PA, 1975.

39. Kim, J., and Anderson, R.W., "Spark Anemometry of Bulk Gas Velocity at the Plug Gap of a Firing Engine", SAE Paper #952459, Society of Automotive Engineers, Warrendale, PA, 1995.

40. Herweg, R. and Maly, R.R., "A Fundamental Model for Flame Kernel Formation in S.I. Engines", SAE Paper #922243, Society of Automotive Engineers, Warrendale, PA, 1992.

41. Thompson, N.D. and Wallace, J.S., "Effect of Engine Operating Variables and Piston and Ring Parameters on Crevice Hydrocarbon Emissions", SAE Paper #940480, Society of Automotive Engineers, Warrendale, PA, 1994.

42. Chan, S.H. and Zhu, J., "The Significance of High Value of Ignition Retard Control on the Catalyst Lightoff", SAE Paper #962077, Society of Automotive Engineers, Warrendale, PA, 1996.

43. Cullen, M.J., Marzonie, R.M., Dona, A.R., Grant, E.J., Yannone, R.A., and Eggers, P.J., "Ignition Timing Control System for Varying Cold Start Spark Advance During Adaptive Learning", U.S. Patent No. 5,540,202, July 30, 1996.

44. Kuroda, H., Nakajima, K., Sugihara, Y., and Muranuka, S., "The Fast Burn with Heavy EGR, New Approach for Low NO_x and Improved Fuel Economy", SAE Paper #780006, Society of Automotive Engineers, Warrendale, PA, 1978.

REPORT DOCUMENTATION PAGE

Form Approved
OMB NO. 0704-0188

AGENCY USE ONLY (Leave blank)	2. REPORT DATE	3. REPORT TYPE AND DATES COVERED
	September1997	Subcontract report

TITLE AND SUBTITLE

ıbrication and Testing of an Enhanced Ignition System to Reduce Cold-Start Emissions in an Ethanol (E85) Light-Duty uck Engine

5. FUNDING NUMBERS

(C) ACI-6-16602-01
(TA) FU702130

AUTHOR(S)

Gardiner, R. Mallory, and M. Todesco

PERFORMING ORGANIZATION NAME(S) AND ADDRESS(ES)

exum Research Corporation
ıermotech Engineering Division
15 Norris Court
ngston, Ontario, Canada K7K 4R9

8. PERFORMING ORGANIZATION REPORT NUMBER

SPONSORING/MONITORING AGENCY NAME(S) AND ADDRESS(ES)

ational Renewable Energy Laboratory
517 Cole Boulevard
olden, CO 80401-3393

10. SPONSORING/MONITORING AGENCY REPORT NUMBER

NREL/SR-540-22967

1. SUPPLEMENTARY NOTES

2a. DISTRIBUTION/AVAILABILITY STATEMENT

ational Technical Information Service
S. Department of Commerce
285 Port Royal Road
oringfield, VA 22161

12b. DISTRIBUTION CODE

UC-1504

3. ABSTRACT *(Maximum 200 words)* This report describes an experimental investigation of the potential for an enhanced ignition system to lower the cold-start nissions of a light-duty vehicle engine using fuel ethanol (commonly referred to as E85). Plasma jet ignition and conventional inductive ignition were compared for a eneral Motors 4-cylinder, alcohol-compatible engine. Tests were aimed at identifying the degree to which calibration strategies such as mixture enleanment and tarded spark timing could lower engine-out hydrocarbon emissions and raise exhaust temperatures, as well as determining how such calibration changes would affect e combustion stability of the engine.

4. SUBJECT TERMS

ternative fuels, transportation fuels, ethanol, E85, light-duty vehicles, enhanced ignition system

15. NUMBER OF PAGES
100

16. PRICE CODE

7. SECURITY CLASSIFICATION OF REPORT	18. SECURITY CLASSIFICATION OF THIS PAGE	19. SECURITY CLASSIFICATION OF ABSTRACT	20. LIMITATION OF ABSTRACT